Escola Superior de Tecnologia da Saúde do Porto
Instituto Politécnico do Porto
António César Andrade Dias Pimenta

Biochemical and Structural characterization of β-lactamases TEM-180 and TEM-201

Mestrado em
Tecnologia Bioquímica em Saúde.
Setembro de 2012

ESCOLA SUPERIOR DE TECNOLOGIA DA SAÚDE
DO PORTO
INSTITUTO POLITÉCNICO DO PORTO

António César Andrade Dias Pimenta

BIOCHEMICAL AND STRUCTURAL CHARACTERIZATION OF B-LACTAMASES TEM-180 AND TEM-201

Dissertação submetida à Escola Superior de Tecnologia a Saúde do Porto para cumprimento dos requisitos necessários à obtenção do grau de Mestre em Tecnologia Bioquímica em Saúde, realizada sob a orientação científica de Doutora Irina de Sousa Moreira, Investigadora Assistente, REQUIMTE e Doutor Rúben Fernandes, Professor Adjunto, área tecnico-científica das Ciências Químicas e das Biomoléculas da ESTSP-IPP e Centro de Investigação em Farmacologia e Biopatologia Química (U38-FCT) da FMUP e co-orientação de Doutora Paula Amador, Professora Adjunta do Instituto Politécnico de Coimbra.

Setembro, 2012

Acknowledgements

To Professor Cristina Prudêncio and Professor Maria João Ramos for the opportunity to work in their groups and stimulating my interest in research.

To Doctor Irina Moreira for accepting me as her student and teaching me what I know in Computational Chemistry. Also for always support my work, for the valuable advices during this and for being available to help me in this project.

To Doctor Rúben Fernandes for accepting me as his student and allowing me to develop the project, making it even more appealing. Also for finding time to guide me through the project at any hour and for the many advices during the entire period of the MSc.

To Carla Oliveira and Claudia Pereira for helping me with the experimental methods and for Claudia Pereira for the support and encouraging during the entire MSc.

To Rui Ramos and João Martins from lab 3.26 for the help since the first day, teaching me how to apply several methodologies that I needed and for the great moments spent every day with the others lab members.

To the colleagues in Professor Maria João Ramos´s group for the quality times spent together.

To my family and friends for the support during the entire project. In particular to my mother for supporting all aspects that allowed me to accomplish this stage in my life and my brother for helping me with informatics problems that I encountered.

To Catarina Moreira for her support, patience and friendship of many years.

Abstract

With the constant development of new antibiotics, selective pressure is a force to reckon when investigating antibiotic resistance. Although advantageous for medical treatments, it leads to increasing resistance. It is essential to use more potent and toxic antibiotics. Enzymes capable of hydrolyzing antibiotics are among the most common ways of resistance and TEM variants have been detected in several resistant isolates. Due to the rapid evolution of these variants, complex phenotypes have emerged and the need to understand their biological activity becomes crucial.

To investigate the biochemical properties of TEM-180 and TEM-201 several computational methodologies have been used, allowing the comprehension of their structure and catalytic activity, which translates into their biological phenotype.

In this work we intent to characterize the interface between these proteins and the several antibiotics used as ligands. We performed explicit solvent molecular dynamics (MD) simulations of these complexes and studied a variety of structural and energetic features.

The interfacial residues show a distinct behavior when in complex with different antibiotics. Nevertheless, it was possible to identify some common Hot Spots among several complexes – Lys73, Tyr105 and Glu166. The structural changes that occur during the Molecular Dynamic (MD) simulation lead to the conclusion that these variants have an inherent capacity of adapting to the various antibiotics. This capability might be the reason why they can hydrolyze antibiotics that have not been described until now to be degraded by TEM variants. The results obtained with computational and experimental methodologies for the complex with Imipenem have shown that in order to this type of enzymes be able to acylate the antibiotics, they need to be capable to protect the ligand from water molecules.

II. Index

III. Index of figures

IV. Index of tables

IV. List of Abbreviations

AMBER - Assisted Model Building with Energy Refinement

ASM - Alanine Scanning Mutagenesis

CHARMM - Chemistry at Harvard Macromolecular Mechanics

ESBL – Extended Spectrum β-Lactamase

FF – Force Field

GAFF - General Amber Force Field

HS - Hot-spot

IRT – Inhibitor Resistant β-Lactamase

MD – Molecular Dynamic

MM – Molecular Mechanics

MM-PBSA – Molecular Mechanics-Poisson-Boltzmann Surface Area

MM-PBSA – Molecular Mechanics-Generalized Born Surface Area

PME - Particle Mesh Ewald

RDF – Radial Distribution Function

RESP – Restrained Electrostatic Potential

RMSD – Root Mean Square deviation

RMSF – Root Mean Square fluctuation

SANDER - Simulating Annealing with NMR-Derived Energy Restraints

S.D. – Standard Deviation

WHO – World Health Organization

PDB – Protein Data Bank

DFT - Density Functional Theory

3D – Tridimensional

CAZ – Ceftazidime

APSM – Ampicillin/Sulbactam

CTX – Cefotaxime

FOX – Cefoxitin

CRO – Ceftriaxine

CXM – Cefuroxime

TZP – Piperacillin/Tazobactam

AZM – Azithromycin

CN – Gentamycin

FD – Fusidic acid

SXT - Trimethoprim/sulfamethoxazole

IMI – Imipenem

VA – Vancomycin

E – Erythromycin

TOB – Tobramycin

DA – Dindamycin

OX – Oxacillin

P – Penicillin G

CIP – Ciprofloxacin

LEV – Levofloxacin

MXF – Moxifloxacin

F – Nitroforantoin

CLR – Clarithrimycin

CEC – Cefaclor

TEC – Teicoplanin

MUP – Mupirocin

RD – Rifampicin

LZD – Linezolid

NA – No halo

TSA - Tryptic soy agar

TSB - Tryptic soy broth

SOC - Super Optimal Culture

FDA - Food and Drug Administration

WHO - World Health Organization

CLSI – Clinical and Laboratory Standards Institute

OXOID - dehydrated form of Mueller-Hinton medium

SAM - S-Adenosylmethionine

Chapter I - Introduction

1. State of the Art

1.1. Beta-lactamases – evolution and relevance

Infectious diseases are nowadays accepted as one of the most important and relevant clinical conditions, and, many times, fatal. With the inclusion of antibiotics in the clinical practice, mankind has taken this problem as a ceased problem in the history of human diseases. However, the infectious agents have the capacity to resist the antibiotics action. Nowadays, the majority of the hospitals isolates are microorganisms highly resistant to antibiotics.[1, 2] The ability to resist antibiotics can be associated with multiple factors but the most common is genetic mutation that leads to the production of a mutated protein. These proteins can be enzymes that increase the catalytic activity towards antibiotics or increase the resistance to the inhibitors binding. Additionally membrane transporters that export antibiotics prior to their binding to the target may be also mutated. The microorganisms that do not possess any mutation in their genome conferring resistance to the antibiotics may obtain these kinds of genes through the acquisition of mobile genetic elements such as plasmids and transposons.[1, 3, 4] These mechanisms can be considered as primary mechanisms of resistance (resistance occur at the primary level of metabolism). Nevertheless, mechanisms of resistance affecting secondary metabolism have also been described (biosynthesis of modified β-lactams that are antagonist of the modified proteins).[5]

Specific primary mechanisms of resistance can be associated with Gram-positive and Gram-negative bacteria. In Gram-positive bacteria, acquisition of resistance is obtained through the production of β-lactamases (inactivation of the antibiotic) and production of mutated Penicillin Binding Proteins (PBPs).[5, 6] Several mechanisms of resistance can be obtained with the mutation of these targets. It is possible that a less sensitive PBP is produced either by mutation of an endogenous protein or with acquisition of a new PBP. It is possible to up regulate the production of PBPs allowing the pathogen to produce peptidoglycan.[7] The most common mechanism in Gram-negative bacteria is the production of β-lactamases but these organisms can also present mutation of outer membrane proteins such as porins. This allows them to avoid one of the mechanisms for the crossing of the antibiotic through the outer membrane to reach the active site (PBPs)

and the production of efflux pumps capable of remove the antibiotics from the periplasma and transporting them out of the bacteria.[5, 6]

Nowadays, it is accepted that the increase of antibiotic resistance is due to the negligent use of antibiotics or the lack of these to perform a proper medical treatment – World Health Organization (WHO). However, the emergent resistance of β-lactams was detected even before penicillin was ever used in medical practice.[1, 2] The first β-lactamase was described, in 1940, by Chain, E. *et al* in *E. coli,* as a penicillinase but soon this resistance had appeared in others species, particularly in *staphylococci*.[1, 8] It is believed that β-lactamases have PBPs as their ancestors and that by the acquisition of new mutations, evolved and gain the capability to acylate and deacylate β-lactams.[9] So, it becomes clear why PBPs and β-lactamases are both serine proteases with similar active sites (in both exists a lysine near the catalytic serine). However, in PBPs the lysine is the initial base but in β-lactamases its role is not yet fully understood. Another major dissimilarity between the active site of these two types of proteins is the presence of a new glutamate residue in the Ω-loop in the β-lactamases.[10]

The most common isolated β-lactamases are TEMs and SHVs, as well as extended spectrum β-lactamase (ESBL). Other examples are OXAs and SHO.[1, 11, 12] After the discovery of TEM-1(1963), its prevalence increased and, in 20 years, various variants of TEM-1 were detected with altered kinetic properties such as the ability to hydrolyze extended spectrum β-lactam antibiotics and to resist inhibition (inhibitor resistant - IRT).[2]

1.2. TEM-1 characterization

The antibiotics action with TEM-1 occurs by hydrolysis of the amide group of the β-lactamic ring by a serine residue in the active binding site, which allows the classification of this enzyme as class A β-lactamase (classification according to Ambler, 1980).[13] Despite this classification still being used, it does not allow to clearly and efficiently differentiate some β-lactamases with distinct properties. To overcome this situation a more complex system of classification was developed by Bush.[14] This system uses several of the enzyme characteristics such as molecular structure, biochemical properties and genetic sequence.[14]

1.2.1. TEM-1 structure

β-lactamase TEM-1 (Figure 1) is organized in three domains that are organized Sandwich-like ((α-Helices /β-sheets/ α-Helices). Its binding site is located between the β-sheets domain and the domain that includes the α2-Helix.[13, 15]

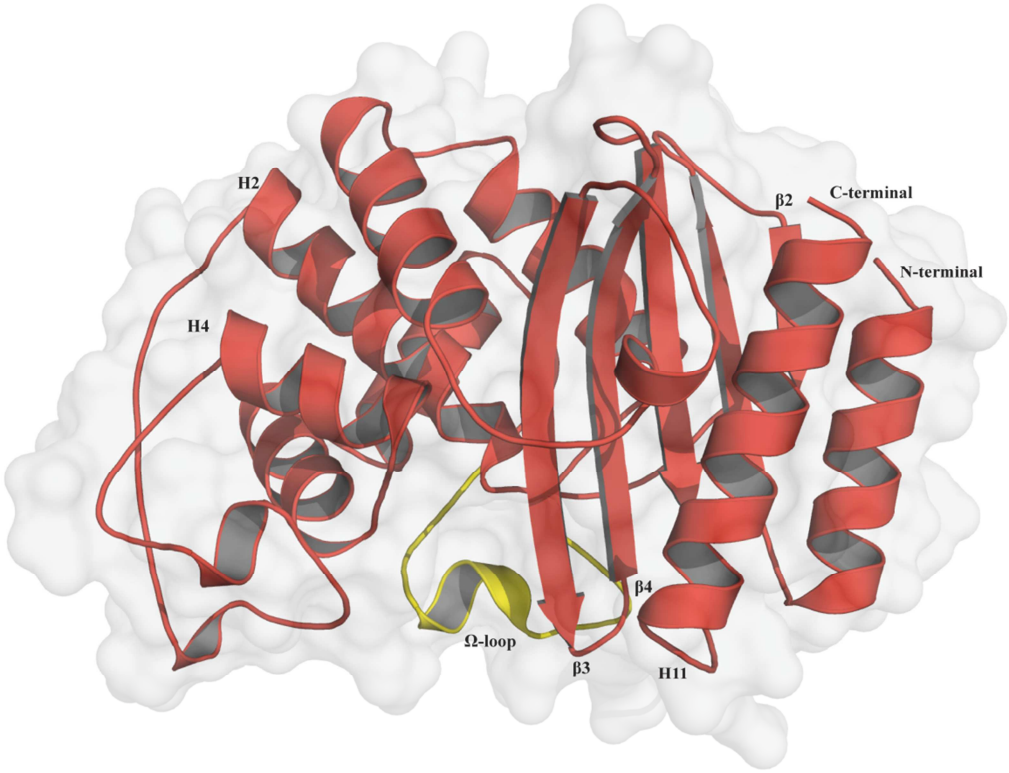

Figure 1: Structural representation of TEM-1 (PDBID:1ZG4[16]) with some of the key secondary structures identified.

The protein backbone is highly ordained and stable and a higher variability is observed in the loops due to the lack of a well defined secondary structure.[17] The high variability of the position of loop Ω, may influence the proximity of water molecules near the active center, more precisely near the Glu166 residue. Figure 2 illustrates the proximity of the residues that do not catalyze the reaction (highlighted in orange) to the catalytic residues, reason why they may influence the ability of this enzyme to hydrolyze substrates (leading to a different orientation of the catalytic residues, enlargement of the catalytic pocket or displacement of water molecules in the catalytic pocket). However, there is a tradeoff: the destabilization of the enzymatic structure. The Ser130 residue has an important role in the catalysis, mainly due to its proximity to the residue Ser70. It is very important in the reaction with inhibitors of β-lactamases as it is the residue that is irreversibly inhibited.[1,

[13, 17-21] Kollman *et al*. [22] have shown that Ser130 can be responsible for the β-lactamic ring opening due to the donation of an hydrogen, after the nucleophilic attack by Ser70.

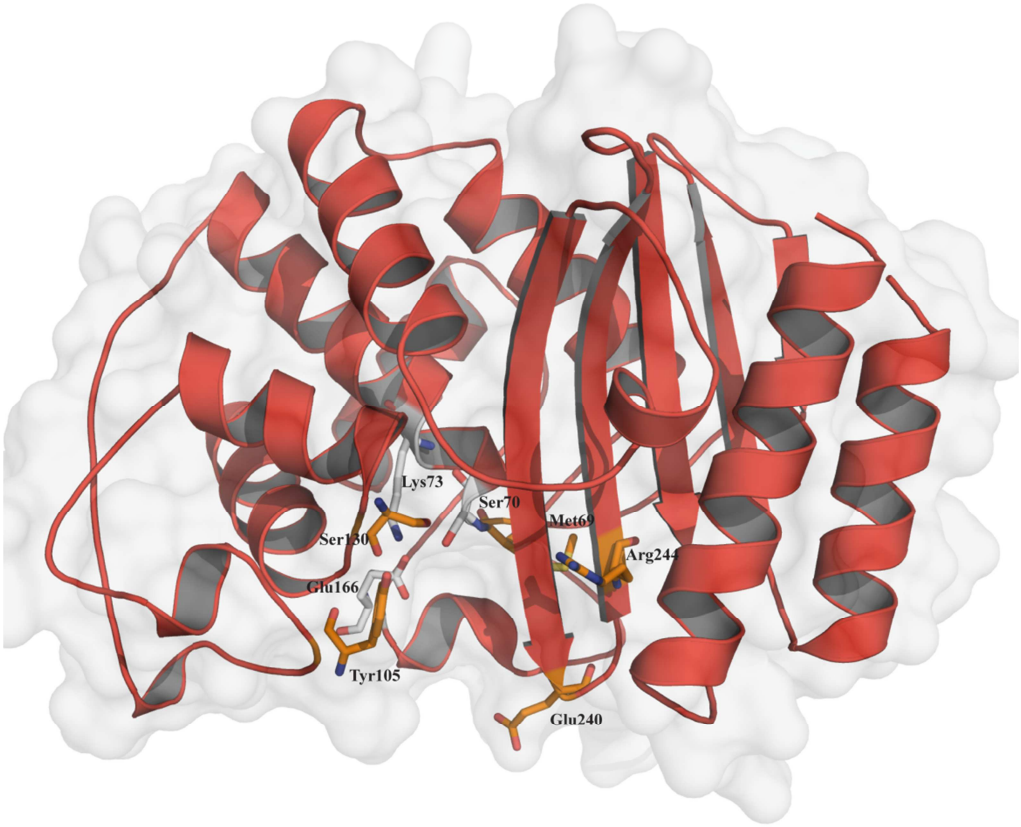

Figure 2: Structural representation of TEM-1 (PDBID:1ZG4[16]) with the catalytic residues in a white stick representation and the residues near the catalytic pocket (the ones that can affect the enzymatic catalyzes) highlighted in orange.

1.2.2. TEM-1's activity

The process responsible for the resistance to antibiotics can be explained by two main processes: acylation and deacylation.[13] In the acylation process, the Ser70 residue is deprotonated in order to perform the nucleophilic attack to the carbon in the carbonyl group in the β-lactamic ring. The deprotonation process is achieved through the interaction of a water molecule with Glu166, being the latter the primary base of the reaction.[18, 23] After accessing the importance of the Lys73 in the process, other theories refer the possibility of this residue act as a base in the enzymatic process. However, it can also be important to stabilize the ligand in the hydrolysis reaction. Thus, the mechanism is yet not fully understood and many theories have been described.[13, 18, 22, 23] The deacylation process of the formed intermediary occurs with an activated water molecule

bound by hydrogen bridges to Glu166, releasing Ser70 from the β-lactamic ring in its protonated form.[13]

1.2.3. Extended spectrum β-lactamases - ESBL

For decades new antibiotics were developed with clinical usability. The usage of new antibiotics induced a selective pressure over microorganisms, which led to a co-development of the latter with production of enzymes capable of antibiotic degradation.[3, 12]

TEM-1 degrades efficiently some penicillins but, despite its poorly filled out active center, it does not possess the needed space to accommodate big lateral chains like the ones in ceftazidine and cephotaxime (3th generation cephalosporins).[2, 12, 24] With the introduction of this type of compounds, these enzymes have evolved. Up to 2001 [1] mutations were observed only on a small number of residues. After Bradford *et al.* compile the mutations on the existent ESBLs, not only several new enzymes have been identified but mutations on several different residues can now be observed. TEM ESBL started to be identified and isolated since the 70s, being nowadays more than 100.[1, 25]

The unusual mutations observed in this phenotype increase the plasticity of the active center, which allowed its enlargement, despite the fact that they do not occur in the active center. This enlargement means that the enzymes with this phenotype can acylate larger β-lactam antibiotics, inactivating them. ESBL have shown to degrade extended spectrum β-lactams (around 100 times more efficient) but with decreased catalytic activity for penicillins (100 fold less efficient).[26] The enlargement and increase of plasticity of the active center do occur but with a decreased enzymatic stability.[27] Having this in consideration, it is understandable that enzymes that present an additional factor that leads to higher enzymatic stability are naturally selected. This is mainly accomplished by evolutionary pressure, by the use of antibiotics with bigger lateral chains.[2, 24] In several ESBL, one factor was identified: the Met182Thr mutation. This mutation does not lead to any effect on the catalytic activity of the enzyme. Therefore, by itself does not bring any evolutionary advantage, which might be the reason why any enzyme was identified with just this mutation.[2, 3, 19, 28] Wang X. *et al*. proved that bacteria that produce enzymes with

the referred mutation are less susceptible to 3th generation cephalosporins, when compared with the wild type. Effect that is observed in a higher degree with the increase of the temperature.[12] These observations may be explained by the increase of the proteic stability but it is still possible that it promotes the correct folding of the TEM variants.[24]

A small amount of amino acids mutations with a high importance for the yield of extended spectrum enzymes have been described. The most common ones are: Leu21Phe, Gln39Lys, Glu104Lys, Arg164His or Arg164Ser, Gly238Ser and Glu240Lys.[1, 2, 25, 29] Figure 3 is a diagram of the various mutations, relative to TEM-1 sequence, of the ESBLs β-lactamases with sequence available in reference [25] at the time of this review.

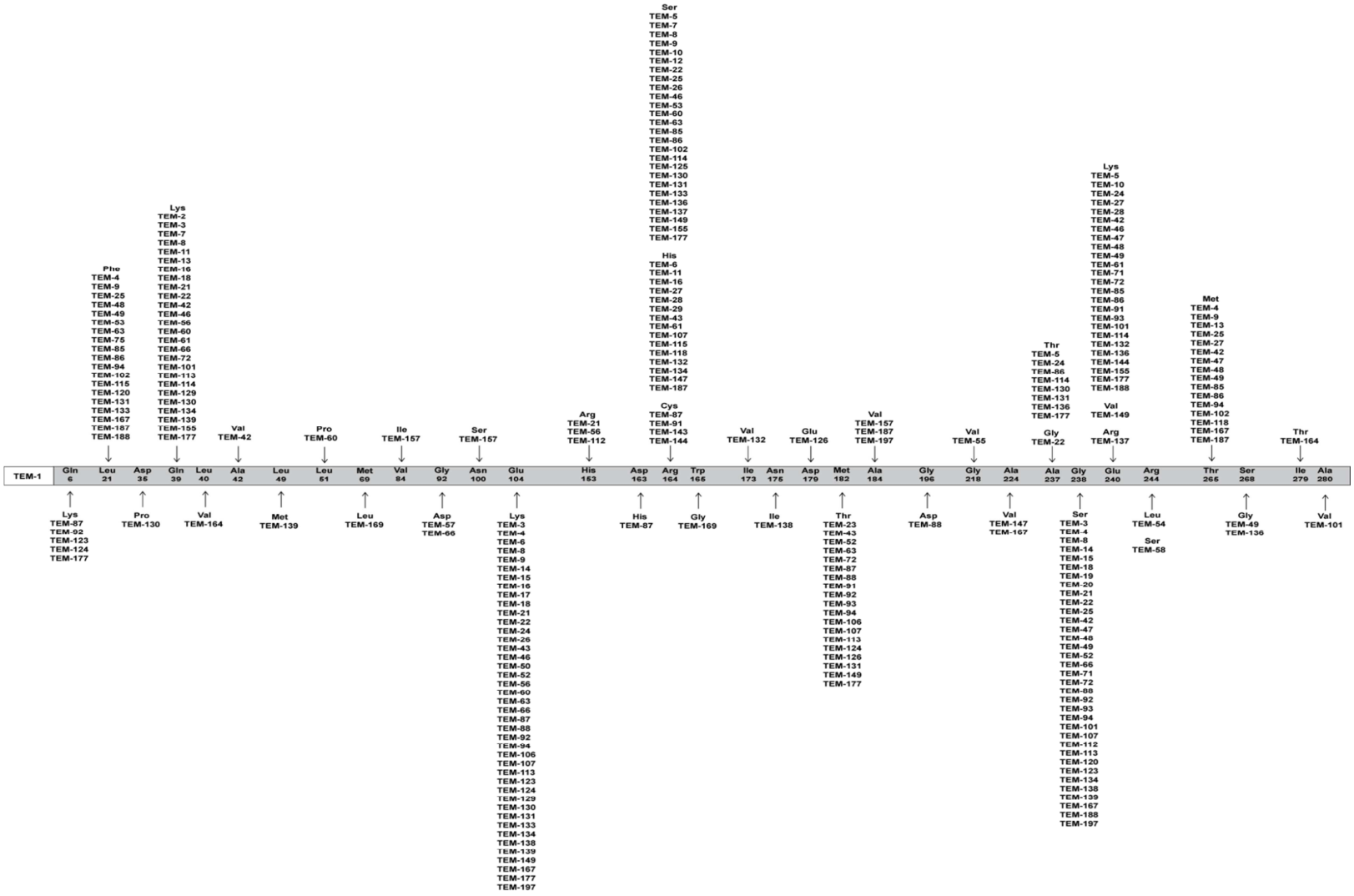

Figure 3: Diagram of the mutations of TEM ESBL enzymes, compared to the TEM-1 sequence. Scheme based on available sequences and phenotype in Jacoby database[25].

1.2.4. Inhibitors resistant beta lactamases - IRT

The β-lactamases with the ability to resist the inhibition by clavulanic acid were discovered in the early 90s.[26] They were identified mainly from samples of *E. coli* but also from samples of other lineages, like *K. mirabilis* and *C. freudii.*[1]

These types of enzymes confer resistance to clavulunate/clavulanic acid and sulbactam. Hence, microorganisms that produces them are resistant to Clavamox® treatment (amoxicillin-clavulanic acid), ampicillin-sulbactam and other inhibitor combinations.[2, 11, 29-31] IRTs remain susceptible to Tazobactam, and this treatment may be performed in combination with piperacillin.[31] Mutations in the residues Met69, Ser130, Trp165, Arg244, Arg275 and Arg276 appear to be relevant in promoting this phenotype and its identification is more common in clinical isolates.[1, 2, 21, 26, 32] Substitutions in the Met69, Ser130, Arg244 and Arg276 residues were identified as resistance promoters ampicillin-clavulanic acid combinations and other studies have shown that mutations in Met69, Trp165 and Arg276 promote resistance to cephtazidine-clavulanic acid treatment.[1, 20, 32, 33] Mutations on the Arg275 residue do not promote considerable resistance to clavulanic acid inhibition. Nevertheless, mutations for Leu and Gln have been identified to increase cefotaxime resistance, suggesting that Arg275 mutations may promote resistance to inhibitors and β-lactam antibiotics.[2, 24] Figure 4 is a diagram of the mutations, relative to TEM-1, of the IRTs β-lactamases with sequence available in reference [25] at the time of this review.

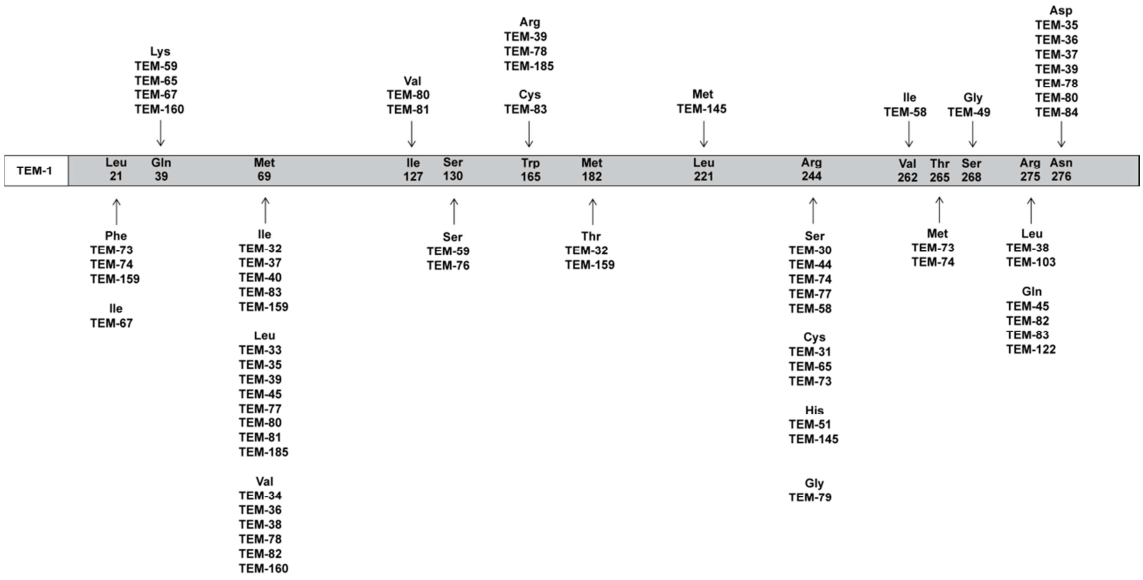

Figure 4: Diagram of the mutations of the TEM IRT enzymes, compared to the TEM-1 sequence. Scheme based on available sequences and phenotype in Jacoby database.[25]

The inherent mechanism of the inhibition is identical for all inhibitors and, unlikely the mechanism of β-lactam hydrolysis, is already well known.[26] It comprehends 8-10 different intermediaries in the inactivation pathway and derives of conventional hydrolysis intermediaries.[20] The inhibitors form a covalent bond between residues Ser70 and Ser130 leading to the irreversible inactivation of the enzyme due to deprotonation of the Ser130 residue.[21, 26] Despite the hydrolytic pathway being 100 times faster than the inactivation pathway, the latter is irreversible, which leads to the inhibition of all the enzymes in the microorganism and loss of its activity.[21] Clearly, Ser130 is essential to the inactivation via and its role is very important to the IRT phenotype.

Other described mutations do not present direct interaction with the inhibitor nor with the proteic neighborhood of the active center. However, it is possible that these mutations cause torsion of Ser130 side chain, deflecting it from the active center, which leads to resistance to inhibitors.[2, 26] IRT TEMs are less capable of hydrolyzing β-lactam antibiotics. As they are resistant to the inhibitors, have the ability to overcome this aspect and therefore, be resistant to the various treatments.[21] Mutants that present mutations in residues that are typically responsible for the EBSL and IRT phenotype, normally present just one of the phenotypes. However, it have been identified some mutants (i.e. TEM-50 or CMT-1) that confer resistance to clavulanic acid and present the ability to

hydrolyze large spectrum cephalosporins. [11, 25] Several others have also been described as CMT or CMT-type enzymes. Although CMT variants present resistance to β-lactamase inhibitors, some can still be inhibited by the clavulanic acid at a higher rate than IRT variants. These are fundamental evidences that β-lactamases with more complex phenotypes and higher potential to promote resistance to treatments are evolving.[34] Figure 5 is a diagram of the mutations described until now regarding the CMT/CMT-type phenotypes in comparison with the TEM-1 gene.[25]

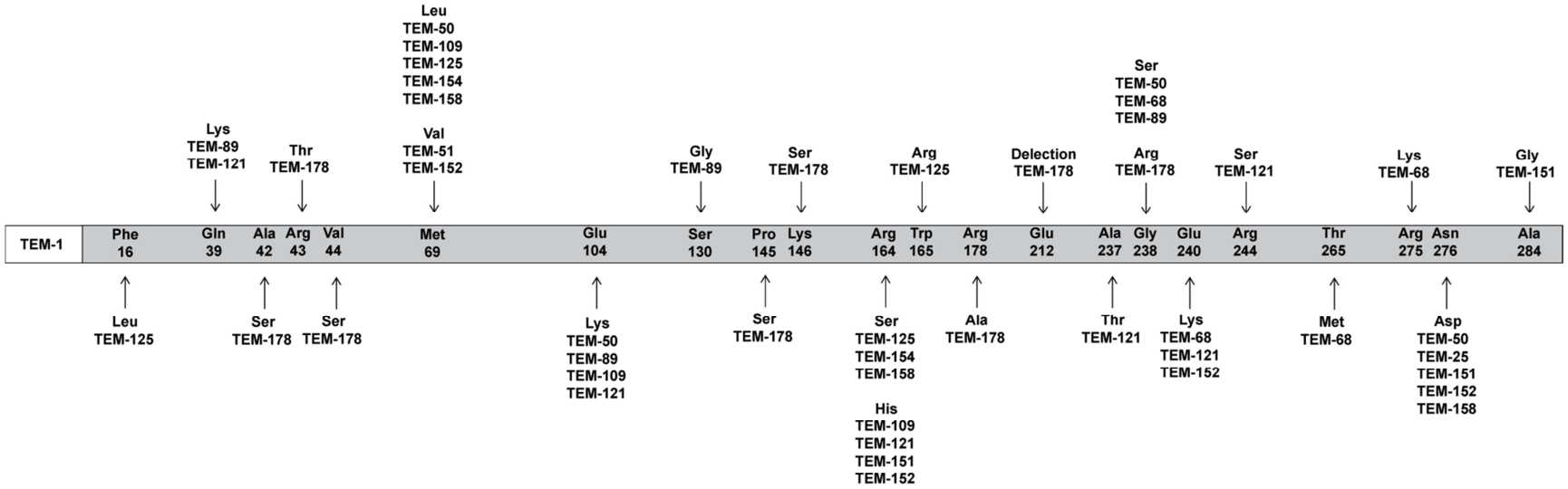

Figure 5: Diagram of the mutations of the TEM CMT/CMT-type enzymes, compared to the TEM-1 sequence. Scheme based on available sequences and phenotype in Jacoby database[25].

1.2.5. Previously described TEM variants

For several years, researchers have study this family of enzymes. Such searching for knowledge concerning TEM enzymes, include the comprehension of their enzymatic mechanisms and shad light into the way they are evolving for better predicting their biological effect (antibiotic resistance). In the medical context, the comprehension of the genetics and biochemistry of the various β-lactamases will allow the development of better therapeutic approaches towards the infection control caused by pathogens that produce TEM enzymes.

Table 6 lists some of the most important and well described variants. It becomes clear the relevance of some residues for their structure and activity.

Table 1: Biological and structural effect of the mutation of key residues of several TEM enzymes.

Variant	Mutation	Biological effect	Structural characteristics	PDB ID
Wild Type (WT)	-	Responsible for β-lactam antibiotics resistance (cephalosporins are moderate resistant). They open the β-lactam ring deactivating the molecule.	-	1ZG4[13]
-	S70G	Less active than WT deactivating β-lactam antibiotics. It can still be active as Ser130 might perform the nucleophilic attack to the β-lactam ring or due the presence of an additional water molecule close to Gly70.	Lack of nucleofilic properties at residue 70 side-chain. The overall structure is very similar to WT except conformation of Ser130 and backbone near this residue.	1ZG6[13, 21]
TEM-76	S130G	Less active than WT deactivating β-lactam antibiotics. Less prone to inhibition by clavulanate and tazobactam (K_1>K_1WT for pre-acylation complexes) More stable at T_m than WT.	Distance between Ser70 and Gly130 is greater than in WT (7,3Å and 6,7Å in WT). Rotation of Lys234 (N shifts 1,5Å). H-Bond between Lys73 and Ser70 does not exist (N of Lys73 moves 0,5Å). New water molecule near Ser130 is responsible for its activity.	1YT4[21]
Frequent in many TEM mutants	M182T	Similar activity than WT. Increased stability (stabilizes ESBL). Differences between TEM with Met182Thr increases with the increase of the temperature.	Met182 is 14,5Å from the active site and therefore, it does not affect β-Lactamase activity.	1JWP/ 1M40[12, 18]
TEM-69	E104K R164S M182T	ESBL	Loss of H-Bond between Arg164 and Asp179 and between Arg164 and Glu171. Loss of secondary structure near residue 170 (α-Helix) increases the catalytic pocket.	1JWP[12]

TEM-32	M69I M182T	More stable than TEM-40 (Met69Ile) and less stable than Met182Thr mutants. Resistance against β-lactamase inhibitors - IRT (Ser130 moves). Catalytic activity is reduced.	RMSD Cα= 0,41Å Ser70 distortion causes a 64^0 ϰ1 of Ser130 (no longer makes H-Bonds with Ser70 and Lys73) Ser130 Oγ - Ser70 Oγ = 5,5Å (3,2Å in WT) Ser130 Oγ - Lys73 Nζ = 5,4Å (3,8Å in WT). New water molecule near Ser130	1LI0[26]
TEM-34	M69V	More stable than WT. Resistant to inhibition (new H-Bond Ser130-Lys234: reduced ability to perform a nucleofilic attack)	RMSD Cα= 0,30Å Ser70 distortion causes a 27^0 ϰ1 of Ser130. H-Bonds between Ser130 with Ser70, Lys73 and Lys234 (Ser130 Oγ - Lys234 Nζ = 2,8Å ; Ser130 Oγ - Lys73 Nζ = 3,2Å). Two lone pairs are used to bond with the two Lys when in WT only one of these was verified. The rate of cross-linking between the two Ser is reduced, which leads to a lower inactivation.	1LI9[26]
TEM-64	N276D	IRT phenotype K_{inact} 35% inferior than in WT with clavulanic acid. Small or nonexistent inhibition with Tazobactam and Sulbactam.	Overall structure similar to WT. Residues 272-290 (β-Sheet surface/α-Helix H_{11}), 26-40 (N-Terminal α-Helix H_1) and 219-224 (α-Helix H_{10}) move. RMSD=0,52Å RMSD(Asp276)=0,75Å. New interaction with Arg244 (Asp276 $O_{\delta 2}$ - Arg244 $N_{\eta 2}$=3,3Å). Nonexistent water molecule in the active site (less prone to inhibition).	1CK3[32]
TEM-30	R244S	IRT phenotype due to water displacement.	Water displacement leads to lower affinity to inhibitor (Schiff's Base from inhibitor goes away from Ser130).	1LHY[26]

Legend 1: RMSD: Random Medium Standard Deviation; WT: Wild Type

1.2.6. Relevant aminoacids

Table 1 stresses out the importance of some residues for the structure and activity of the various TEM variants. Their importance is related to their position in the protein as well as to specific pair interactions with residues in their microenvironment. Here we will characterize them:

(i) Met69

The side chain of Met69 lies behind β3 forming a wall of the oxyanion pocket. By means of steric interactions it influences the position of Ala237 and Gly238. Due to the proximity with Ser70, it has an important role influencing the structural position of this residue and also of Ser130. (Figure 6-A)[1, 26, 35]

(ii) Glu104

This glutamic acid residue is located in a conserved loop, highlighted in yellow (101-111) and its hydrophilic side chain is exposed at the entrance of the binding site. Due to its direct contact with Asn132 (part of the conserved SDN loop, highlighted in green (130-132), if mutated it might affect the entry of bulky ligands. (Figure 6-B)[1, 29]

(iii) Ser130

Serine 130 is part of a complex hydrogen bounding network that contributes for the stability of the active site and the deprotonation process of Ser70. This residue is highly conserved. However, even tough with consequences in the enzyme activity mutations or displacement of the side chain are tolerated. (Figure 6-C)[1, 20, 21, 31]

(iv) Arg164

This arginine residue is underneath the binding site in the Ω-loop (162-179). The side chain is linked with Glu171 and Asp179 by salt bridge interactions and hydrogen bonds. An alteration in this residue might lead to an altered stability and conformation of the loop, and therefore, changes in the active site and the position of the catalytic residues. (Figure 6-D)[1, 29, 36]

(v) Met182

Methionine 182 is distant from the active site but it has contact with the secondary structure in which Met69 is located. Mutations in this residue have been detected on clinical isolates but its role is not fully understood. (Figure 6-E)[1, 26, 28, 29]

(vi) Ala237

The side chain of alanine 237 is on the exposed side of β3, which faces the catalytic pocket. Therefore, the position of this residue influences the stability of β-lactam

antibiotics binding by hydrogen bonding with them (groups NH and CO of the backbone). (Figure 6-F)[1, 19, 29, 37]

(vii) Gly238

The side chain of glycine 238 is on the internal and more protected side of β3, close to the residue Met69. It has been demonstrated the importance of this residue both for the position of the β3, as well as the position of the Ω-loop (steric conflict model). This affects the active site volume. (Figure 6-G)[19, 25, 29, 38](1, 12, 17, 22)

(viii) Glu240

This residue is located at the end of β3 and its side chain can interact with the substituents of bulky β-lactam antibiotics (i.e. cephalosporins). Mutations in this residue alone would not modify significantly the catalytic properties of the enzyme but it might compensate the destabilization of other mutations (i.e. Arg164Ser or Gly238Ser). (Figure 6-H)[1, 2, 39-41]

(ix) Arg244

Arg244 is located in the β4 and its long side chain reaches over to the adjacent β-strand (β3) to the edge of the binding site. It is kept in place by two hydrogen bonds with Asn276. Arg244 together with Val216 can be responsible for holding a water molecule in place, which is thought to be important for the enzyme inactivation process. (Figure 6-I)[1, 29, 36, 42]

(x) Asn276

This residue is located on the C-terminal α-helix (H11) and its carbonyl group interacts with Arg244 by two hydrogen bonds (Asn276 carbonyl group with guanidinium group of Arg244). A mutation in residue 276 will not affect the position of the surrounding residues (i.e. Arg244). However, the rotamer of the mutant will be substantially different for TEM-1. As consequence, α1 and α10 will be displaced. (Figure 6-J)[1, 29, 30, 32, 36]

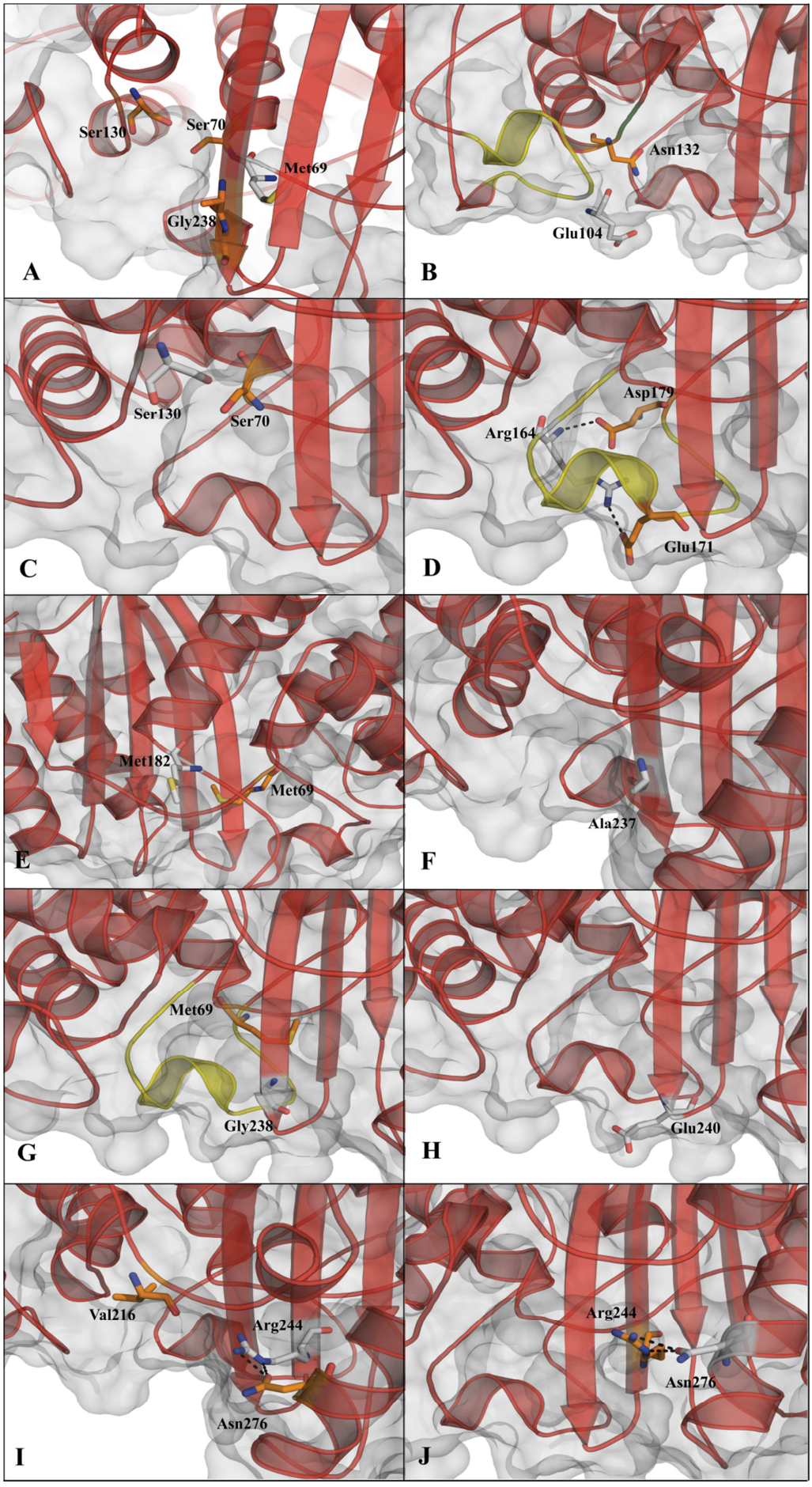
Ser130
Ser70
Met69
Gly238
A
Asn132
Glu104
B
Ser130
Ser70
C
Asp179
Arg164
Glu171
D
Met182
Met69
E
Ala237
F
Met69
Gly238
G
Glu240
H
Val216
Arg244
Asn276
I
Arg244
Asn276
J

Figure 6: Structural representation of key residues of TEM-1 (PDBID: 1ZG4[16]). In orange are highlighted the interacting residues. A: Met69; B: Ser104; C: Ser130; D: Arg164; E: met182; F: Ala237; G: Gly238; H: Glu240; I: Arg244 and Asn276.

1.3. β-lactam structure and classification

The first β-lactam antibiotic to be used in clinical practice was penicillin. It was discovered and rapidly described by Alexander Fleming in 1928 but was only used with success in medical practice in 1941, after the work of Howard Walter Florey and Ernst Chain.[43]

β-lactams target the PBPs with success because this type of antibiotics mimics the D-ala-D-ala dipeptide in the peptidoglycan and form a very stable acyl-enzyme complex inhibiting PBPs from synthesizing peptidoglycan.[44] In fact, the deacylation step of these antibiotics can be up to six times slower when compared with β-lactamases.[45]

β-lactam antibiotics always feature a very reactive cyclic amid – β-lactam ring - which is a part of the bicyclic structure that forms the "core" of the antibiotic. A few common ring rearrangements can be appointed: penam, penem, carbapenem, cefem and monobactam.

Other class of antibiotics within the β-lactams is the β-lactamase inhibitors, which have a different structure and role in treatment. By themselves inhibitors do not treat infections but they are used to surpass the capability of infectious agents to degrade antibiotics used in the medical treatment.

1.3.1. Penams

After Fleming's discovery of penicillin, several antibiotics with different activity spectrums have been developed for medical use. Methicillin is not used anymore in medical practice due to the use of more active penicilliase-resistant penicillins. Nevertheless, it is still in use in laboratory to determine the susceptibility of *Staphylococcus aureus* to the penicillinase-resistant penicillins. This class of β-lactam antibiotics has as bicyclic structure the β-lactam ring and a thiazolidinic ring. Both natural and synthetic antibiotics exist within this class.[46]

Table 2: Spectrum, pharmacodynamics and chemical structures of several penicillins.

Class	Name	Type	Mechanism of action	2D Structure
Penicillins	**Penicillin V**	β-lactamase sensitive	By binding to specific PBPs located inside the bacterial cell wall, Penicillin V inhibits the third and last stage of bacterial cell wall synthesis. Cell lysis is then mediated by bacterial cell wall autolysins.	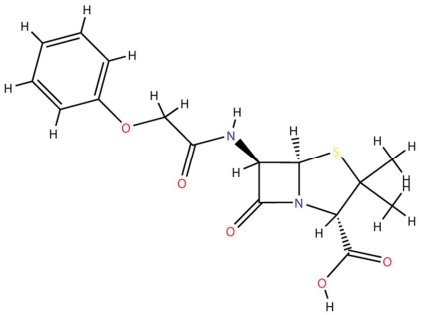
	Methicillin	Penicilli-nase-resistant penicillin	Methicillin acts by inhibiting the synthesis of bacterial cell walls. It inhibits the transpeptidase enzyme (PBP2a) used by bacteria to cross-link the peptide (D-alanyl-alanine) used in peptidoglycan synthesis.	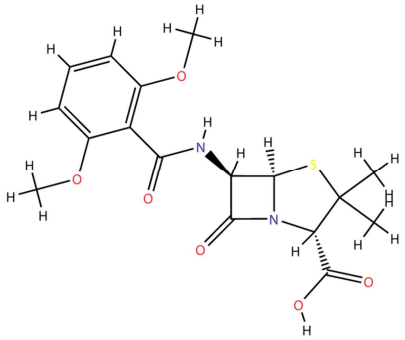
	Cloxacillin	Penicilli-nase-resistant penicillin	By binding to specific PBPs located inside the bacterial cell wall, cloxacillin inhibits the third and last stage of bacterial cell wall synthesis. Cell lysis is then mediated by bacterial cell wall autolytic enzymes such as autolysins.	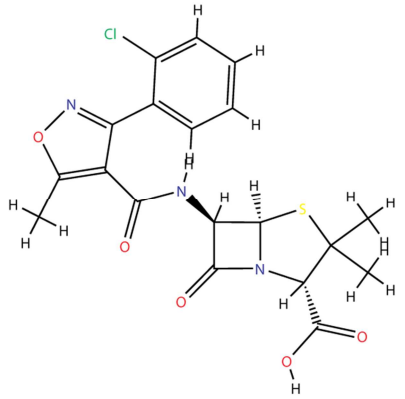
	Amoxicillin	Moderate-spectrum penicillin	Amoxicillin binds to PBP-1A located inside the bacterial cell well. Penicillins acylate the penicillin-sensitive transpeptidase C-terminal domain by opening the lactam ring. The inactivation of the enzyme prevents the formation of a cross-link of two linear peptidoglycan strands, inhibiting the third and last stage of bacterial cell wall synthesis.	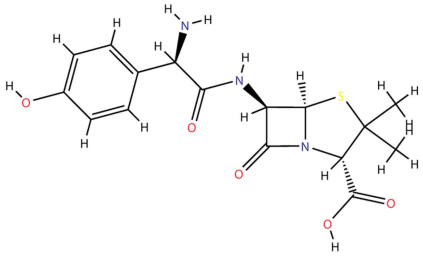

	Ampicillin	Moderate-spectrum penicillin	By binding to specific PBPs located inside the bacterial cell wall, Ampicillin inhibits the third and last stage of bacterial cell wall synthesis. Cell lysis is then mediated by bacterial cell wall autolytic enzymes such as autolysins.	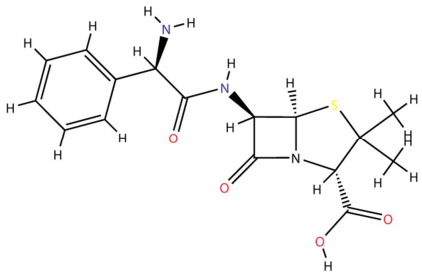
	Carbenicillin	Extended-spectrum penicillin	Carbenicillin exerts its antibacterial activity by interference with final cell wall synthesis of susceptible bacteria via PBPs inhibiting the third and last stage of bacterial cell wall synthesis.	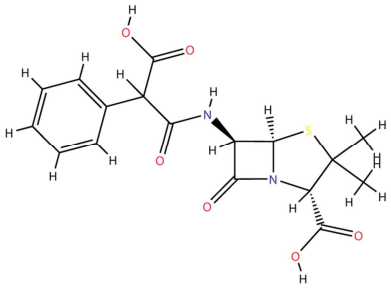

Legend 2: PBP: Penicillin Binding Proteins

1.3.2. Cefems

Cefems can be classified into five different classes depending on the bicyclic structure and substituents: cephalosporins, cephamycins, oxa-1-cephems, carba-1-cephems and others. More typically, they are divided according to their microbiological classification: division in classes, 1st-5th generation according to their microbial spectrum. According to this classification scheme cefoxitin (cephamycin) is often included with the 2nd generation cephalosporins, which present broad-spectrum activity. These antibiotics demand more refinement than penicillins to be effective.

Table 3: Spectrum, pharmacodynamics and chemical structures of several cephalosporins.

Class	Name	Type	Mechanism of action	2D Structure
Cephalosporins	Cefazolin	1st gen, broad-spectrum Cephalosporin	Bacterial cell wall synthesis inhibition via PBPs affinity. It inhibits the third and last stage of cell wall synthesis. Effective against some species of Gram-positive bacteria.	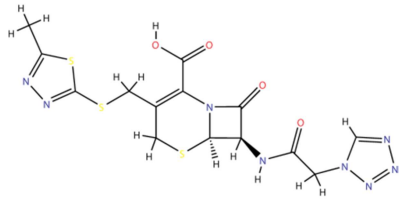
	Cefuroxime	2nd gen, broad-spectrum Cephalosporin	Bacterial cell wall synthesis inhibition via PBPs affinity. It inhibits the third and last stage of cell wall synthesis. Effective against Gram-positive and Gram-negative bacteria. It can cross the blood–brain-barrier	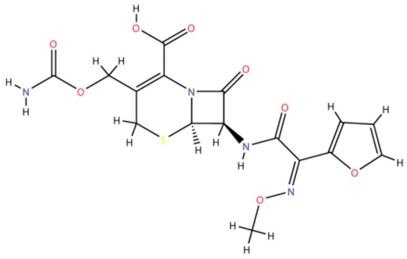
	Cefotaxime	3rd gen, extended-spectrum Cephalosporin	The bactericidal activity of cefotaxime results from the inhibition of cell wall synthesis via PBPs. Cefotaxime shows high affinity for penicillin-binding proteins in the cell wall including PBP Ib and PBP III.	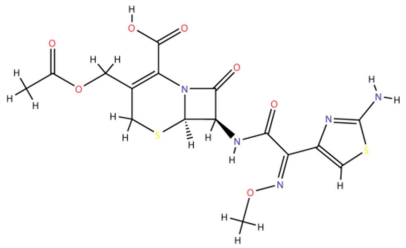
	Ceftazidime	3rd gen, extended-spectrum Cephalosporin	Bacterial cell wall synthesis inhibition via PBPs affinity. Effective against Gram-positive and Gram-negative bacteria	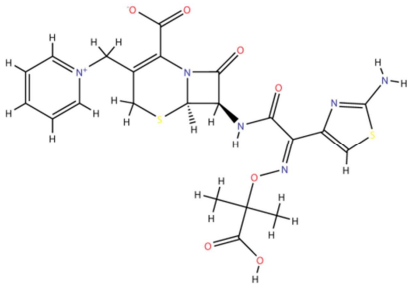
	Cefpirome	4th gen, extended-spectrum Cephalosporin	Bacterial cell wall synthesis inhibition via PBPs affinity. Effective against Gram-positive and Gram-negative bacteria.	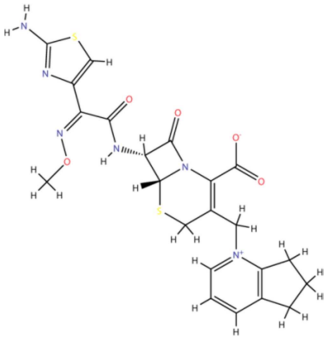
	Ceftobiprole	5th gen, extended-spectrum Cephalosporin	Bacterial cell wall synthesis inhibition via PBPs affinity. It inhibits the PBP IIa in MRSA PBP IIx in penicillin-resistant S. pneumoniae. Effective against Gram-positive and Gram-negative bacteria.	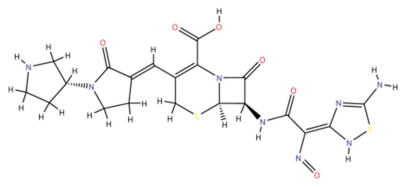

Legend 3: PBP: Penicillin Binding Proteins; MRSA: Methicillin-resistant *Staphylococcus aureus*

1.3.3. Carbapenems

This class of antibiotics is structurally similar to the β-lactam antibiotics and is effective against Gram-negative rods and Gram-positive organisms. Initially, these antibiotics were used only to treat severe infections cause by Gram-negative pathogens that did not respond to treatment with other antibiotics.[47] These antibiotics are effective inhibitors of the L,D-transpeptidase, which is resistant to the majority of β-lactams.[48] This transpeptidase uses L-Lys-D-Ala (instead of D-Ala-D-Ala) as acyl donor in the cross-linking reaction of the peptidoglycan.[49]

Its bicyclic structure is similar to penams but it does not possess the sulfur atom (the 2nd ring is not a thiazolidinic ring).

Main difference between the two antibiotics presented in the next table relies on toxicity and resistance to peptidases.[50]

Table 4: Spectrum, pharmacodynamics and chemical structures of several carbapenems.

Class	Name	Type	Mechanism of action	2D Structure
Carbopenems	**Imipenem**	Broad-spectrum	Imipenem acts as an antimicrobial through the inhibition of cell wall synthesis of various gram-positive and gram-negative bacteria. This inhibition of cell wall synthesis in gram-negative bacteria is attained by binding to PBPs. In E. coli and selected strains of P. aeruginosa, imipenem has shown to have the highest affinity to PBP-2, PBP-1a, and PBP-1b. It results in the direct conversion of the individual cell to a spheroblast, which leads to rapid cell lysis and death without filament formation. It is inactivated by dihydropeptidases in the renal tubules.	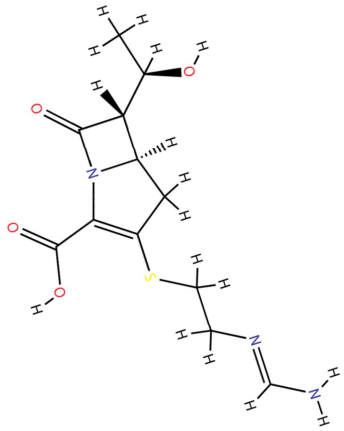

	Meropenem	Broad-spectrum	The bactericidal activity of meropenem results from the inhibition of the cell wall synthesis. Meropenem readily penetrates the cell wall of most Gram-positive and Gram-negative bacteria to reach PBP targets. Its strongest affinities are toward PBPs 2, 3 and 4 of E. coli and P. aeruginosa; and PBPs 1, 2 and 4 of S. aureus. It is not inactivated by dihydropeptidases and is less toxic than Imipenem.	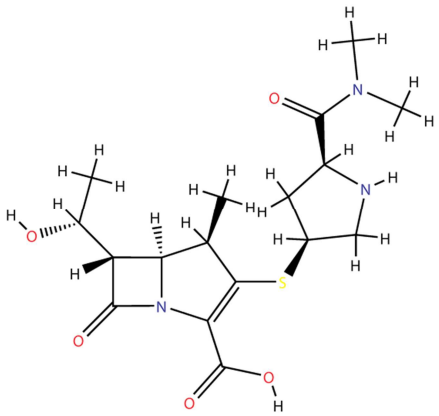

Legend 4: PBP: Penicillin Binding Proteins

1.3.4. Monobactams

Monobactams have a monocyclic "core" (only one β-lactam ring). The first drug of this class available was Aztreonam and it is only effective against Gram-negative aerobic bacteria without major toxic effects reported. Because of its activity spectrum it is recommended that initial treatment is performed with broader spectrum β-lactams.[50, 51]

Table 5: Spectrum, pharmacodynamics and chemical structure of Aztreonam.

Class	Name	Type	Mechanism of action	2D Structure
Monobactam	**Aztreonam**	β-lactamase resistant	The bactericidal action of aztreonam results from the inhibition of the third and last stage of bacterial cell wall synthesis due to a high affinity of aztreonam for PBP III.	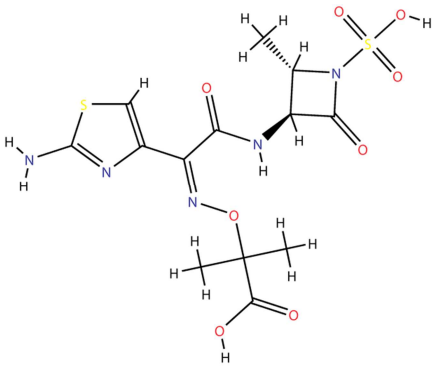

Legend 5: PBP: Penicillin Binding Proteins

1.3.5. β-lactamase inhibitors

These antibiotics are used to irreversibly inhibit serine dependent β-lactamases increasing the effect of other antibiotics that would be degraded to become more effective in treatment.[52-54]

Clavulanic acid, Sulbactam and Tazobactam (sulbactam and Tazobactam are penicillin sulfones) do not inhibit metallo-β-lactamases (MBLs). No efficient inhibition of MBLs is currently used in medical practice but progresses have been made in this way.[52, 55]

Table 6: Spectrum, pharmacodynamics and chemical structures of the β-lactamase inhibitors: clavulanic acid and the penicillin sulfones sulbactam and tazobactam.

Class	Name	Type	Mechanism of action	2D Structure
β-lactamase inhibitors	Clavulanic acid	β-lactamase inhibitor	Clavulanic acid competitively and irreversibly inhibits a wide variety of □-lactamases, commonly found in microorganisms resistant to penicillins and cephalosporins. It results in a restoration of the antimicrobial activity of β-lactam antibiotics against lactamase-secreting-resistant bacteria by inactivating β-lactamase.	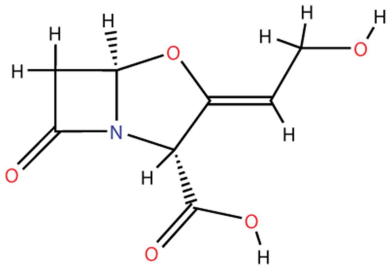
	Sulbactam	β-lactamase inhibitor	Sulbactam competitively and irreversibly inhibits a wide variety of β-lactamases, commonly found in microorganisms resistant to penicillins and cephalosporins. It results in a restoration of the antimicrobial activity of □-lactam antibiotics against lactamase-secreting-resistant bacteria by inactivating □-lactamase. It is used in combination with other β-lactam antibiotics when the infectious agent shows resistance to clavulanic acid.	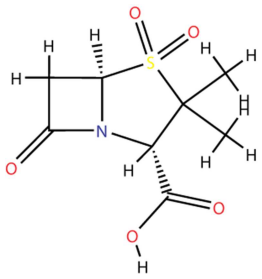
	Tazobactam	β-lactamase inhibitor	Tazobactam broadens the spectrum of piperacillin by making it effective against organisms that express β-lactamase and would normally degrade piperacillin.	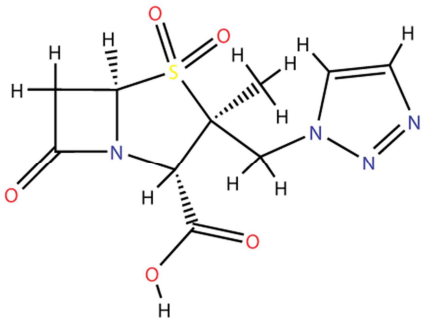

Legend 6: PBP: Penicillin Binding Proteins

1.4. Computational chemistry

The use of computational methods to predict results in molecular systems have increased due to its success, which has allowed important advances in Science that made experimentally, could mean years and high costs.

Therefore, Computational Chemistry is a chemistry branch that allows the application of theoretical chemistry and physics, integrated in computer programs efficiently. It has as primary goal to obtain results that explain a given chemical problem.[56] This area of chemistry must be seen as an integrating part for scientific development. It should be in constant interaction with other areas as physical, inorganic and organic chemistry as well as molecular biology, in order to understand the structural and biological concepts that are essential to Science development.

Nowadays theoretical chemistry allows, for example, the study of individual properties of the molecule (ionization energies, spectroscopic properties, molecular energy and structure, among others), and also resulting properties of the interaction between molecules (structural properties, molecular docking, geometry optimization of molecular complexes and protein structure predictions, to name just a few).

Due to the amount of problems that computational chemistry is able to study, several methodologies were developed – *ab initio* method, semi-empirical (based on mechanical quantic' laws and, in case of semi-empirical methods, empirical parameters are used in order to simplify calculus), *density functional methods* (electronic density calculus) and classical mechanics based methods (sub-atomic particles are not discriminated and, therefore, the atom is treated as a non-deformable spherical particle with a given radius (Van der Walls radius)).[57, 58]

1.4.1. Molecular Mechanics

The molecular systems simulations, with high number of atoms, by methods that consider subatomic particles, demand high computational capacity and can be potentially expensive due to the time required. Sometimes the computational resources and time

involved are too high. To bypass this problem, classic mechanics have been of great importance to study large dimension proteins.[56]

Molecular mechanics treats molecules as particles cluster (atom is the base unit of the system), with a given mass and bound together by coils, which allows the molecule to be study by classical mechanics laws (Newton's Laws). This way, allows the study of the movement upon a force action without observing the bonds break due to the applied force. The total energy of the system can be described through force fields parameterization.[58]

1.4.1.1. Force fields

A force field can be described as a mathematical function that permits to calculate the energy according to the position of the atom that constitute it, being necessary an ensemble of parameters that allows its application (due to the quantic character implied).[57]

The energy of the system is composed by independent terms that describe not only the molecular distortion (related to intramolecular bounds) but also interactions with the surrounding atoms (VDW and electrostatic energy) and even crossed terms.[57, 58]

$$E_t = E_{str} + E_{bend} + E_{tor} + E_{VDW} + E_{el} + E_{cross} \quad (1)$$

The mathematical function represents the different terms necessary to calculate the total energy of the system (E_t) being E_{str} the energy term that corresponds to the alteration in the atomic bond lengths, E_{ang} the energy term associated to the angle bond variations, E_{tor} the energy term for dihedral angle torsions, E_{VDW} and E_{el} the terms for the interactions of Van der Walls and electrostatics and, finally, E_{cross} referent to crossed terms.

1.4.1.1.1. Energy due to bond length alteration

The most accurate form to describe/calculate the energy associated with stretching or compression of the bond length is using the Morse potential function:

$$E_{Bond}^{Morse} = \frac{1}{2} D_0 \left[e^{-\alpha(l-l_{eq})} - 1 \right]^2 \quad (2)$$

Where D_0 corresponds to the minimum value that the Morse potential can have, α is $\alpha = \sqrt{\frac{K_{bond}}{2D_0}}$ (K_{bond} is the force constant that the system has at *equilibrium)*.

Although this is more accurate than using a Hook potential function (harmonic potential), especially when applied to very high distances between two atoms, it demands longer computational times then Hook's potential. Therefore Hook's potential is commonly used in many force fields to describe bond lengths:[57, 58]

$$E_{Bond}^{Hook} = \frac{1}{2} K_{bond} \left(l - l_{eq} \right)^2 \quad (3)$$

To be able to reduce the computational time using the Harmonic potential the system should have lengths close to *equilibrium* so that the two potentials have similar values.

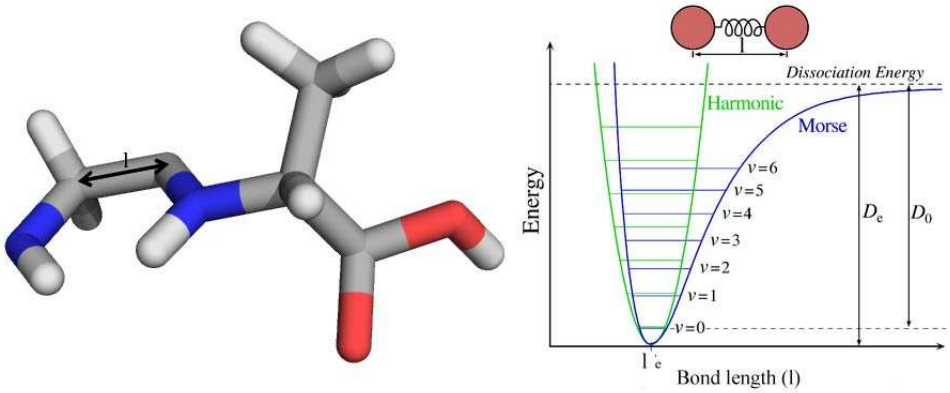

Figure 7: Graphical representation of the Energy variation in Harmonic and Morse Potentials in relation with bond lengths.

1.4.1.1.2. Energy due to bending

Like the previously described "bond length alteration" term, the energy related to the increase or decrease of an angle can be described with Harmonical potential with reasonable accuracy (it has limitations when there are multiple *equilibrium* values or when working with geometries that are very different compared to *equilibrium*).[57, 58]

$$E_\theta = \frac{1}{2}K_\theta(\theta - \theta_{eq})^2 \quad (4)$$

In this equation θ and θ_{eq} represent the angle between atoms and the angle at equilibrium and K_θ is the force constant associated with bending.

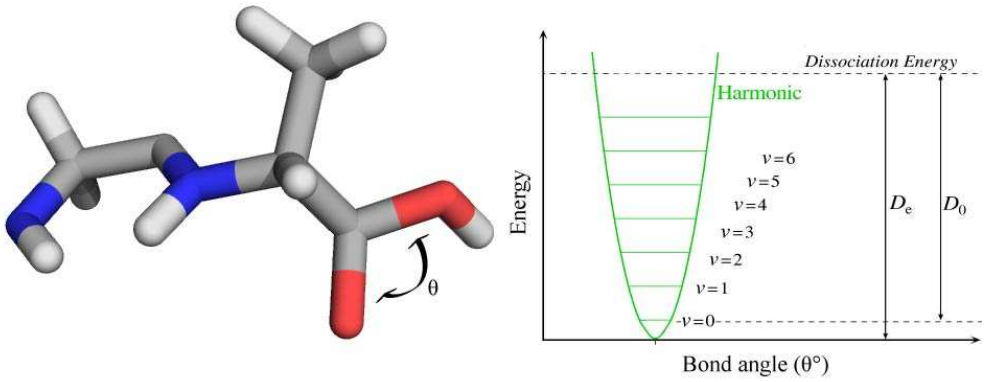

Figure 8: Graphical representation of the Energy variation in Harmonic Potential in relation to bond angles.

1.4.1.1.3. Energy due to torsion

Torsional energy can be obtained estimating the energy variation when a bond rotates. To perform this calculation the dihedral angle is analyzed. This angle varies within [0°, 360°] or [-180°, 180°]. Unlike E_θ and E_{Bond}^{Hook}, if θ rotates 360° energy returns to the original value.[57, 58]

A mathematical expression to calculate this energy can be:

$$E_\omega = \frac{1}{2}K_\omega[1 + \cos(n\omega - \gamma)]^2 \quad (5)$$

Where K_ω is the constant related to the minimum energy necessary to rotate a bond, ω is the dihedral angle, n represents the number of minimums that the function presets when rotated 360° (multiplicity) and γ represents where the angle has its minimum energy.

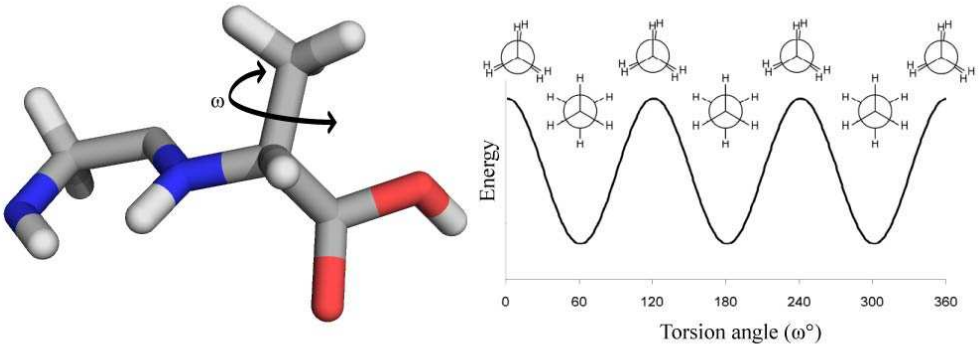

Figure 9: Graphical representation of the Energy variation in relation to bond torsion angles.

1.4.1.1.4. Van der Walls energy

Van der Walls energy describes the attraction or repulsion of nonbonded atoms and it's not taken into account by the electrostatic energy and therefore isn't affected by atoms charges.

Van der Walls force and the corresponding energy are inversely proportional to distance. The maximum value when the distance between to atoms equals the sum of the van der Waals radii and as the distance in between increases, Van der Walls force will tend towards 0. If the atoms are brought closer than distance for Van der Walls energy maximum value, a very repulsive interaction occurs because the electron cloud overlap.[57, 58]

The energy expression for these forces can be represented by the mathematical expression:[57]

$$E_{vdw}(i,j) = 4\varepsilon_{ij}\left[\left(\frac{\sigma_{ij}}{r_{ij}}\right)^{12} - \left(\frac{\sigma_{ij}}{r_{ij}}\right)^{6}\right] \qquad (6)$$

This equation represents the Lennard-Jones potential for a pair of atoms (i,j) and it has an attractive term, $-4\varepsilon_{ij}\left(\frac{\sigma_{ij}}{r_{ij}}\right)^{12}$ and a repulsive term $-4\varepsilon_{ij}\left(\frac{\sigma_{ij}}{r_{ij}}\right)^{6}$. $-4\varepsilon_{ij}$ corresponds to the minimum energy of the function for Lennard-Jones potential and r_{ij} is the sum of the Van der Walls radii.

1.4.1.1.5. Electrostatic energy

Electrostatic energy describes interactions of atoms that are not directly bonded that are a result of point charges. These interactions can be described with Coulomb's law mathematically represented by the equation:[57, 58]

$$E_{ele}(i,j) = k_e \frac{|q_i\, q_j|}{r^2} \qquad (7)$$

Where r is the distance between the atoms and $q_i\ q_j$ the point charges of the atoms. k_e is the Coulomb's constant (or the Coulomb force constant) and can also be represented by:

$$k_e = \frac{1}{4\pi\varepsilon} \qquad (8)$$

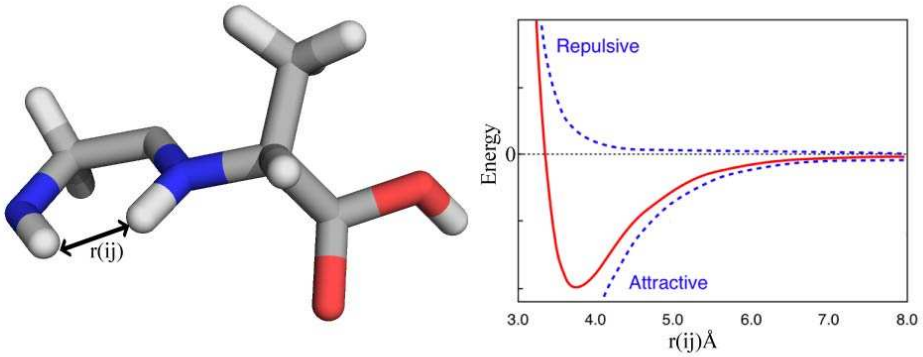

Figure 10: Graphical representation of the Energy variation due to VDW interactions (repulsive) and due to electrostatic interactions (Attractive).

1.4.1.1.6. Cross terms energy

With the inclusion of these terms in molecular mechanics force fields, it becomes possible to establish a correlation between different terms of the force field like bond length and bond angle, bond length and torsion, among others.[58] The downfall of adding this term is that it becomes much more computationally expensive.

1.4.1.2. Common force fields

When performing biological systems MD simulation, the most commonly used force fields are AMBER (Assisted Model Building with Energy Refinement), which is used mainly for proteins and nucleic acids, and CHARMM (Chemistry at HARvard Macromolecular Mechanics), which can be used in simulations of systems with variable size and complexity.[58-60]

Force fields that give parameters for all the atoms in the system (all atom type) were developed with the downside of being more time consuming. The mathematical function has been described by Case D. *et al*.[59], and is represented by equation 9:

$$U(\vec{R}) = \sum_{bonds} K_b (b - b_0)^2 + \sum_{angles} K_\theta (\theta - \theta_0)^2 + \sum_{dihedrals} \frac{V_n}{2}(1 + \cos(n\phi - \delta)) + \sum_{nonbond} \left[\frac{A_{ij}}{R_{ij}^{12}} - \frac{B_{ij}}{R_{ij}^{6}} + \frac{q_i q_j}{\varepsilon_1 R_{ij}} \right] \quad (9)$$

The terms that compose the mathematical function of AMBER force field have been described in section 1.4.1.1.

CHARMM is also a force field that gives parameters for all the atoms (all atom type). It has been described by Brooks C. *et al*.[60], and is represented by the equation 10:

$$U(\vec{R}) = \sum_{bonds} K_b (b - b_0)^2 + \sum_{UB} K_{UB} (S - S_0)^2 + \sum_{angles} K_\theta (\theta - \theta_0)^2 + \sum_{dihedrals} K_\chi (1 + \cos(n\chi - \delta)) + \sum_{impropers} K_{imp} (\varphi - \varphi_0)^2 + \sum_{nonbond} \varepsilon \left[\left(\frac{R_{\min_{ij}}}{r_{ij}} \right)^{12} - \left(\frac{R_{\min_{ij}}}{r_{ij}} \right)^{6} \right] + \frac{q_i q_j}{\varepsilon_1 r_{ij}} \quad (10)$$

1.4.2. Molecular Dynamics

Molecular dynamics (MD) have been applied for the past three decades to study macromolecules with biological interest. The first biomolecule of interest to be studied using MD was bovine pancreatic tripsyn inhibitor (BPTI). This publication had a major role to the evolution of the general understanding of protein structure. As up to 1975, proteins were seen as rigid body structures.[61] Nonetheless, it was initially described in 1959 by Alder and in 1964 by Rahman.[61-63] These methods calculate, with detail, individual motions of particles as a function of time and can be used to address some questions about a system such as investigating the structure, thermodynamic proprieties and others.[64] Some structural motions investigated by MD are local motions: atomic fluctuations, up to large scale motions like dissociation/association of subunits.

Given the complexity of the systems with biological interest it becomes clear that the evolution of the computational methodologies was made alongside the evolution of computers and other related hardware. The increasing power of computers have led to a proportional increase in the complexity of the calculus inherent to MDs, allowing bigger molecules to be studied, more detailed studies and even complexes. There also some noticeable disadvantages: (i) the need to parameterize all the intervenient species, (ii) not be able to study systems with breakage or formation of new bonds and (iii) not being as accurate as *ab initio* or DFT

Molecular dynamics simulations allow the study of the macroscopic properties of a system (state functions), generating information at a microscopic level (atoms positions and velocities). Examples of state functions used to characterize the macrostate of the system are volume (V), number of particles (N), pressure (P), temperature (T) and others.[65]

In order to define the thermodynamic state of a system, α+2 state functions need to be specified, where α is the number of components of the system. All the remaining proprieties can be calculated through the thermodynamic fundamental laws.

To any macrostate corresponds an infinite number of microstates therefore the ensemble of microstates of the system will have the same value for α+2 state functions (an

ensemble has different microscopic characteristics but similar macroscopic thermodynamic state).[65]

Table 7: Constant state functions in the most common ensembles

Ensemble	Constant state functions
Microcanonical ensemble (**NVE**)	number of atoms, **N**, volume, **V**, energy, **E**
Canonical Ensemble (**NVT**)	number of atoms, **N**, volume, **V**, temperature, **T**
Isobaric-Isothermal Ensemble (**NPT**)	number of atoms, **N**, pressure, **P**, temperature, **T**
Grand canonical Ensemble (**mVT**)	chemical potential, **m**, volume, **V**, temperature, **T**

Molecular dynamic simulations generate successive microstates (trajectory) solving algorithms based on Newton's second law or equation of motion, which allows the calculation of the trajectory for all the particles of the system.

$$\vec{a}(t_0) = \frac{\vec{F_i}(t_0)}{m_i} \qquad (11)$$

The position of a particle can be obtained for $t_0 + \Delta t$ solving equation 12:

$$\vec{r}(t_0 + \Delta t) = \vec{r}(t_0) + \vec{v}(t_0).\Delta t + \frac{\vec{a_i}(t_0)}{2}.\Delta t^2 \qquad (12)$$

The velocity of a particle can be estimated for $t_0 + \Delta t$ solving equation 13:

$$\vec{v}(t_0 + \Delta t) = \vec{v}(t_0) + \vec{a_i}(t_0).\Delta t \qquad (13)$$

Where $\vec{r}$ is the initial position of the particle, $\vec{v}$ is the velocity and Δt is the time step. Δt must be small enough so that the force that is applied to the particle remains the same from t_0 to $t_0 + \Delta t$ – the force that acts on a particle is dependent of all the particles position surrounding the first so during Δt changes on the position of surrounding particles should be small enough that the force remains constant.

With the wide variety of subjects that can be studied using MD it becomes clear that the time of simulation and time step are two critical aspects of the simulation. It should be chosen accordingly to the type of system and movement to be investigated.

Choosing the right time step becomes critical. If it is too small the computational cost will be too high, and if it is not small enough the inaccuracy of the integration of the motion equations will increase.

A common method to define the integration step is to choose one that is one order smaller than the time associated with the fastest movement in the system (in biomolecular systems this is usually the time scale for bond-stretching of bonds with hydrogen atoms – 10fs). These high frequency movements are rarely relevant and an integration step this small would make the simulation more expensive. A common solution to this problem is to restrain hydrogen bonds to their *equilibrium* length, allowing a longer integration step to be used (2fs instead of 1fs). A popular method to make constrains is to use the SHAKE algorithm. [66]

Another important aspect when performing MD simulations is the temperature. The equations used with this methodology are conservative so it is usually necessary to maintain the temperature of the system constant – a thermostat is applied.[67]

Different types of thermostats were developed being the most common Nosé-Hoover[68], Berendsen[69] and Langevin thermostats[70, 71].

When a thermostat is applied, the integration of the motion equations will take into account the friction coefficient, χ, as an additional acceleration, either positive or negative, for all the particles in the system.[67]

The additional acceleration is obtained by:

$$\chi(t).\vec{v}(t) \qquad (14)$$

where $\chi(t)$ is calculated with the differential equation:

$$\frac{d\chi(t)}{dt} = \frac{1}{\tau_T^2}\left(\frac{\tau}{T_{ext}} - 1\right) \qquad (15)$$

Where τ_T^2 is the temporal constant, τ is the initial temperature and T_{ext} the temperature to which the system converges.

1.4.2.1. Periodic boundary conditions

In the MD simulations, systems under simulation have an atom count within the thousands which are contained in simulation cell. Simulation cells can be cubic, octahedral or parallelepiped and can also present other shapes, although less used, because of the additional complexity that those would cause.

With this type of approach to the simulation the problem of surface effects arises. Particles close to the walls of the simulation cell are subject to a different set of interactions when compared to those in the center of the cell.

One way to overcome this problem is creating periodic boundary conditions. By doing so, it is considered that the simulation cell is the central cell of a network made with an infinite number of its replicas. The motion equations are numerically solved only for the particles in the central cell and the particles in the replica cells will mimetize the motions of the first particles- image particles.

The calculation of the intermolecular interactions has to be an approximation because they can only be calculated for a finite number of particles. To perform this calculus there are two methods: the minimum image or the spherical cut methods. Both have as base principle to ignore interactions above a certain interatomic distance.

When using the minimum image method, it is centered on each atom a cell with same size and shape as the simulation cell and if the spherical cut method is applied it is centered on each atom a sphere with pre-determined radii. All the atoms within this "atom-centered" cells are taken into account for the calculus of the intermolecular interactions and all the remaining are excluded. It is of great importance to choose a cut-off radii or cell dimension large enough so that the atom that is defined as the center to have low energy interactions with its images. Otherwise, non-physical effects might result from these methods. When working with a system having as its components a protein and explicit water, the size of the simulation cell shall be, at least, the size of the protein plus twice the cut-off length that is considered for the calculus the interactions.

Intermolecular interactions can be separated in short or long range interactions. The first are usually described by Lennard-Jones terms and the latter by Coulomb potential. To calculate the interaction energy a cut-of-radii needs to be chosen, which is not a problem for short range interactions because for a computational acceptable radii the interaction energy is very low. Therefore does not affect the final result (a corrective term is added to compensate the energy not taken into account for the calculus). Unlike these, Columbic interactions would need a large cut-off radii in order to make the remaining interactions despicable. If it is set to a distance that is too short it will produce considerable distortions.

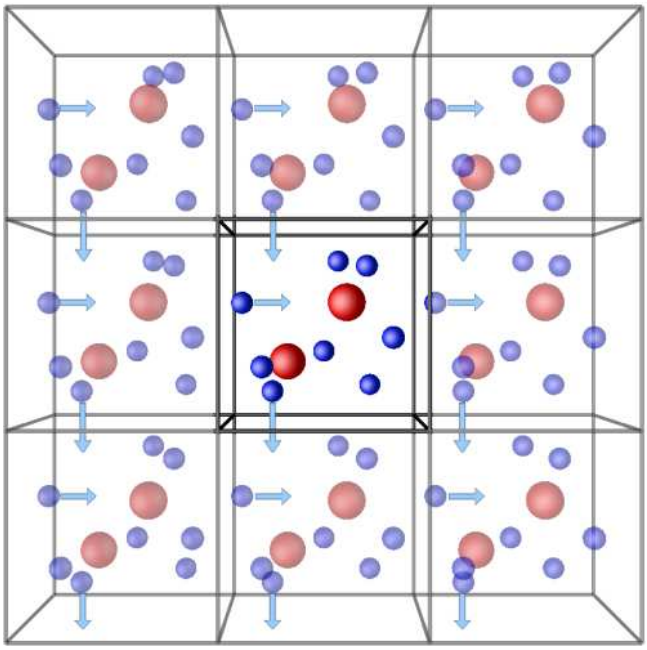

Figure 11: Schematic representation of the Periodic Boundary Conditions. In the center is the simulation cell, surrounded by replica cells that reproduce the movement of the particles in the center cell.

1.4.2.2. Particle Mesh-Ewald method (PME)

The Particle Mesh-Ewald method[72] was developed by theoretical physics, which had as foundation for their work the Ewald summation[73], before computers were used. However, it started to be widely used with the development of technology and with it computers, allowing the simulation of systems with electrostatic interactions. PME method introduces two changes in the system.[73] The first, every punctual charge is neutralized, at long distances, with the addition of a spherical charge cloud equal in magnitude to the point charge with density given by a Gaussian function centered on the

point charge. After this, the interactions of the system can be treated as discussed previously – simple cut-off. The second change consists on canceling the effect of the introduction of the first charges adding a second set of opposite Gaussian charges (counter-ions).[74, 75] The potential caused by the charges added can be obtained with Poisson equation and calculated a Fourier series.

After the calculation of the Ewald summation it is necessary to subtract the energy of self-interaction. This constant can be calculated.

1.4.3. Molecular docking

With the development of new techniques that allowed to obtain macromolecules 3D structures (like crystallography techniques, for example), the number of macromolecules of interest with known crystallographic structures has been increasing (in the order of tens of thousands in the RCSB-PDB).[16] Despite all the advances in this type of techniques, to crystalize protein – protein and protein – ligand complexes is still slow and expensive. To overcome this problem, some methods as molecular docking were developed. In molecular docking the goal is to understand and predict the association of from a structural and energetic point of view.

According to the study object, the methodologies may vary and its choice may influence considerably the outcome of the study in question. The critical steps to take into account in these methodologies are the choice of the flexibility of the molecules, the searching and scoring function algorithm. In molecular docking is possible to divide methodologies in protein – protein or protein – ligand docking.

1.4.3.1. Protein – protein

In this type of methodology the goal is to predict the structure of a 2 proteins complex (the structure of both exists previously) by complementarity of shape, charge or energy between them.

1.4.3.2. Protein – ligand

This methodology tries to predict most favorable configuration of the ligand (small molecule) when bounded to the protein and to evaluate this bound intensity. This method allows the evaluation of several of the orientations of the ligand as well as their different conformations (it is possible to analyze all the degrees of freedom of the ligand). The different complexes obtained in this type of docking are evaluated according to the orientation and conformation of the ligand, bounds energy and, in some cases, bound spot (active centers of already studied enzymes).

1.4.3.3. Docking algorithms

1.4.3.3.1. Searching algorithms

Despite apparent sensibility in docking methodologies, it is necessary to consider important aspects in this type of work. In a molecular docking methodology between macromolecules and ligands the complexity is very high due to the degrees of freedom present in the two molecules, which leads to high computational resources necessity. All the software's initiate by a looking of the best fitted pose for the complex under study: the searching part.

1.4.3.3.1.1. Rigid algorithms

By using rigid algorithms, both molecules (receptor and ligand) will be treated as rigid. Consequentially, the docking process will be very quick compared to the docking if both structures were treated as flexible. With the development of technology, the calculus speed increased considerably allowing this type of algorithm to be progressively replaced by others that treat the ligand, and sometimes also the receptor, as flexible. This preference is due to the fact that, by limiting the molecules freedom degrees, it is also blocked the opportunity to find the most appropriated conformation.[76-78]

1.4.3.3.1.2. Semi – flexible algorithms

In this type of algorithm the receptor is considered rigid but the ligand is now treated as a flexible molecule. There are two distinct methods that consider the ligand as flexible: the systematic method and the random method.

1.4.3.3.1.2.1. Systematic method

Algorithms of systematic search try to use all the degrees of freedom of the molecule. This can be divided in search methods of:[79]

Conformation – all the bounds that may suffer rotation twirl 360° to form all ligand's possible combinations of the ligands, which results in accentuated increase the number of combinations.

Fragmentation – initial docking may come from ligands fragments in the active spot followed by covalent bond between fragments or may be done with the rigid part of the ligand with posterior addition of the flexible zones.

Data base – libraries with already generated conformations are used to count all possible conformations due to the flexibility of the ligand.[80]

1.4.3.3.1.2.2. Random methods

In random methods the structure of the protein where the docking is made is submitted to random variations of the conformation of the ligand being the final result accepted or not. There are 3 types of algorithms for this method:[79]

Monte Carlo – based on an energy function, not needing additional information.[81]

Genetic Algorithm (GA) – application of algorithms based on natural selection and genetic concepts in docking. This method has an initial population, unlike other methods, composed by several conformations of the ligand towards the protein. This allows the possibility to explore different regions of the search space leading to enhanced performance. [82]

One of the great advantages using this type of algorithm is that it allows a comprehensive design of the algorithm taking into account the type of problem to be solved, which is why this type of algorithms can be used for a variety of problems and not only docking. This can be done with the definition of some essential components and procedures.

Genetic algorithms will encode the input parameters into solutions or strings where each string represents a chromosome (candidate solution in initial population). To select the better candidates to lead to next generation a fitness function is applied, measuring the quality of the candidate solutions. The fitness function to be applied can vary. It can be obtained with a mathematical function or a more complex computer simulation. It is also possible to select the best candidates from the initial population with a more subjective evaluation.

To further evolve the obtained individuals a series of genetic operations can take place (crossover and mutation) and also in this step there is several possibilities to adjust the genetic operators to better suit the problem to be solved (type of crossover and mutations).

Although genetic algorithms can vary greatly a general procedure can be appointed:

Step 1. Origin – Generate the initial population (P_0)

Step 2. Fitness Evaluation and Selection – Selection of the best individuals (P_1) from P_0

Step 3. Crossover – Apply crossover to population P_1 to generate a offsring O_0

Step 4. Mutation – Mutate O_0 to obtain O_1

Step 5. Replacement – Replace P_0 with O_1

Step 6. Termination – Select final population/solutions

Tabu search – with this method the docking process is stopped in already studied receptor areas promoting, this way, new docking regions.

1.4.3.3.1.3. Flexible algorithms

This type of algorithm is used when the receptor's flexibility (by increase to the ligand) cannot be rejected. Some systems may suffer alteration in their structure after the ligand bonding such as near side chains rearrangement.

To make this kind of methods more viable from a programing point of view, the molecule target's partial flexibility is considered. In this type of methodology it can be use molecular dynamics and Monte Carlo methods (a more powerful but not so used technique due to the amount of time required), rotamers libraries, protein grids and flexible receptor modulation.

1.4.3.3.2. Scoring functions

This type of functions allows the evaluation and classification of ligand conformations and the differentiation of molecules that bound to the target molecule or not.[79] A scoring function that would allow the proper evaluation of all bond aspects would be very demanding from a programing point of view. For that reason some simplifications are made in order to reduce its complexity.[83] Scoring functions can be divided into three categories: based on force fields, of empirical bases or based on knowledge:

1.4.3.3.2.1. Based on force fields

These functions are based on the application of force fields that quantify the energy's interaction between receptor and ligand and the ligand's internal energy. For this quantification VDW and electrostatic energy are considered.[83, 84]

1.4.3.3.2.2. Based on empirical data

This type of function is created to reproduce experimental data and is based on the possibility of bond energies being able to be obtained, approximately, by the sum of some unrelated individual terms.[83]

1.4.3.3.2.3. Based on knowledge

In this case general principles and rules are followed so that certain structures obtained experimentally are reproduced. These methods are based on atom-atom interaction potentials that are defined by the frequency of different atom-atom interactions observed on known data base of complexes protein – ligand structure.[79]

This type of scoring functions, although fast, either neglect solvation or approximate the effect from solvation with relative simple models (e.g. empirically derived group additive desolvation parameters).

In recent years, there have been reports on a number of methods that use explicit water molecules in the system, to calculate solvent-dependent energies more accurately. Thermodynamic integration (TI), Free Energy Perturbation (FEP) and Grand Canonical Monte Carlo (GCMC) are very accurate and rigorous methods but also extremely time consuming (great statistical sampling must be carried out) which prevents their use in docking algorithms.[85]

Scoring functions based on continuum solvent models offer a good compromise between using explicit water molecules and neglect the contribution of interactions with solvent. All atom methods have been developed using continuum solvent namely MM-PBSA and MM-GBSA. These methods treat the solvent as a high dielectric continuum field which enables the approximation of the energies of desolvation to move charged atoms into and out of the dielectric field of the protein and ligand in a time efficient manner.[85]

1.4.4. Autodock

Autodock is free use software for noncommercial purposes and is particularly effective in protein – ligand docking.[86] It is one of the most quoted software by the scientific community and is currently used on the *FightAIDS@Home* (Olson Laboratory). This software is composed by two main programs:

AutoGrid: allows the calculation of the grids that describe the target protein

AutoDock: effects the ligand docking with pre-calculated grids assembly

In the AutoGrid the protein is placed in a three dimensional grid and, in each grid point is placed a probe that corresponds to each atom found in the ligand. The dispersion/repulsion energies, and when necessary also energies associated with hydrogen bridges, are calculated all the atoms the atoms of the receptor until 8Å of each grid point.[86] The resulting data are saved in grid files, separately. The AutoDock uses a semi-empirical force field to calculate the associated energies to the protein(P) – ligand(L) bond. The bonding free energy is estimated in two steps: first the two molecules' transition between their conformation when bonded and not bonded is energetically evaluated, and secondly the intermolecular energies associated with the complex formation process is evaluated – equation 16. It is also estimated the entropy variation associated to this process ($\Delta Sconf$).[87]

$$\Delta G = \left(V^{L-L}_{ligado} - V^{L-L}_{não\ ligado}\right) + \left(V^{P-P}_{ligado} - V^{P-P}_{não\ ligado}\right) + \left(V^{P-L}_{ligado} - V^{P-L}_{não\ ligado} + \Delta Sconf\right) \quad (16)$$

1.4.5. Free energy calculations

Free energy is a thermodynamic value that allows the understanding of how biochemical molecules associate and react.[88] It is usually expressed as Helmholtz function (F) or Gibbs function (G). These two functions are applied for different ensembles where Helmholtz function is used for NVT and Gibbs function is more suited for NPT ensembles.

In order to obtain a good estimation of absolute free energy all the possible states for the system should be sampled, which is not viable due to the amount of calculus. Instead, the difference of free energy between two states is calculated and in result we have the probability of finding one of them and not the other.

For the past decades, several methodologies have been developed to calculate free energy using MD. These methods allow us to predict protein stability, drug affinity to a target, among other aspects. Among these methods are TI, FEP and MM-PBSA and the

choice will take in consideration several factors (i.e. time). TI and FEP are the most rigorous but demand long simulation times.[89] In these methods a gradual transformation between two states of interest occurs. Although MM-PBSA is less rigorous it is the most often used as it is less time consuming. In any of these methods it is necessary to carefully choose time of simulation, force field, among others because these will affect the accuracy of the calculus.

1.4.5.1. Molecular Mechanics/Poisson-Boltzman Surface Area

In MM-PBSA the MD trajectory is analyzed and a continuous solvent model is used.[90, 91] Free energy is calculated using equation 17:

$$G = E_{MM} + G_{PBSA} - TS_{MM} \quad (17)$$

E_{MM} is the energy from molecular mechanics (includes all the parameters discussed previously for molecular mechanics), G_{PBSA} is the solvation free energy estimated by the numerical resolution of Poisson Boltzamn equation. PB equation describes the electrostatic interaction between molecules in ionic solutions and is often used in MD and related fields because it can be used to approximate the effects of solvent on structures of biomolecules – implicit solvent.[90] PB equation can be represented as in equation 18:

$$-4\pi\rho(r) = \nabla\varepsilon(r)\nabla\phi(r) - k'(r) \quad (18)$$

Where $\phi(r)$ is the electrostatic potential, ε(r) is the dielectric constant, ρ(r) the charge desnsity and k' is the inverse of the Debye-Huckel lengh.

G_{PBSA} and E_{MM} are obtained by calculating the average of several geometries from the MD simulation. $-TS_{MM}$ refers to the solute entropy and often is not taken into account because it is considered to have the same value for molecules with similar dimensions.

Delphi is a software that calculates electrostatic potential and energies in systems of biomolecules by numerically solving the Poisson-Boltzman equation. In this software the first step is to overlap a cubic shaped grill to both solvent and solute. Values for electrostatic potential, charge density, dielectric constant and ionic force are calculated

for each point of the grill. Because atomic charges usually are not coincident with the grill points, this is allotted to the nearest eight points.

The boundary between solute and solvent is defined by the molecular surface and all the grill points that are placed out of it have dielectric values and ionic force assigned of the solvent. The points within the grill have dielectric constant for solute assigned.

After this, Poisson-Boltzman equation is solved for each grill point until convergence is achieved.

The calculus of the electrostatic component of the free solvation energy is obtained when a solute is transferred from a low dielectric constant to a high dielectric constant condition causing a variation is electrostatic energy. This can be obtained through the resolution of equation 19:[91]

$$\Delta G_{PB} = \frac{1}{2}\sum q_i(\phi_i^4 - \phi_i^1) \qquad (19)$$

In this equation "q" represents punctual charges of the solute.

The non-electrostatic contributions for free solvation energy have greater importance when working with non-charged or low polarity solutes and are obtained with the equation 20:

$$\Delta G_{np} = \gamma A + b \qquad (20)$$

Where A is the solvent accessible area and γ and b are constants obtained from experimental data – γ is 0,00542 kcal $Å^{-2}$ mol^{-1} and b 0,92 kcal mol^{-1},

1.4.5.2. Protein-Ligand binding affinity

To calculate ligand binding affinity, it is necessary to calculate energies for complex, receptor and ligand for the structures that were obtained from the MD simulation In continuum solvent. This calculus follows the equation:[92]

$$\Delta G_{molecule} = \left(G_{complex}\right) - \left(G_{receptor}\right) - \left(G_{ligand}\right) \qquad (21)$$

Where $\Delta G_{molecule}$ corresponds to the binding free energy and the other terms are the energy associated with the complex, receptor and ligand.

Internal energy, electrostatic energy and Van der Walls energy are obtained using the force field. The external dielectric constant is solvent-dependent but the internal dielectric constant cannot be assigned universally because any protein is highly complex. Therefore, each case should be analyzed carefully and this constant should be adjust for the specific system being studied.

1.4.6. Protein-ligand interface

One important field of molecular biology is the discovery and understanding of all interactions between molecules especially those with highly relevant biologic role.

Protein-ligand interfaces are of noticeable relevance when studying enzymes given the relevance of this type of proteins for many biological mechanisms which include disease related mechanism such as drug-target interaction or drug resistance mechanism.

Protein-ligand interfaces are usually very complex and have a high number of residues but only a few participate in the protein-ligand interaction.[93] It becomes clear that the study of these interfaces becomes necessary to the better understanding of the structural and energetic features of interfacial residues. More knowledge on this field can help to understand the biologic role and activity of the protein and/or ligand under study.

The forces that influence the formation and stabilization of these complexes (protein-ligand) can vary due to the structure of the ligand itself and the type of aminoacid residues that form the interface and even others that at a first glance might look of less relevance. The residues in the interface can interact with the ligand via hydrophobic interactions, hydrogen bonds, salt bridges, electrostatic forces and VDW forces and π-interactions. Covalent bonds tend to be minor contributors to molecular recognition and if present they are often irreversible due to the bond strength. [94, 95]

Most interfaces have a high number of conserved residues and form a high complementary pocket, in shape and hydrophobicity and hidrophilicity regions between protein and ligand.[96]

The type of aminoacid residue becomes clearly relevant to the interactions in the interface but is important to refer that the nature of the ligand as also high impact on the interface (different ligands having similar M.W. and general structure might behave in a different manner due to the existence or not of double or triple bonds and different position of polar atoms).[94]

1.4.7. Alanine Scanning Mutagenesis (ASM)

Although protein-ligand interfaces are large and complex they can all be characterized by size, shape and complementary and single residues can be appointed as being responsible for the majority contribution for binding energy – Hot-Spots (HS).[92, 97]

To define HS of the interface ASM can be performed in two different approaches: computational analyses or a more practical analysis. The practical approach can be performed to provide empirical data but it has major disadvantages associated with not only the time necessary to perform the experiment but also the high cost inherent to this. Unlike the computational method where, in general, there is only the need to mutate *in silico* the residue to be studied, removing the side-chain past the β-carbon and have a single MD simulation, doing this in bench work involves mutation of the gene of interest, expression of the protein, isolation and sometimes refolding. These methods are all cost and time consuming and are prone to practical complications that can arise.

Thus, ASM can infer the role of the side-chain and the energetic contributions for binding energy. To analyze the contribution of each side chain binding free energy is estimated as in equation 22:4

$$\Delta\Delta G_{binding} = \Delta G_{binding-mutant} - \Delta G_{binding-wild\ type} \quad (22)$$

When after the alanine mutation cause an increase of binding free energy of 2kcal/mol or more, that given residue is considered an HS and when the increase reaches 4kcal/mol or higher, the residue has a major role in binding. However these are unusual.[98] Glycine could also be used but would introduce flexibility in the protein backbone.[94] The problem with this methodology is that the contribution of the residues backbone cannot be studied in this manner, which might lead to erroneous results since the contributions that

it has for the interface is, in average, one fifth of the interface area and it contributes with almost two thirds of the hydrogen bonds.[99]

Systematic analyses of hotspots have shown that they have a distinctive aminoacid composition – tyrosine (12.3%), tryptophan (21.0%), arginine (13.3%) and are usually conserved residues.[95, 98, 100] Aromatic residues clearly have high incidence as HS as they can contribute with cation-π interactions, having a large hydrophobic surface and capability to form H-bonds. Arginine can form up to 5 H-bonds and a salt bridge (guanidinium group is positively charged).[94, 101]

Systematic studies of HS have shown propensity for HS to be inaccessible to the solvent, shielded by other residues in an O-ring structure.[95] This lead to the O-ring theory, which states that residue with high impact on binding free energy are protected from bulk solvent.

When performing the mutation for alanine the effect of the side chain removal over the orientation of surrounding residues is not treated explicitly in the single trajectory. To overcome this downfall, it is mimicked by the internal dielectric constant that increases with the polarity of the mutated residues. It allows for a better prediction of HS when charged residues and highly polar residues are involved. Previously, the relative binding free energy calculated for charged residues was an important limitation to ASM.[92] It was demonstrated that instead of a single dielectric constant, different dielectric constants should be used to obtain a good accuracy: 2 for non-polar residues, 3 for polar residues and 4 for charged residues. Although these constants have led to great results, adjustments might be needed due to the extreme complexity and variation between protein interfaces.[92]

1.5. Objectives

1.5.1. Computational studies

In this work the aim was to characterize two TEM variants (TEM-180 and TEM201) both structurally and in terms of their activity against antibiotics. Since no 3D structure is available, they were constructed by *in silico* mutation of TEM-1 structure. To analyze their activity against antibiotics Molecular Docking was performed and complexes structures analyzed. To accomplish these objectives more specific objectives were appointed:

a) Verify which are the mutations present in the proteins of interest (variants TEM-201 and TEM-180) by alignment with the wild-type protein (TEM-1)
b) Construct the enzymes TEM-201 and TEM-180 by *in sillico mutation* of TEM-1
c) Verify if there are any differences in the conformation of important residues in the catalytic process of the enzymes
d) Perform molecular docking for the wild-type protein, TEM-201 and TEM-180 with a data base with different antibiotics
e) Justify any alterations in the hydrolysis ability of different ligands based on the determined structural and energetic characteristics of the different complexes

1.5.2. Experimental studies

To characterize the biologic activity of TEM-180 and TEM-201 clones, producing these enzymes, were subjected to growth with several antibiotics. In order to achieve this, a series of specific objectives were appointed:

a) Synthetize high expression vectors with the sequences of TEM-201 and TEM-180
b) Clone *E. coli* 25922 with the synthetized vector
c) Test biological resistance of the cloned *E. coli* against several antibiotics
d) Compare results obtained in the different methodologies concerning the antibiotics bonds

Chapter II - Methodology

2. Theoretical Methods

2.1. Structure preparation

To determine the mutations of the TEM variants an alignment of the sequences of TEM-180, TEM-201 and TEM-1 was performed using ClustalW.[102] TEM-180 has the mutations: I84V, V184A, M272T and D273E, and TEM-201 has the mutations: L30V, I84V, V184A and S268G.

The structures of the TEM variants (TEM-180 and 201) were obtained by *in silico* mutations of TEM-1 (PDB ID: 1ZG4[16]) and protonation states were assigned using Schrödinger Software, LLC[103].

2.2. Molecular Dynamics simulation

The protein structures obtained in the previous step were was stabilized and refined by MD simulation with the modified Cornell force field, by Duan *et al.* – ff03.[104, 105] The MD simulation was carried out in explicit solvent with the TIP3P[106] water model using the AMBER9 program[59], First, the water was equilibrated in the presence of the fixed complex (25 ps), then only the side chains were relaxed (200 ps) - minimization, and finally a production run of 16 ns was done for the system. During the initial 2 ns of the production run temperature was increased from 0 to 300K (ensemble NVT) followed by 14 ns of production at constant 300K (ensemble NPT). In the restrained simulations, the atoms were subjected to a harmonic restraining force of 10 kJ $mol^{-1}.nm^{-2}$. In all MD simulations, the bond lengths involving hydrogens were constrained using the SHAKE algorithm[66], the equations of motion were integrated with a 2 fs time step, and the Langevin algorithm[70, 71] was used to regulate the temperature of the system. All of the crystallographic waters were removed from the structure subjected to the MD simulation. Periodic boundary conditions were applied using PME[72, 73] to treat long-range electrostatic interactions, and counter-ions were added to keep the whole system neutral. We used a 10-Å separation between each edge of the box and the closest solute atom to minimize electrostatic interactions between periodic images of the solute. We calculated Root-Mean-Square-Deviation (RMSD) profiles using the average structure as reference. For each of the last 6 nanosecond of the MD simulation, the structure with lowest RMSD was selected for the following procedures.

2.3. Molecular Docking

Protein-ligand docking was performed using the six microstates ensemble from the protein MD simulation as targets and several antibiotics: Penams or penicillins (Amoxicillin, Ampicillin, Benzylpenicillin or Penicillin G, Phenoxymethylpenicillin or Penicillin V, Cloxacillin and Methicillin), Carbapenems (Imipenem and Meropenem), Cephems or Cephalosporins (Cefoxitine, Cefotaxime, Cepholosporin C and Cefpirome) and β-lactamase inhibitors (Clavulanic acid, Sulbactam and Tazobatcam) selected, according to their clinical relevance. Their structures were obtained from PubChem Compound.[107] The AutoDock 4.2 package[86] was used for the entire docking procedure. An energy grid of 46 Å × 40 Å × 40 Å in dimension, with a 0.375-Å grid spacing (the center of the Grid Box and dimension were previously tested) were generated with the program AutoGrid. Gasteiger charges were assigned to the ligand atoms. AutoDock 4 was used to evaluate ligand-binding energies over the conformational search space using the Genetic Algorithm-local search method. Default docking parameters were used with the following exceptions: ga-pop-size, 200; ga-num-evals, 10,000,000; and ga-run, 50. The structural poses that resulted from the docking were analyzed taking into account several parameters: (i) the binding energy should be negative; (ii) the complexes should have either low energy and form clusters with a higher number of complexes; (iii) the β-lactam ring should be on the more internal part of the catalytic pocket and, if possible, facing the catalytic Ser70; and (iv) the complexes should have a high number of interactions (protein-ligand). To this purpose interaction maps of the complexes were made for the various solutions with the LIGPLOT package[108].

2.4. Molecular Dynamics simulation of protein-ligand complexes

The final complexes obtained from molecular docking were stabilized and refined with MD simulations following the procedure described in section 2.2.

To obtain the parameters for the different ligands, partial atomic charges were derived with standard HF/6–31G* RESP[109] methodology using the program Antechamber

implemented in the Amber package[59]. Atom types and missing force-field parameters of the ligands were assigned from with GAFF force field.[110]

2.5. Structural analysis

RMSDs and Root-Mean-Square-Fluctuations (RMSFs) of the protein backbone and the various ligands were calculated for all the MD simulations in order to investigate their stability. For a detail study of the binding interface, significant residues were selected: Met69, Ser70, Lys73, Tyr105, Ser130, Asn132, Glu166, Asn170, Val216, Lys234, Ser235, Glu239, Arg244 and Arg275. This selection took into account the literature[2, 11, 29] and the manual inspection of the binding site to ensure that crucial residues were selected. For these residues, RMSF and B-factors were calculated to investigate the deviation of these compared to a reference position. The environment around the same residues was carefully characterized. For this step, all residues and water molecules within 5 Å of each interfacial residue were selected and their occupancy was estimated. We have also analyzed the radial distribution function, g(r) or RDF, as well as, the average number of waters within a given distance, of all interfacial residues. G(r) gives the probability of finding an atom at distance r from another atom, in relation to the probability expected for a bulk solvent distribution at the same density. It was calculated by compiling a histogram with a spacing of 0.02 and a range of 8 Å. These two procedures, as well as, the visual inspection of the MD simulations were performed with the VMD package and tailor-made scripts.[111] Crucial inter-atomic distances for the enzyme catalytic activity and enzymatic inhibition were measured for all the MD simulations. All structural representations were made by the PYMOL package[112].

2.6. Energetic profile

The MM-PBSA (Molecular Mechanics Poisson Boltzmann Surface Area) script[113] integrated into the AMBER9 package[114] was used to calculate the binding free energy difference upon alanine mutation. The alanine mutations were performed on the interface residues that were previously selected in the structural analysis with the exception of alanine, glycine or proline residues. These were not mutated since have usually a primary role in

the protein stability and the mutation could lead to protein degradation. Due to the limitations of the method, residues that would only interact via backbone couldn't be analyzed with computational ASM. This method combines a continuum approach to model solvent interactions with a MM-based approach to atomistically model protein-protein interactions. It provides speed and accuracy and has been quite used in the last years[113, 115-128]. The MM-PBSA approach first developed by Massova *et al.*[113] was improved by Moreira *et al.*[119] and can now be applied with an accuracy of 1 kcal/mol. The mutant complexes are generated by a single truncation of the mutated side chain, replacing Cγ with a hydrogen atom and setting the Cβ-H direction to that of the former Cβ-Cγ. For the binding energy calculations, a total of 25 snapshots of the complexes were extracted in the last 1 ns of the run. The ΔΔG is defined as the difference between the mutant and wild type complexes defined as:

$$\Delta\Delta G = \Delta G_{cpx-mutant} - \Delta G_{cpx-wild\ type} \quad (23)$$

Typical contributions to the free energy include the internal energy (bond, dihedral, and angle), the electrostatic and the van der Waals interactions, the free energy of polar solvation, the free energy of nonpolar solvation, and the entropic contribution:

$$G_{molecule} = E_{internal} + E_{electrostatic} + E_{vdW} + G_{polar\ solvation} + G_{non-polar\ solvation} - TS \quad (24)$$

For the calculations of relative free energies between closely related complexes, it is assumed that the total entropic term in equation 2 is negligible as the partial contributions essentially cancel each other.[124] The first three terms of equation 2 were calculated with no cutoff. The $G_{polar\ solvation}$ was calculated by solving the Poisson-Boltzmann equation with the software DELPHI[129, 130]. In this continuum method, the protein is modeled as a dielectric continuum of low polarizability embedded in a dielectric medium of high polarizability. We used a set of values for the DELPHI parameters that proven in a previous study to constitute a good compromise between accuracy and computing speed[131]. We used a value of 2.5 grids/Å for scale (the reciprocal of the grid spacing); a value of 0.001 kT/c for the convergence criterion; a 90% for the fill of the grid box; and the coulombic method to set the potentials at the

boundaries of the finite-difference grid. The dielectric boundary was taken as the molecular surface defined by a 1.4 Å probe sphere and by spheres centered on each atom with radii taken from the Parse[132] vdW radii parameter set. The key aspect of the new improved approach is the use of a three dielectric constant set of values (ε=2 for nonpolar residues, ε=3 for polar residues and ε=4 for charged residues plus histidine) to mimic the expected rearrangement upon alanine mutation (the method is described at [117, 119]). It is important to highlight that we used only one trajectory for the computational energy analysis as it has been proven to give the best results[119] Side-chain reorientation was implicitly included in the formalism by raising the internal dielectric constant. The nonpolar contribution to the solvation free energy due to van der Waals interactions between the solute and the solvent was modeled as a term dependent of the solvent accessible surface area (SASA) of the molecule. It was estimated by 0.00542×SASA+0.92 using the molsurf program developed by Mike Connolly[133].

3. Experimental Methods

3.1. Molecular Genetic Techniques

3.1.1. Competent Cell preparation

a) Inoculate 50ml of OXOID medium with the *E. coli* strains *E. coli* DH5α and *E. coli* BL21, at 37°C.

b) Inoculate 200ml of OXOID medium previously warmed at 37°C with 2ml of the previous culture and incubate at 37°C with stirring, until OD_{600} between 0.2 and 0.375 is achieved.

c) Place the culture in pre-cooled tubes and put them in ice for 15min.

d) Centrifuge at 3000rpm for 15 minutes, at 4°C.

e) Elutriate the supernatant and ressuspend, slowly, the sediment in 20ml of pre-cooled 100mM $CaCl_2$ solution. Incubate in ice for 20 minutes

f) Centrifuge the cells in 0.5ml of 100mM $CaCl_{2\ solution,}$ at 4°C. Incubate in ice between for 24 hours for maximum transformation efficiency (efficiency increases in time, up to 24h. After that period cells rapidly lose their competency).

g) Add glycerol to the competent cells for a final concentration of 10% V/V and freeze the mixture at -70°C.

Transformation was performed with the synthetized plasmids, with the sequences of interest inserted.

The sequences inserted had the following structure:

CCATGG-GC-TEM sequence without termination codon TAA-CACCATCACCATCAC-TAA-CTCGAG

Sequences in orange are sequences detected by restriction enzymes (restriction sites), sequence in blue was used to keep the sequence for TEM enzymes in the correct open reading frame, the termination code was rejected from the sequence because we want a Tag on the produce protein (His Tag was chosen – sequence in red) and TAA is the termination code.

3.1.2. Bacterial Transformation

a) Unfreeze the competent bacteria in ice.
b) Put 5µl of plasmidic DNA solution in microtubules and keep them in ice.
c) Add 50µl of competent cells to each microtubule and use circular movements to mix them, with the tip of the pipette.
d) Incubate in ice for 20 minutes.
e) Put each microtubule in a bath at 37°C for 2 minutes – Thermic shock.
f) Place the microtubules in ice for 2 minutes.
g) Add 200µl of OXOID medium and incubate at 37°C with stir.
h) Plate 10µl of cells for each Petri plate.
i) Incubate the plates at 37°C over-night.

3.2. Microbiology Technics

3.2.1. Bacterial strains

Bacterial strains used in the present study included *E. coli* strain ATCC 25922 from American Tissue and Cell Culture, for antimicrobial susceptibility testing. Other strains of *E. coli* included *E. coli* DH5α and *E. coli* BL21 for cloning procedures.

3.2.2. Culture media and buffers

3.2.2.1. General transport and store media

3.2.2.1.1. Tryptic soy media

TSA and TSB are a basic media used for culturing many kinds of microorganisms. Tryptic soy agar is mainly used as an initial growth medium observation of colony morphology, developing a pure culture, achievement of sufficient growth for further biochemical testing, and culture storage (Finegold *et al*., 1978; MacFaddin, 1985).

A dehydrate commercial form of these media was used (CULTIMED) and the hydratation was made according manufacturer indications. The medium was confirmed for pH 7.3 prior to autoclaving for 15 min at 121 °C. Before plating the medium was cooled until 55 ºC.

3.2.2.1.2. SOC (Super Optimal Culture) medium

SOC medium was used in cloning procedures since it is referred to as a good medium for *E. coli* growing (Hanahan, 1983). This medium is composed by tryptone 20g, yeast extract 5 g and NaCl 0.5g. Then, when all solutes were dissolved in 950 mL of water, it was added 10 mL of 250 mM (1.86g/100 mL) of KCl and pH was adjusted to 7.0 with 0.5 M NaOH (~0.2 mL). The volume was adjusted up to 1 L. The medium was sterilized by autoclave at 121 ºC for 15 minutes. When the solution was cooled down to room temperature (RT) 20 mL of 1 M sterile glucose (18 g /100 mL and sterilize by passing through a 0.22 µL filter) were added. Just before use 5 mL of autoclaved 2M MgCl2 (19g of MgCl2 in 100 mL) were added (Sambrook & Russel, 2001).

3.2.2.1.3. Antibiotic susceptibility medium: Mueller-Hinton

Mueller-Hinton agar is recommended for the disk diffusion method of antibiotic susceptibility testing by FDA from WHO and CLSI for testing most commonly encountered aerobic and facultative anaerobic bacteria in food and clinical material. The medium shows good batch-to-batch reproducibility. It yields satisfactory growth of most non-fastidious pathogens. Beef infusion and casein provide nitrogenous compounds, vitamins, carbon, sulphur and amino acids in Mueller-Hinton media. Starch is added to absorb any toxic metabolites produced.

Mueller-Hinton medium was purchased as a dehydrate form (OXOID) and the hydratation was made according manufacturer suggestions. The medium was confirmed for pH 7.3 prior to autoclaving for 15 min at 121 °C. Before plating the medium was cooled until 55 ºC.

3.2.3. Antibiotics' stock solutions

3.2.3.1. Ampicillin

Ampicillin (APPLICHEM) stock solution was prepared to a final activity of 50 mg/mL on distilled water being further sterilized and aliquots were passed through a prerinsed 0.22 µm filter. Ampicillin aliquots were stored at -20 ºC.

3.2.4. Susceptibility methods

Antimicrobial susceptibility testing was performed by disc diffusion (Kirby-Bauer) method according to the CLSI guidelines, using as control E. coli strain ATCC 25922.

3.2.4.1. Kirby-Bauer Disc diffusion method

When a filter paper disc impregnated with a chemical is placed on agar the chemical will diffuse from the disc into the agar. This diffusion will dispense the chemical in the agar only around the disc. The solubility of the chemical and its molecular size will determine the size of the area of chemical infiltration around the disc. If an organism is placed on the agar it will not grow in the area around the disc if it is susceptible to the chemical. This area of no growth around the disc is known as a "zone of inhibition" (Joyce & Woods, 2004).

Many conditions can affect a disc diffusion susceptibility test. When performing these tests several parameters were held constant so only the size of the zone of inhibition is variable. Conditions that must be constant from test to test include the agar used, the amount of organism used, the concentration of chemical used, and incubation conditions such as time, temperature, and atmosphere (Pfaller & Jones 2006). The amount of organism used is standardized using a turbidity standard. This may be a visual approximation using a McFarland standard 0.5 or turbidity may be determined by using a spectrophotometer (optical density of 1.0 at 600 nm). For antibiotic susceptibility testing the antibiotic concentrations are predetermined and commercially available. Each test method has a prescribed media to be used and incubation at 35-37 ºC in ambient air for 18-24 hours (CLSI, 2003; CLSI, 2005).

The agar used was Mueller-Hinton (OXOID) agar. This method is well documented and standard zones of inhibition have been determined for susceptible and resistant values. Quality control strains E. coli ATCC 25922 were also used according CLSI guidelines. Discs purchased from OXOID that were used in the present study included APSM 30/10µg,

CXM 30µg, FOX 30µg, CTX 30µg, CAZ 30µg, IMI 10µg, GEN 30µg, CIP 5µg, SXT 25µg, CRO.30 µg, TZP 110 µg, AZM 15 µg, FD 10 µg, VA 30 µg, E 15 µg, TOB 10 µg, DA 2 µg, OX 1 µg, P 10 units, NOR 10 µg, LEV 5 µg, MXF 5 µg, N 300 µg, CLR 15 µg, CEC 30 µg, TEC 30 µg, MUP 5 µg, RD 5 µg and LZD 30 µg.

Chapter III – Results &Discussion

4. Theoretical results and discussion

4.1. Docking protein-ligand

4.1.1. Enzymatic ensemble

To inquire the stability of the docking complexes through the MD simulation, the RMSD was calculated for the protein backbone and for the ligand (C, N, O and S atoms were all selected). The RMSD presented in Figure 12, shows that the MD simulations are very stable (RMSD lower than 2Å). It can be seen that the variance along the MD simulation never surpasses 0.6Å. Therefore, the proteins backbone is very stable.

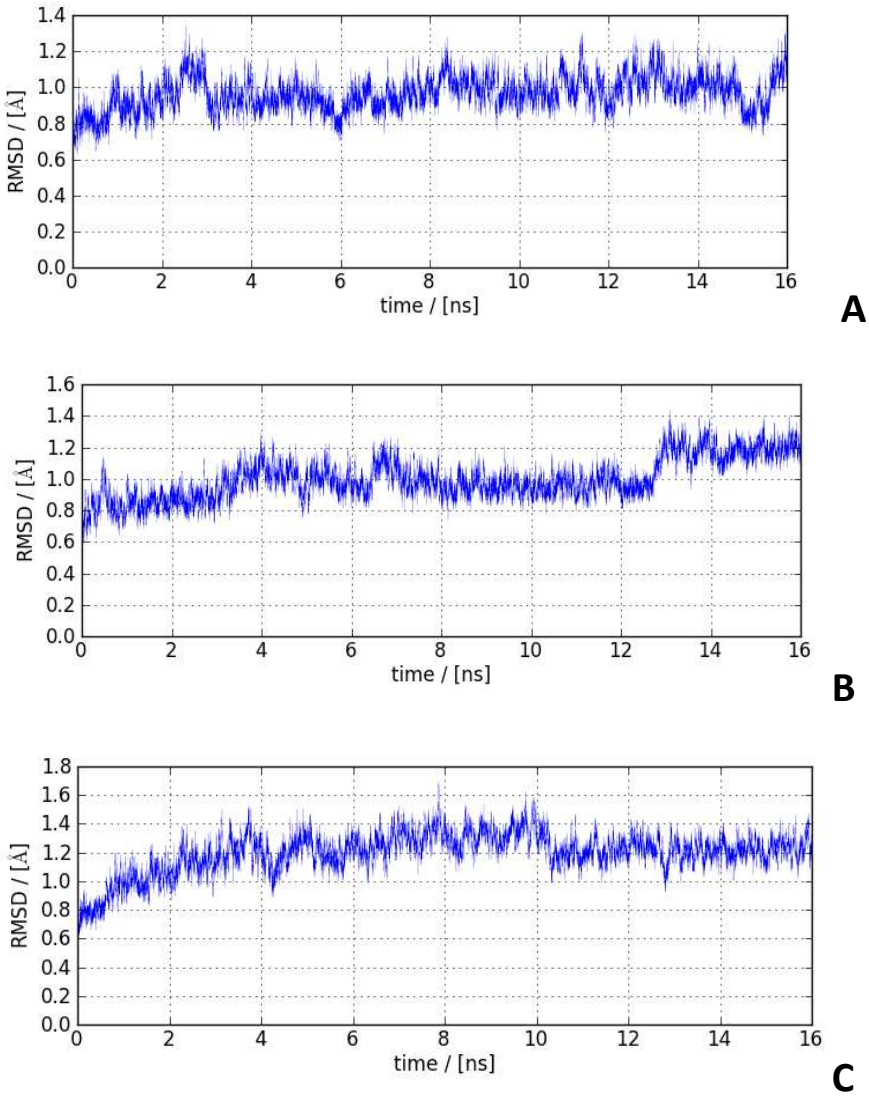

Figure 12: Graphical representation of the RMSDs of the backbone for TEM-180 (A), TEM-201 (B) and TEM-1 (C).

Although RMSD analysis of the three simulations have shown good backbone stability through the 16ns, after visual inspection it becomes clear the importance of the enzymatic ensemble. Visible changes in the secondary structures of β3 and β4 – H11 did indeed occur during the MD simulation. The selected microstates for TEM-1 (Figure 13-C) show less noticeable structural differences than TEM-180 (Figure 13-A) and TEM-201 (Figure 13-B), which is consistent with the RMSD data. In the last 6ns, the backbone is more stable for TEM-1 than for TEM-180, and the latter more stable than the TEM-201 backbone. For TEM-180 the most relevant differences occur in the lower portion of β4 strand (near Arg244) and H11 (near Arg275). In TEM-201 there are more noticeable differences in the β4 strand and H11 than in TEM-180. This appears to lead to the formation of a helical structure between these two domains, most likely due to a greater distance between them. Also, the Ω-loop shows greater variance in TEM-201 than in the TEM-1 and TEM-180. It becomes clear that it is important to take into account the structural variance of the proteins in time.

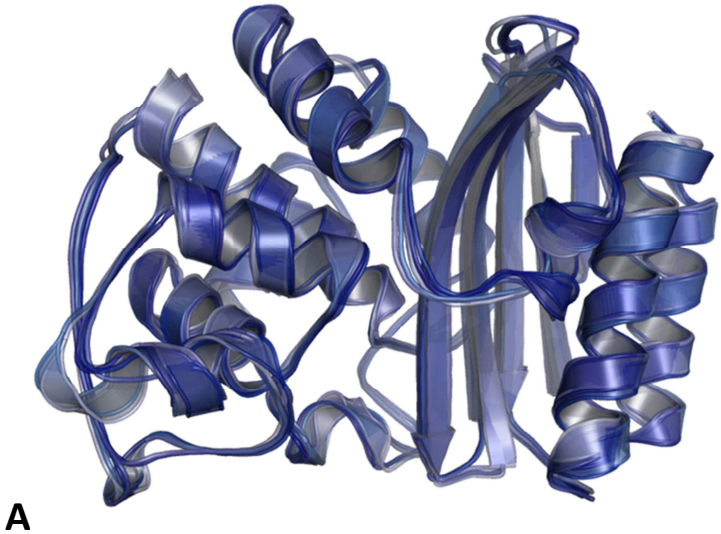

A

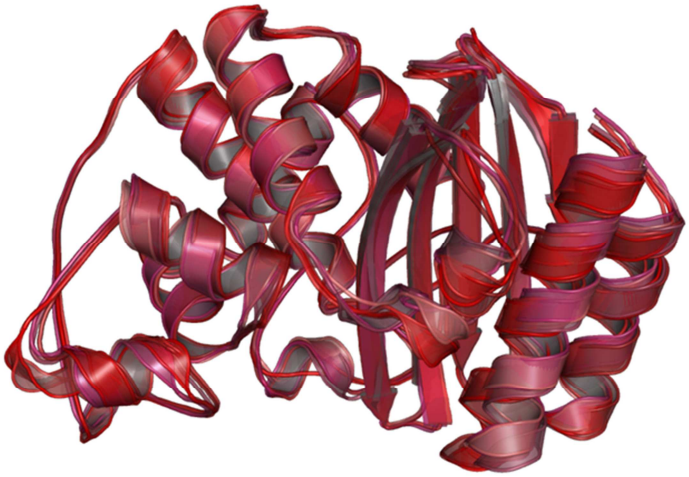

B

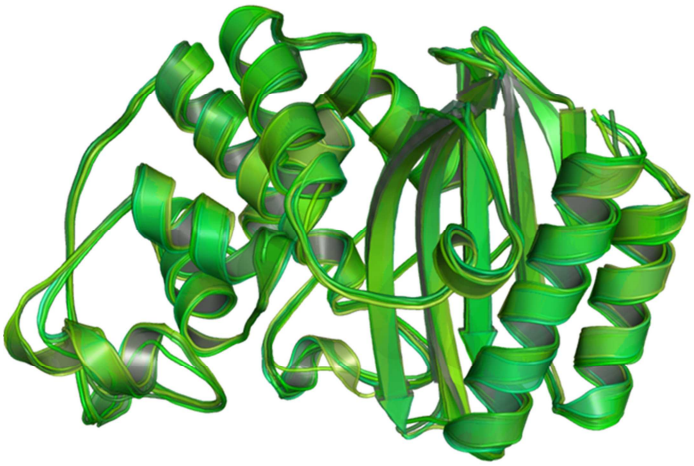

C

Figure 13: Representation of the six microstates (ensemble) selected from the MD simulation of TEM-180 (A), TEM-201 (B) and TEM-1 (C)

4.1.2. Organic compounds docking

To better analyze the Docking results it was beneficial to have an X-ray structure of a TEM enzyme in complex with some of the chosen antibiotics. However, no structure was found with TEM enzymes and these antibiotics, previously to acylation. Two complexes were found with TEM variants and two different antibiotics: these were of intermediates of the acylation reaction complexes. Given these shortcomings, the structural poses that resulted from the docking procedures were analyzed with several parameters as described in 2.3 Molecular Docking. The TEM variants under study formed complexes with all Penicillins (ampicillin, amoxicillin and methicillin), carbapenemes (Imipenem and meropenem) and Cefpirome. TEM-1 only formed complexes with ampicillin, amoxicillin and clavulanic acid.

Complexes shown in Figure 14, present ampicillin deep into the catalytic pocket with the same general orientation. The carbonyl group of the β-lactam ring faces Ser70 and the entire ligand is positioned between the back wall of the catalytic pocket and Tyr105. This ligand position would be the perfect one for this type of complex but it might not be an eliminating factor due to the rotating capacity of the ligand molecules within the catalytic pocket.

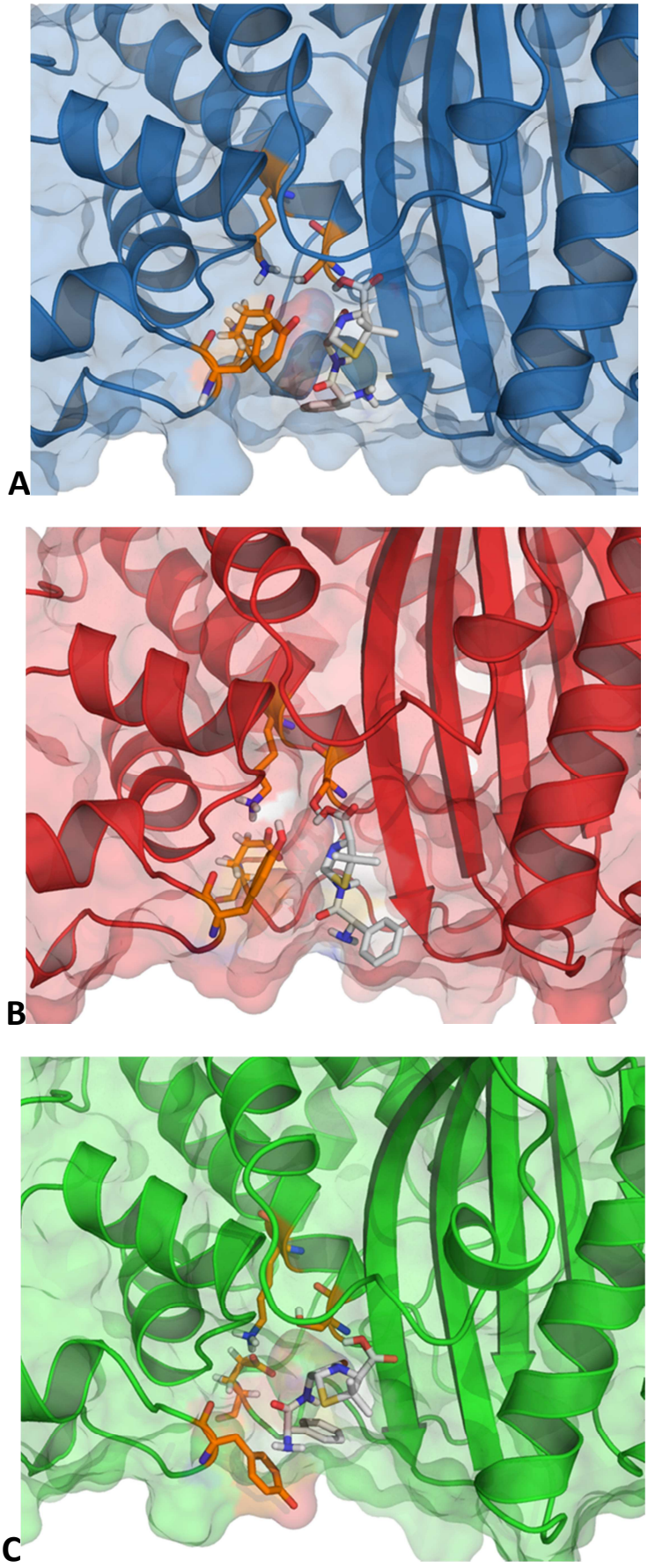

Figure 14: Structural representation of the complex TEM-180/Ampicillin (A), TEM-201/Ampicillin (B) and TEM-1/Ampicillin. Ampicillin is in white stick representation and the interfacial residues are in orange stick representation.

The three complexes obtained with Amoxicillin are represented in Figure 15. They show the ligand in the same position in the catalytic pocket. The geometry of the ligand in TEM-1 complex (Figure 15-C) is not the most favorable. However, as it is still protected by Tyr105, it was selected. The geometry shown for TEM-1 complex might be one of the facts that justify TEM-1 having less activity against Amoxicillin than against Ampicillin.

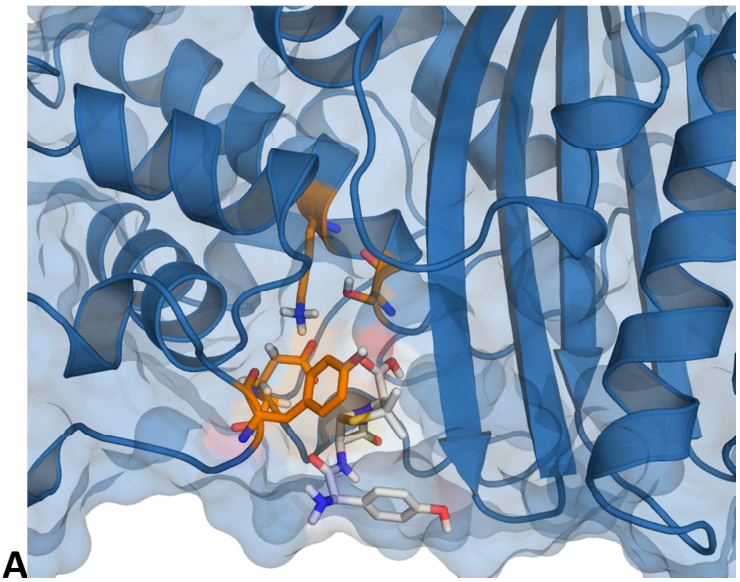

A

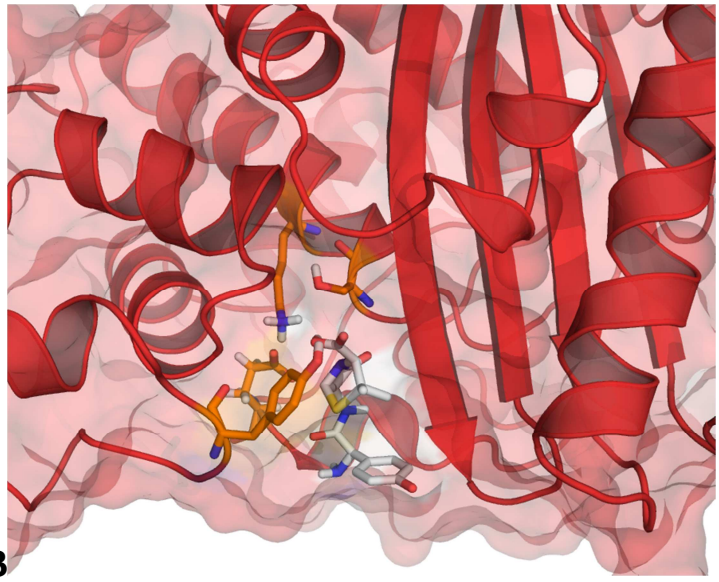

B

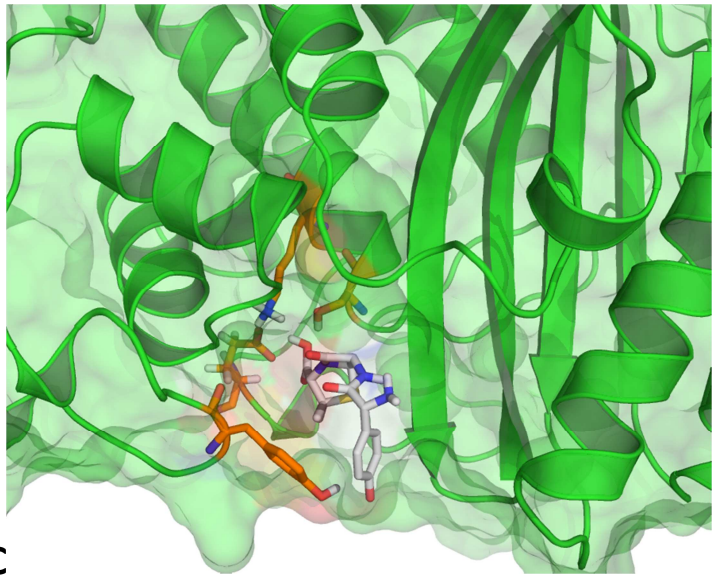

C

Figure 15: Structural representation of the complex TEM-180/Amoxicillin (A), TEM-201/Amoxicillin (B) and TEM-1/Amoxicillin. Amoxicillin is in white stick representation and the interfacial residues are in orange stick representation.

The complexes with Clavulanic acid (Figure 16) present very similar position of the ligand, within the catalytic pocket, with the carboxyl group of the β-lactam ring facing Ser70. It is noticeable that all three complexes have the ligand molecule close to the β3 strand.

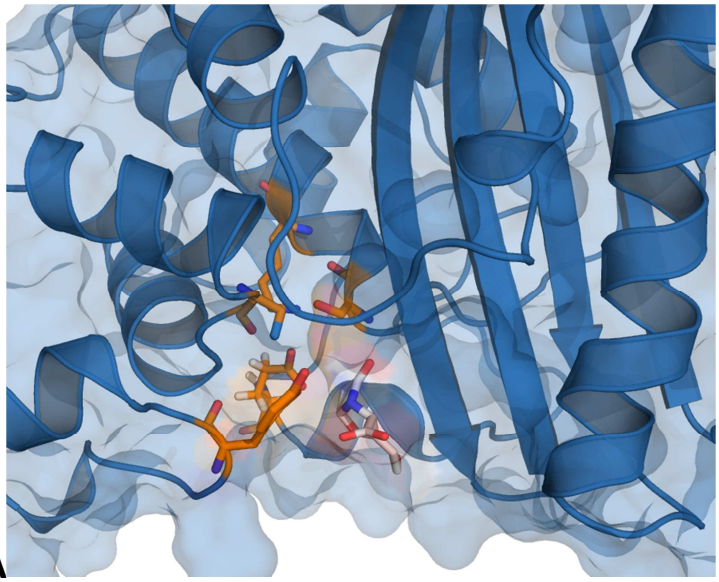

A

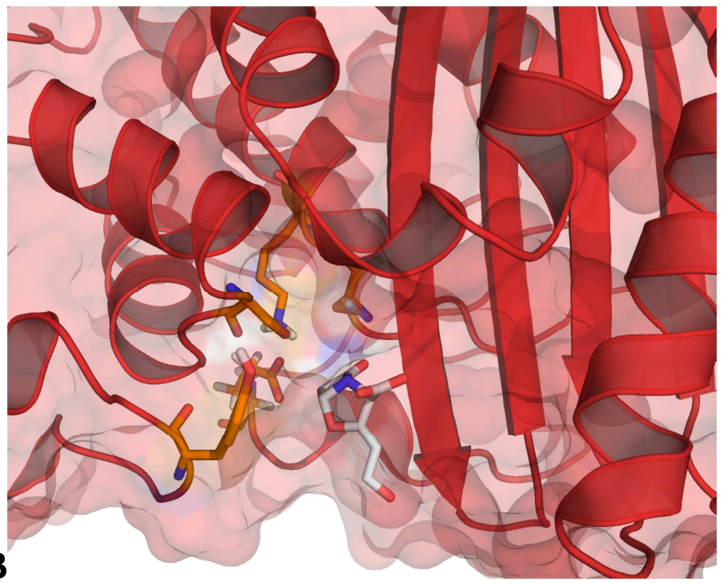

B

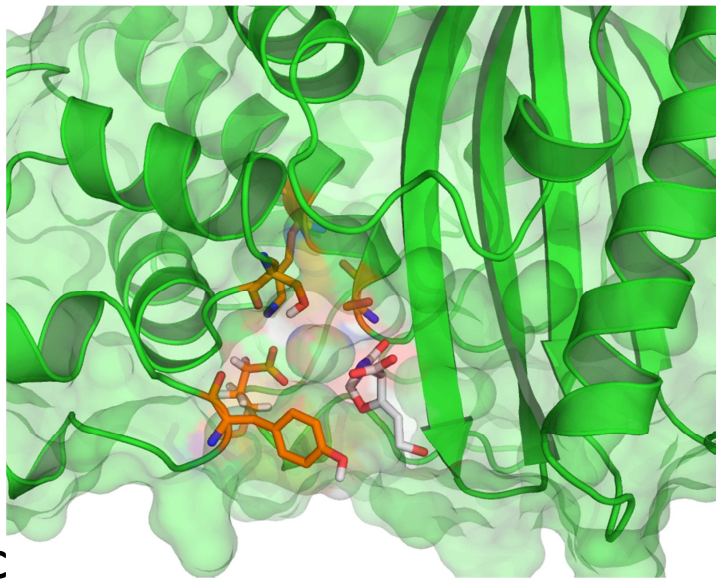

C

Figure 16: Structural representation of the complex TEM-180/Clavulanic acid (A), TEM-201/Clavulanic acid (B) and TEM-1/Clavulanic acid. Clavulanic acid is in white stick representation and the interfacial residues are in orange stick representation.

The complexes obtained from Molecular Docking with Cefpirome present similar ligand location and overall geometry for TEM-180 (Figure 17-A) and TEM-201 (Figure 17-B). In both cases, the carbonyl group of the β-lactam ring faces Ser70 and the entire molecule is located near β3 strand with the ring that contains a sulfur atom interacting with the β3-β4 loop. The other aromatic substituent follows β3 strand and faces to the exterior of the pocket.

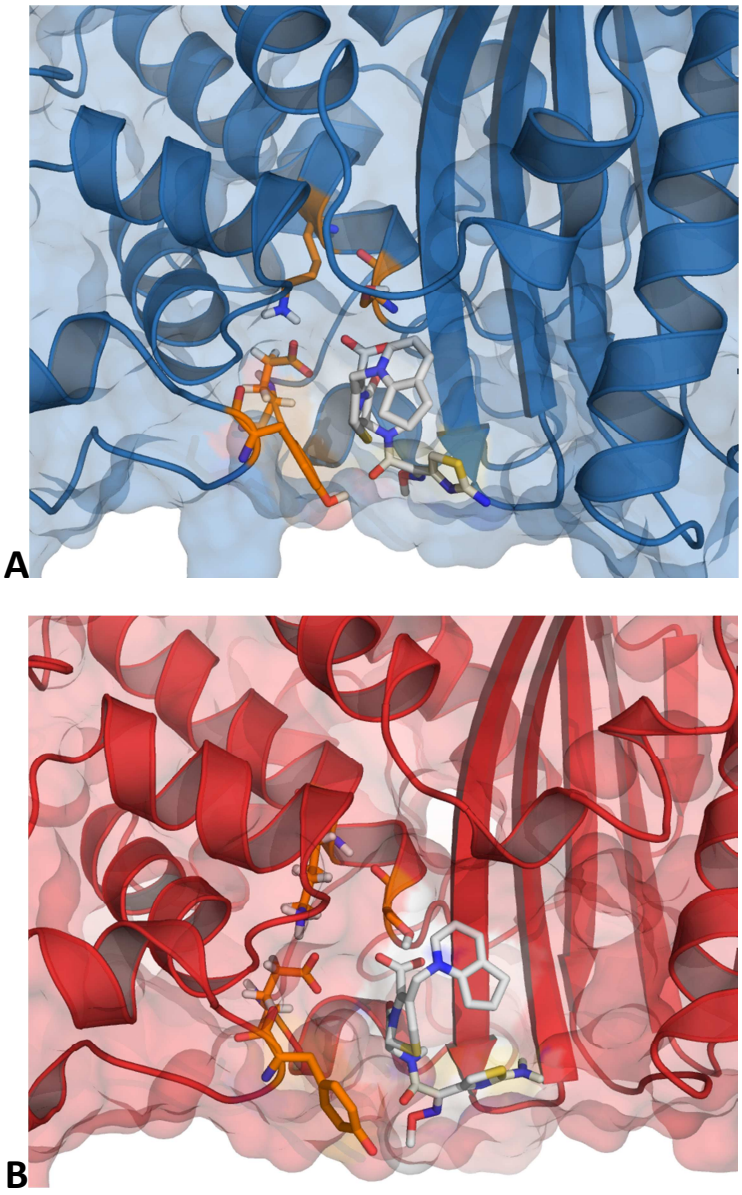

Figure 17: Structural representation of the complex TEM-180/Cefpirome (A), TEM-201/Cefpirome (B). Cefpirome is in white stick representation and the interfacial residues are in orange stick representation.

The complexes with Imipenem show similar ligand location but the complex with TEM-180 (Figure 18-A) has the ligand closer to the catalytic serine (Ser70) than the complex with TEM-201(Figure 18-B). The main difference observed between the two is on the orientation of the side chain of the ligand. In Figure 18-A Imipenem side chain is located closer to Tyr105, possibly interacting with it, while in Figure 18-B the same side chain is closer to β3 strand and H11.

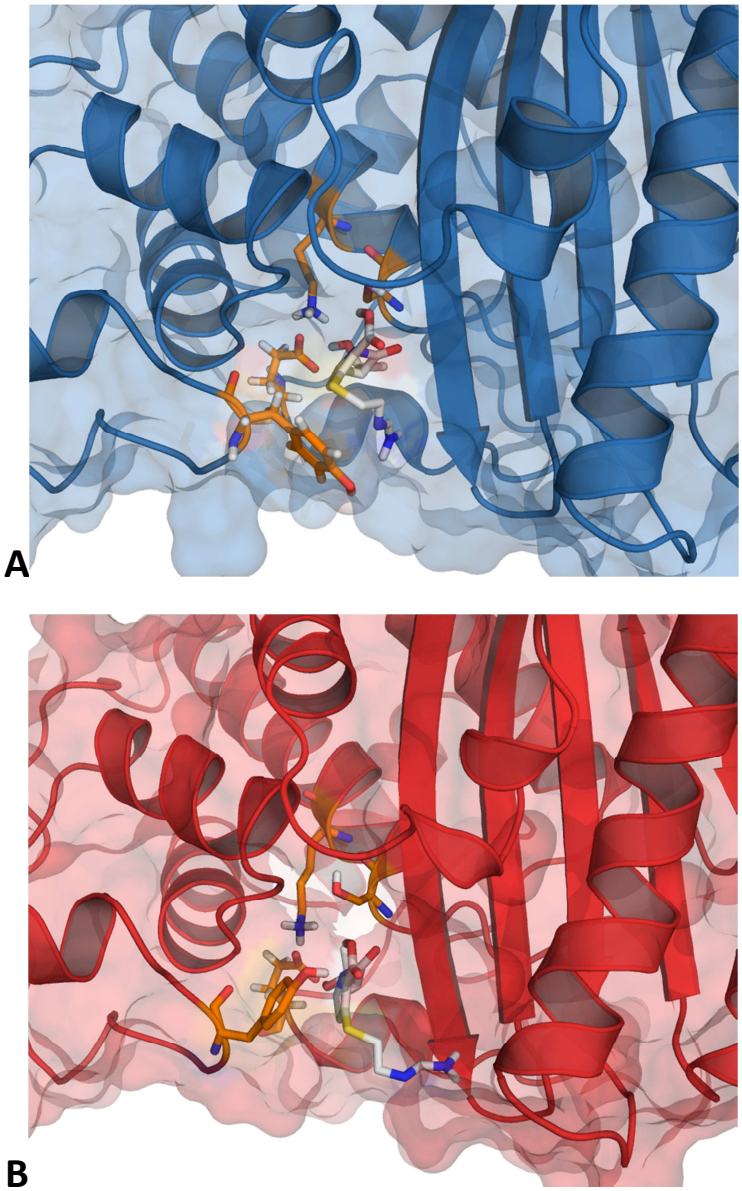

Figure 18: Structural representation of the complex TEM-180/Imipenem (A), TEM-201/Imipenem (B). Imipenem is in white stick representation and the interfacial residues are in orange stick representation.

As shown in Figure 19, both complexes have the ligand in the same position and relative orientation within the catalytic pocket. The carboxyl group is facing Ser70 and Meropenem is placed along the β3 strand in both cases with a minor difference in the position of the side chain ring. In complex with TEM-180 (Figure 19-A) this ring has its substituent facing the opposite side of the pocket to β3 and in complex with TEM-201 (Figure 19-B), the same substituent it is closer to the β3-β4 loop.

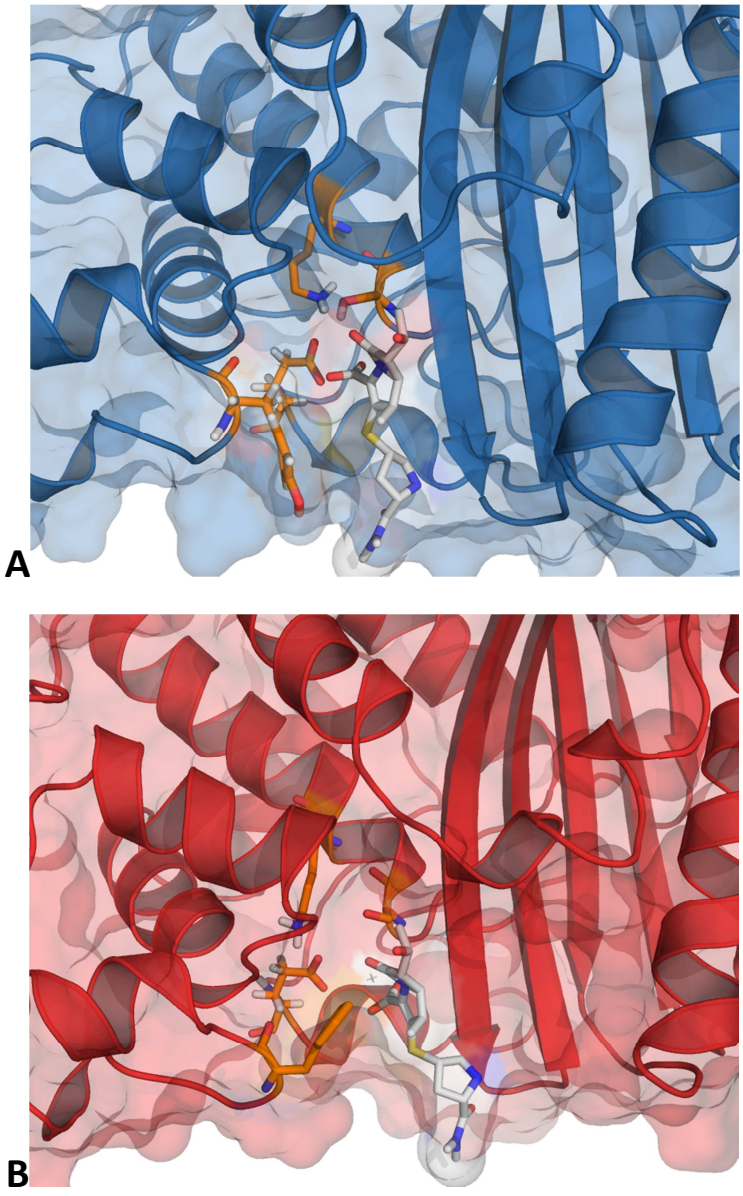

Figure 19: Structural representation of the complex TEM-180/Meropenem (A), TEM-201/Meropenem (B). Meropenem is in white stick representation and the interfacial residues are in orange stick representation.

Although Methicillin has been described as resistant to the TEM family of β-lactamases because of its bulky ortho-dimethoxyphenyl group, directly attached to the side-chain carbonyl group of the penicillin nucleus, it was included in the study and so Molecular Docking was performed and good complexes were obtained for both TEM variants.

As seen in Figure 20 the large cavity of these TEM variants can receive the ligand molecule in the best orientation for the acylation reaction (carboxyl group of the β-lactam ring facing catalytic Ser70) and protecting the ortho-dimethoxyphenyl group from solvent. It might be the reason for its resistance to this type of β-lactamases. It is noticeable that for TEM-201 (Figure 20-B) the referred group appears to be more protected from the solvent because it is closer to the β3-H11 interface instead of being position in the center of the pocket like in TEM-180 (Figure 20-A).

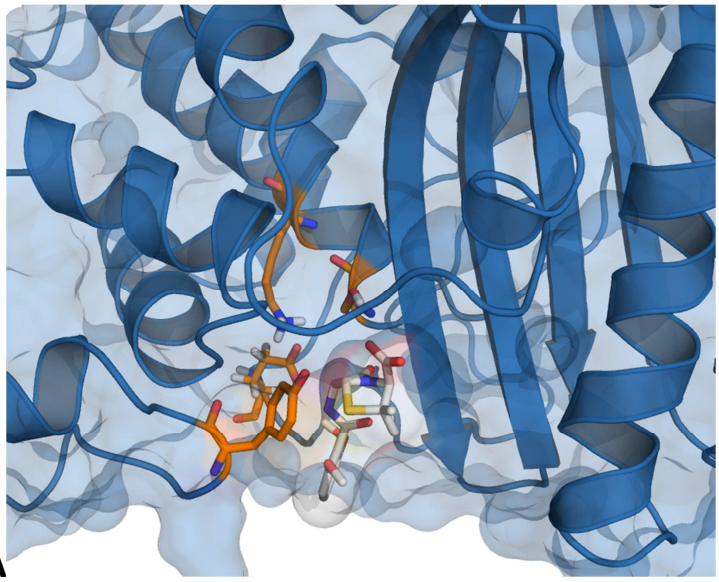

A

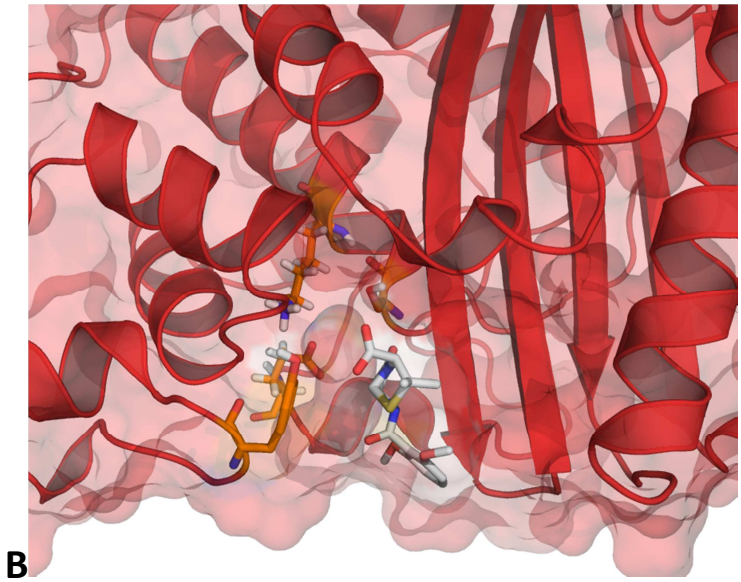

Figure 20: Structural representation of the complex TEM-180/Methicillin (A), TEM-201/Methicillin (B). Methicillin is in white stick representation and the interfacial residues are in orange stick representation.

4.2. Molecular Dynamics- Structural and Energetic Analysis

4.2.1. MD stability

To investigate the stability of the complexes visual we have visually inspected the MD simulation to better understand the variances observed in RMSD graphics (Figure 21-A to C; Figure 34-49)

The RMSD for complexes protein/Ampicillin shows more variation for TEM-180 (Figure 21-A) and for TEM-1 (Figure 21-C) than for the complex with TEM-201 (Figure 21-B). This can be explained due to the inferior stability of the aromatic ring in the side chain, which leads to more movement of this structure. In TEM-201 the aromatic ring interacts with β3 strand leading to higher stability.

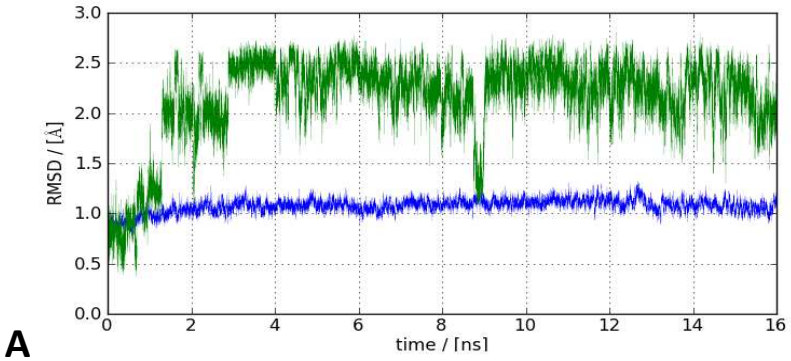

A

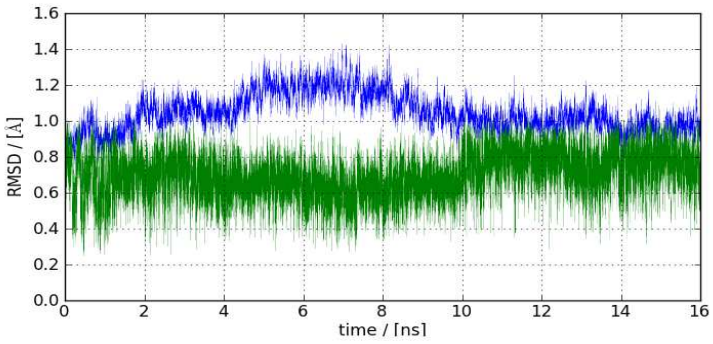

B

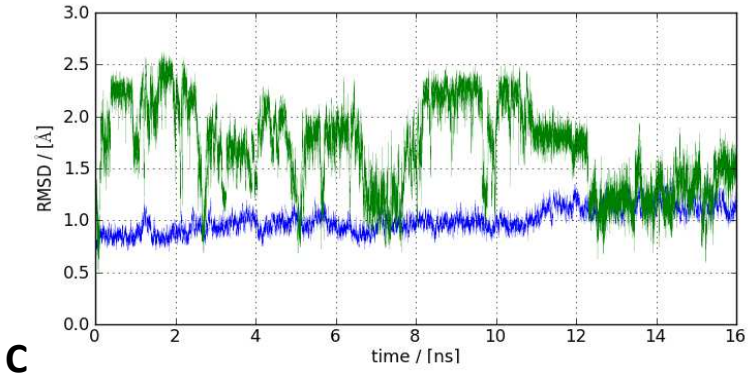

C

Figure 21: Graphic representation of the RMSD of the complexes TEM-180/Ampicillin (A), TEM-201/Ampicillin (B) and TEM-1/Ampicillin (C). In blue is the RMSD for the protein backbone and in green the RMSD of Ampicillin

The complexes of the proteins TEM-180, TEM-201 and TEM-1 with amoxicillin (Figure 34, Figure 35, Figure 36 respectively – S.I.) present very good stability for both for the ligand and the backbone. The difference between these RMSDs and the RMSDs of complexes with Ampicillin might be the result of the extra hydroxyl group in the aromatic ring of the ligand side chain, which might interact with nearby residues leading to higher stability during the MD simulation.

The MD simulations of complexes with Clavulanic acid present very low RMSD in all three complexes as does not possesses a bulky and long side chains. Therefore, the only deviations that can be observed are the result of the torsion of the two rings that are the core structure of it. The differences observed in TEM-201/Clavulanic acid complex (Figure 38 – S.I.) are not significant as no relevant differences were found.

The complexes with Cefpirome have shown two different behaviors during the MD simulation. The complex with TEM-180 (Figure 40) was very stable during the MD for both protein and ligand. In this system Cefpirome was kept very stable with the bulky substituents being stabilized efficiently by nearby residues. The complex with TEM-201 (Figure 41) had a major repositioning of the aromatic substituent linked to the core of the antibiotic. After this, the ligand shows great stability.

The complexes of the two TEM variants with Imipenem (Figure 42 for complex with TEM-180 and Figure 43 for complex with TEM-201 – S.I.) apparently show a considerable RMSD fluctuation. However, in fact, for both cases this is the result of the movement of the long side chain within the catalytic pocket and does not have a major effect on the ligand stability. The core of the antibiotic is very stable.

The complexes of the TEM variants with Meropenem show the same RMSD behavior as with Imipenem and fluctuation (Figure 44 and Figure 45 – S.I.). Although similar, the complexes with Meropenem are more stable than the ones with Imipenem. It is the result of interactions with β3 strand, which are present on this ligand and not with Imipenem (new ring at the end of the side chain that contains a nitrogen atom).

The complexes with Methicillin had a different behavior between them. The complex TEM-180/Methicillin (Figure 46) presented a more erratic behavior during the MD simulation, which translates into significant RMSD variations. This ligand within this TEM variant has shown the capability to rotate inside the catalytic pocket after the 6^{th} ns. This rotation is happens with periodicity which causes the variation observed in Figure 46. It always takes similar time interval to make 180° rotation, inverting the ligand within the pocket and then making it return to the original position.

The complex TEM-201/Methicillin (Figure 47) suffers a slight rotation in the beginning of the simulation but after this it remains very stable during the MD simulation. These differences might be the result of a larger β3 and β4-H11 interface, which increases the capability of TEM-201 to interact with the bulky side chain, stabilizing it and also protecting it from solvent.

All the performed MD simulations have shown great stability for the backbone of the proteins, which is in accordance with the bibliography that states that these type of β-lactamases have an extremely stable backbone that gives them the high tolerance that to mutations.

4.3. Structural and Energetic profiling

The TEM variants presented in this study have shown to form complexes with all the various ligands referred in the Organics Compound Docking part. However, given the complexity of the reactions involved in the hydrolysis and inhibition of this class of enzymes and since the stability of a ligand does not necessarily translate into degradation/enzyme inhibition, it is not adequate to rely only on the absolute free binding energy ($\Delta G_{binding}$) to distinguish the capacity of the organic compounds. It is well

known that the reaction of acylation of the β-lactam ring does not involve only the catalytic residues but also a complex network of H-bonds that lead to an abstraction of a hydrogen of the Serine residue. It has been previously proposed that Glu166 might be the initial reaction base residue (after the abstraction of a hydrogen by a water molecule), abstracting an hydrogen from Lys73, which would then abstract the hydrogen from the hydroxyl group of the Ser70. Lys73 has been described not only as a possible initial base but also as a stabilizer of nearby residues (Ser130 and Ser70) and as having a possible stabilizing effect as far as ligand position goes. Other theories have arisen with the study of various TEM variants and it has been proposed that Lys73 might be, in certain cases, the initial base residue. Although, it was shown the importance of these residues, it is not clear the definite purpose of some of them and how they might influence the reactions on the catalytic site. It becomes necessary to take into account several aspects of the enzyme itself and the complexes formed for a correct comprehension of the crucial system.

To analyze the structure of the complexes, more specifically the interfacial residues, B-factor values (Table 8) were calculated (B-factor describes the displacement of the atomic positions from an average value). The number of water molecules (Table 9) was also calculated to investigate the presence of water molecules near the catalytic residues, as well as, others that might contribute to the stability of the complex. It also allowed a better comprehension of the capability of the enzymes to hydrolyze the antibiotics. To investigate if the H-bond network between the catalytic residues is maintained through the simulation, relevant distances were also calculated (Table 10).

Table 8: Calculated B-factor of interfacial residues both for backbone (BB) and all-atom (AA) for the analyzed complexes

B-Factor																		
Residue	Clavulanic acid						Ampicillin						Amoxicillin					
	BB			AA			BB			AA			BB			AA		
	TEM-180	TEM-201	TEM-1	TEM-180	TEM-201	TEM-1	TEM-180	TEM-201	TEM-1	TEM-180	TEM-201	TEM-1	TEM-180	TEM-201	TEM-1	TEM-180	TEM-201	TEM-1
Met 69	5,14	8,87	8,50	6,73	14,50	11,16	5,05	3,84	8,72	8,56	5,48	13,72	3,77	4,05	6,19	5,13	5,09	11,00
Ser 70	5,41	7,71	10,34	6,80	9,68	19,28	5,09	5,60	9,57	12,95	8,85	25,17	3,79	5,13	6,25	4,83	12,64	16,97
Lys 73	3,73	3,86	6,01	5,63	5,48	8,65	3,18	3,15	4,83	4,13	4,55	6,48	3,23	3,30	3,93	3,92	4,72	5,17
Tyr 105	9,30	17,25	19,98	23,37	86,49	62,95	9,26	9,87	11,15	13,82	41,16	34,95	10,75	13,30	12,82	47,13	15,28	37,42
Ser 130	6,03	11,15	8,16	14,39	22,18	12,40	5,02	7,17	7,34	11,32	8,86	11,68	4,48	7,90	9,80	5,20	16,47	13,75
Asn 132	4,03	6,14	8,39	9,51	12,22	13,44	2,86	4,74	5,02	5,70	13,62	36,22	3,50	6,70	5,09	6,48	8,27	7,40
Glu 166	5,18	9,68	15,98	11,01	13,32	20,37	7,43	5,87	9,64	12,18	11,55	13,38	4,36	4,70	7,01	5,41	5,92	11,99
Asn 170	6,75	12,47	9,06	11,91	25,74	23,30	7,24	6,19	10,69	20,12	7,27	32,14	4,64	6,00	13,69	5,21	6,30	21,09
Val 216	8,58	11,80	10,39	20,84	9,43	15,10	6,23	13,24	10,42	8,34	27,27	15,26	12,45	21,07	13,97	26,18	34,38	59,64
Lys 234	3,42	4,43	4,82	7,80	11,00	7,59	2,95	4,04	4,42	4,27	5,44	7,57	5,37	4,31	4,67	5,92	7,70	8,39
Ser 235	4,31	4,89	6,61	5,52	13,28	8,38	5,22	3,78	5,73	10,45	13,95	7,47	9,87	4,53	6,70	13,63	16,07	8,25
Glu 239	6,85	10,07	7,02	21,07	30,69	27,15	6,86	6,06	16,14	44,68	37,28	38,54	9,91	7,22	8,41	39,46	29,29	22,33
Arg 244	4,66	5,50	4,77	17,57	27,23	19,74	4,80	3,61	4,64	31,21	21,10	19,87	5,10	3,63	5,08	41,48	15,72	22,21
Arg 275	11,15	11,57	9,93	31,57	18,43	18,65	12,21	9,43	8,63	21,10	24,08	52,42	31,84	10,36	9,07	49,02	22,65	15,39

B-Factor																
Residue	Cefpirome				Imipenem				Meropenem				Methicillin			
	BB		AA		BB		AA		BB		AA		BB		AA	
	TEM-180	TEM-201	TEM-180	TEM-201	TEM-180	TEM-201	TEM-180	TEM-201	TEM-180	TEM-201	TEM-180	TEM-201	TEM-180	TEM-201	TEM-180	TEM-201
Met 69	6,78	4,95	11,64	8,42	6,61	6,99	14,87	8,14	6,27	4,90	7,62	6,28	9,68	5,10	28,50	5,97
Ser 70	5,10	4,74	9,32	14,03	8,73	7,13	28,52	14,58	7,79	4,63	14,22	7,27	12,43	5,63	45,53	6,92
Lys 73	3,90	3,46	6,60	4,10	4,28	3,65	7,14	5,77	3,31	3,59	4,70	5,76	3,76	4,32	4,07	6,96
Tyr 105	13,26	9,09	32,35	40,68	7,58	10,08	13,29	88,97	8,60	11,82	7,14	101,74	13,00	14,01	123,12	41,18
Ser 130	8,12	5,39	17,94	10,61	6,18	7,57	11,08	12,77	4,94	11,89	8,92	16,07	7,32	7,62	23,46	10,67
Asn 132	7,61	3,83	19,62	13,57	3,43	5,56	4,71	6,65	3,65	5,66	5,82	11,07	4,68	5,01	13,31	11,69
Glu 166	13,67	5,07	17,69	14,44	5,08	5,10	5,77	6,14	5,84	6,60	15,46	13,57	9,40	7,52	24,41	12,76
Asn 170	8,04	11,01	10,23	14,86	10,14	7,86	26,63	9,76	4,61	7,15	6,06	11,76	18,36	8,07	49,87	9,63
Val 216	38,58	10,77	36,46	15,74	9,40	48,97	19,86	67,35	11,47	10,71	22,47	13,32	13,32	19,68	20,89	24,59
Lys 234	4,98	5,24	9,92	7,35	5,52	5,76	6,01	15,88	3,53	3,50	5,51	13,49	5,23	8,64	6,09	14,36
Ser 235	6,60	9,74	8,84	16,02	12,08	15,07	18,91	20,58	3,93	4,36	6,31	6,10	12,76	7,31	20,83	15,86
Glu 239	7,68	14,34	34,04	50,29	7,57	15,41	26,73	60,50	5,27	8,14	25,03	37,82	7,30	9,90	47,30	33,93
Arg 244	5,34	8,68	43,16	45,07	5,19	8,50	26,48	16,71	4,07	5,01	22,65	20,44	6,11	5,73	6,86	25,89
Arg 275	19,30	20,80	33,15	52,12	16,04	11,68	44,69	13,16	11,56	39,83	28,54	218,54	14,81	18,99	28,09	35,70

Table 9: Number of water molecules in the micro-environment of the interfacial residues, for the analyzed complexes, at 4Å. Highlighted in red is the number of water molecules around the HS

Number of water molecules																	
Residues	Clavulanic acid			Ampicillin			Amoxicillin			Cefpirome		Imipenem		Meropenem		Methicillin	
	TEM-180	TEM-201	TEM-1	TEM-180	TEM-201	TEM-1	TEM-180	TEM-201	TEM-1	TEM-180	TEM-201	TEM-180	TEM-201	TEM-180	TEM-201	TEM-180	TEM-201
Met 69	0,00	0,01	0,00	0,00	0,00	0,01	0,00	0,00	0,00	0,00	0,00	0,00	0,00	0,00	0,00	0,00	0,01
Ser 70	0,77	0,26	3,23	0,55	0,50	1,71	0,09	1,59	1,84	0,25	1,35	0,84	0,75	1,58	3,39	4,76	3,56
Lys 73	0,60	2,29	1,61	0,86	0,48	1,62	0,00	1,03	0,87	3,04	0,00	0,66	0,72	0,60	1,46	1,50	1,99
Tyr 105	3,41	3,61	3,10	2,84	1,46	1,84	2,14	1,01	1,90	2,42	2,30	1,52	1,63	1,57	1,77	2,07	2,71
Ser 130	1,99	2,29	2,04	0,00	0,90	2,06	1,62	1,76	3,08	1,42	1,94	1,23	2,38	1,27	5,04	2,31	4,38
Asn 132	0,26	2,80	3,39	1,46	0,34	2,84	1,80	2,74	1,77	3,05	1,80	1,48	0,23	0,85	2,58	3,07	2,72
Glu 166	0,42	2,62	1,53	1,44	0,52	1,84	0,19	1,03	0,05	3,28	0,83	0,57	0,00	0,55	1,49	2,25	1,08
Asn 170	0,01	4,61	3,28	1,44	0,79	2,22	0,04	1,06	1,70	1,79	1,44	0,16	0,27	0,57	1,27	2,23	1,51
Val 216	1,64	3,59	3,72	0,00	2,17	2,48	1,04	2,35	3,57	3,41	3,28	0,37	2,10	2,37	3,82	1,42	4,38
Lys 234	0,27	2,07	1,10	0,00	0,47	1,35	0,00	1,70	1,50	0,57	1,13	0,00	1,87	1,04	3,69	0,09	2,56
Ser 235	0,00	0,85	0,00	0,53	0,03	0,00	1,32	0,00	0,00	1,14	2,17	1,23	1,68	0,89	2,57	1,22	2,63
Glu 239	6,22	6,27	6,40	6,06	5,98	6,24	5,96	5,82	5,43	5,67	5,87	1,77	4,95	3,68	5,81	5,38	4,13
Arg 244	2,98	4,32	2,77	3,57	3,92	3,15	5,24	2,97	2,77	3,42	5,44	4,28	3,38	2,28	5,84	4,83	4,33
Arg 275	4,45	1,43	4,21	3,62	4,19	2,57	5,12	4,32	4,09	5,79	3,97	2,40	2,75	3,50	3,93	4,57	4,09

Table 10: Average distances (Å) between catalytic residues through the MD simulation

TEM-180																					
χ ± σ	**Amoxicillin**			**Ampicillin**			**Cefpirome**			**Clavulanic acid**			**Imipenem**			**Meropenem**			**Methicillin**		
Ser70-Lys73	3,77	±	0,22	4,74	±	0,83	6,39	±	0,51	4,46	±	0,31	4,89	±	1,40	3,40	±	0,68	4,07	±	0,30
Ser70-Ser130	4,57	±	0,26	4,85	±	0,43	4,77	±	0,56	6,28	±	1,03	4,35	±	0,54	3,84	±	0,38	7,39	±	0,61
Lys73-Glu166	4,72	±	0,17	2,84	±	0,13	4,03	±	0,30	2,76	±	0,08	3,65	±	0,24	3,64	±	0,72	3,07	±	0,23
TEM-201																					
χ ± σ	**Amoxicillin**			**Ampicillin**			**Cefpirome**			**Clavulanic acid**			**Imipenem**			**Meropenem**			**Methicillin**		
Ser70-Lys73	3,82	±	0,26	3,46	±	0,38	4,00	±	0,24	7,01	±	0,35	3,95	±	0,42	3,57	±	0,30	4,18	±	0,25
Ser70-Ser130	4,58	±	**0,31**	5,47	±	0,72	7,44	±	0,51	5,38	±	0,87	6,48	±	0,73	6,47	±	0,40	7,48	±	0,36
Lys73-Glu166	2,86	±	0,15	2,73	±	0,08	3,04	±	0,21	2,83	±	0,12	3,00	±	0,21	2,80	±	0,10	2,98	±	0,28

TEM-1									
χ ± σ	**Amoxicillin**			**Ampicillin**			**Clavulanic acid**		
Ser70-Lys73	5,48	±	0,85	5,06	±	0,99	4,92	±	1,24
Ser70-Ser130	4,50	±	0,61	5,28	±	1,26	4,47	±	0,51
Lys73-Glu166	3,42	±	0,31	3,19	±	0,30	3,32	±	0,45

Table 11: Relative free binding energy and S.D. for the interfacial residues of the various complexes using computational ASM

$\Delta\Delta G_{binding}$/[kcalmol^{-1}]																								
Residue	Clavulanic acid									Ampicillin									Amoxicillin					
	TEM-180			TEM-201			TEM-1			TEM-180			TEM-201			TEM-1			TEM-180			TEM-201			TEM-1		
	ΔΔG	±	S.D.	ΔΔG	±	S.D.	ΔΔG	±	S.D.	ΔΔG	±	S.D.	ΔΔG	±	S.D.	ΔΔG	±	S.D.	ΔΔG	±	S.D.	ΔΔG	±	S.D.	ΔΔG	±	S.D.
Met 69	0,15	±	0,65	0,29	±	0,60	0,18	±	0,61	-0,12	±	0,88	0,44	±	0,70	-0,13	±	1,07	0,68	±	0,67	0,48	±	1,04	-0,10	±	0,81
Ser 70	1,03	±	0,55	0,74	±	0,59	0,25	±	0,57	0,25	±	0,70	0,27	±	0,64	0,24	±	0,87	0,96	±	0,65	1,81	±	0,84	0,24	±	0,68
Lys 73	3,98	±	0,63	0,72	±	0,57	-0,02	±	0,61	2,42	±	0,70	2,19	±	0,60	2,30	±	0,85	3,23	±	0,62	-3,36	±	0,77	1,84	±	0,69
Tyr 105	2,00	±	0,56	-0,80	±	0,60	0,25	±	0,57	4,35	±	0,77	3,59	±	0,61	4,03	±	0,88	3,72	±	0,61	0,95	±	0,79	2,95	±	0,67
Ser 130	-0,15	±	0,55	1,91	±	0,52	0,17	±	0,58	1,08	±	0,73	1,27	±	0,64	0,24	±	0,87	0,04	±	0,62	-2,12	±	0,80	-0,05	±	0,69
Asn 132	0,31	±	0,55	0,23	±	0,64	0,24	±	0,57	3,75	±	0,73	3,53	±	0,60	0,02	±	0,89	2,11	±	0,64	-1,37	±	0,80	1,22	±	0,70
Glu 166	6,86	±	0,62	0,23	±	0,58	0,27	±	0,62	1,24	±	0,73	2,41	±	0,61	0,62	±	0,91	5,97	±	0,70	8,49	±	0,74	7,18	±	0,56
Asn 170	1,51	±	0,53	0,16	±	0,62	0,27	±	0,58	0,46	±	0,74	5,41	±	0,66	1,62	±	0,79	3,62	±	0,65	-8,34	±	0,93	1,07	±	0,67
Val 216	0,77	±	0,62	1,11	±	0,59	0,52	±	0,61	2,76	±	0,87	0,96	±	0,70	-0,41	±	1,00	0,00	±	0,68	0,75	±	1,02	-0,56	±	0,85
Lys 234	0,67	±	0,57	7,59	±	0,64	-0,02	±	0,61	1,41	±	0,67	3,61	±	0,67	1,30	±	0,80	0,11	±	0,66	-2,38	±	0,81	-0,10	±	0,66
Ser 235	-0,03	±	0,58	0,00	±	0,57	0,10	±	0,59	-0,02	±	0,70	-0,02	±	0,61	-0,13	±	0,89	-0,06	±	0,61	-0,24	±	0,84	-0,17	±	0,70
Glu 239	0,02	±	0,56	0,19	±	0,60	0,16	±	0,61	0,09	±	0,67	-0,10	±	0,59	1,20	±	0,81	0,02	±	0,66	7,86	±	0,71	0,86	±	0,62
Arg 244	0,25	±	0,56	0,02	±	0,60	0,11	±	0,61	1,92	±	0,67	0,08	±	0,58	-0,09	±	0,81	0,35	±	0,67	-6,49	±	0,72	-0,19	±	0,67
Arg 275	-0,02	±	0,55	-0,80	±	0,59	0,13	±	0,62	-0,15	±	0,68	-0,01	±	0,59	-0,06	±	0,81	0,14	±	0,64	-5,51	±	0,71	-0,17	±	0,65

$\Delta\Delta G_{binding}$/[kcalmol^{-1}]																								
Residue	Cefpirome						Imipenem						Meropenem						Methicillin					
	TEM-180			TEM-201			TEM-180			TEM-201			TEM-180			TEM-201			TEM-180			TEM-201		
	ΔΔG	±	S.D.	ΔΔG	±	S.D.	ΔΔG	±	S.D.	ΔΔG	±	S.D.	ΔΔG	±	S.D.	ΔΔG	±	S.D.	ΔΔG	±	S.D.	ΔΔG	±	S.D.
Met 69	0,83	±	1,08	0,37	±	0,70	0,78	±	0,74	0,16	±	0,76	0,30	±	0,94	0,71	±	0,68	0,16	±	0,61	0,03	±	0,73
Ser 70	1,82	±	0,98	1,57	±	0,66	0,45	±	0,66	0,00	±	0,74	1,19	±	0,89	1,82	±	0,54	0,01	±	0,52	-0,69	±	0,67
Lys 73	4,59	±	0,93	10,66	±	0,73	1,36	±	0,65	2,38	±	0,79	6,80	±	0,86	1,55	±	0,47	1,61	±	0,54	0,84	±	0,60
Tyr 105	0,87	±	0,97	2,58	±	0,61	4,41	±	0,67	4,06	±	0,70	3,23	±	0,78	3,31	±	0,52	5,82	±	0,56	2,38	±	0,65
Ser 130	1,44	±	0,94	0,32	±	0,66	0,03	±	0,67	0,15	±	0,75	0,88	±	0,84	0,09	±	0,51	0,03	±	0,52	0,16	±	0,63
Asn 132	-0,12	±	0,97	1,71	±	0,62	1,07	±	0,63	1,72	±	0,71	1,54	±	0,75	-0,90	±	0,50	-0,05	±	0,52	-0,33	±	0,64
Glu 166	-1,40	±	0,92	0,23	±	0,66	5,84	±	0,69	6,89	±	0,68	4,81	±	0,80	1,37	±	0,46	-0,47	±	0,56	0,25	±	0,62
Asn 170	2,64	±	0,95	2,56	±	0,68	0,32	±	0,64	1,65	±	0,76	3,95	±	0,83	2,61	±	0,54	1,12	±	0,51	1,83	±	0,61
Val 216	2,94	±	1,03	2,00	±	0,67	0,18	±	0,77	0,08	±	0,78	0,62	±	0,87	-0,10	±	0,67	0,63	±	0,51	-0,22	±	0,70
Lys 234	5,12	±	1,00	10,34	±	0,66	0,21	±	0,65	-0,13	±	0,73	1,11	±	0,77	1,95	±	0,45	0,29	±	0,53	0,19	±	0,59
Ser 235	0,06	±	0,99	-0,15	±	0,65	0,03	±	0,67	0,00	±	0,74	-0,10	±	0,83	0,09	±	0,51	0,11	±	0,55	0,19	±	0,63
Glu 239	1,06	±	0,93	0,12	±	0,68	0,50	±	0,62	-0,07	±	0,73	1,41	±	0,77	0,41	±	0,46	0,75	±	0,56	1,17	±	0,58
Arg 244	-0,27	±	0,96	0,35	±	0,66	0,27	±	0,65	-0,30	±	0,76	-0,20	±	0,79	0,33	±	0,48	0,40	±	0,55	0,00	±	0,60
Arg 275	-0,82	±	0,95	-0,14	±	0,68	0,05	±	0,65	0,30	±	0,75	-0,04	±	0,80	0,00	±	0,47	-0,09	±	0,54	0,11	±	0,60

4.3.1. Analysis of complexes with Clavulanic acid

The complexes formed with clavulanic acid have clearly shown different behavior between the three TEM variants under study.

From the B-factor values (Table 8) measured for the three MD simulations, we can observe that Ser70, Lys73, Tyr105, Glu166, Asn170 are the residues that present the most distinct behavior between the TEM-1 and the mutant forms. With the exception of Asn170, these residues have a more stable backbone in TEM-180 and TEM-201 than in TEM-1. The side chain of Tyr105 in TEM-201 appears to be less stable than in the others (greater difference between the B-factor of all-atom and backbone). The water structure can be depicted in terms of RDF. We analyzed the RDF profiles and calculated the average number of waters within 4 Å (cutoff for meaningful interactions), which are listed in Table 9. Ser70 and Glu166 show a clear different behavior when comparing the variants with TEM-1. The number of water molecules at a 4 Å cutoff of Ser70 is: 0.77 in TEM-180, 2.29 in TEM-201 and 3.23 in TEM-1. At a 4 Å cutoff of Glu166 are: 0.42 in TEM-180, 2.62 in TEM-201 and 1.53 in TEM-1. As mentioned before, the existence of a conserved water is fundamental for the enzymatic process. In contrast with TEM-180 and TEM-1, TEM-201 does not have a conserved water molecule near Glu166. This can lead to a decreased acylation of clavulanic acid, which translates into resistance to this β-lactamase inhibitor.

The hydrogen network responsible for the acylation process has been altered for TEM-201 with a significant increase in the distance between Ser70 and Ser130 (5.38 ± 0.87 Å for TEM-201 in opposition to 4.47 ± 0.51 Å for the TEM-1). Another important structural feature for the irreversible inhibition of the enzyme is altered. Ser70 and Lys73 are at greater distance in TEM-201 than in TEM-1 (7.01 ± 0.35Å for TEM-201 and 4.92 ± 1.24Å in TEM-1). The distance between the two serine residues that form an intermediary of the reaction (Ser70 and Ser130) is higher in TEM-180 than in TEM-1 (6.28 ± 1.03Å for TEM-180 in opposition to 4.47 ± 0.51Å for TEM-1) avoiding in this manner the inhibition of Ser130 by covalent bonding (Table 10). TEM-180 presents a conserved water molecule near Glu146 but with a lower occupancy when compared with WT (51% against 86%), which might lead to decreased acylation and therefore, resistance to clavulanic acid.

The difference in the distance between Ser70 and Ser130 becomes clear when observing its variation during the MD simulation (Figure 22).

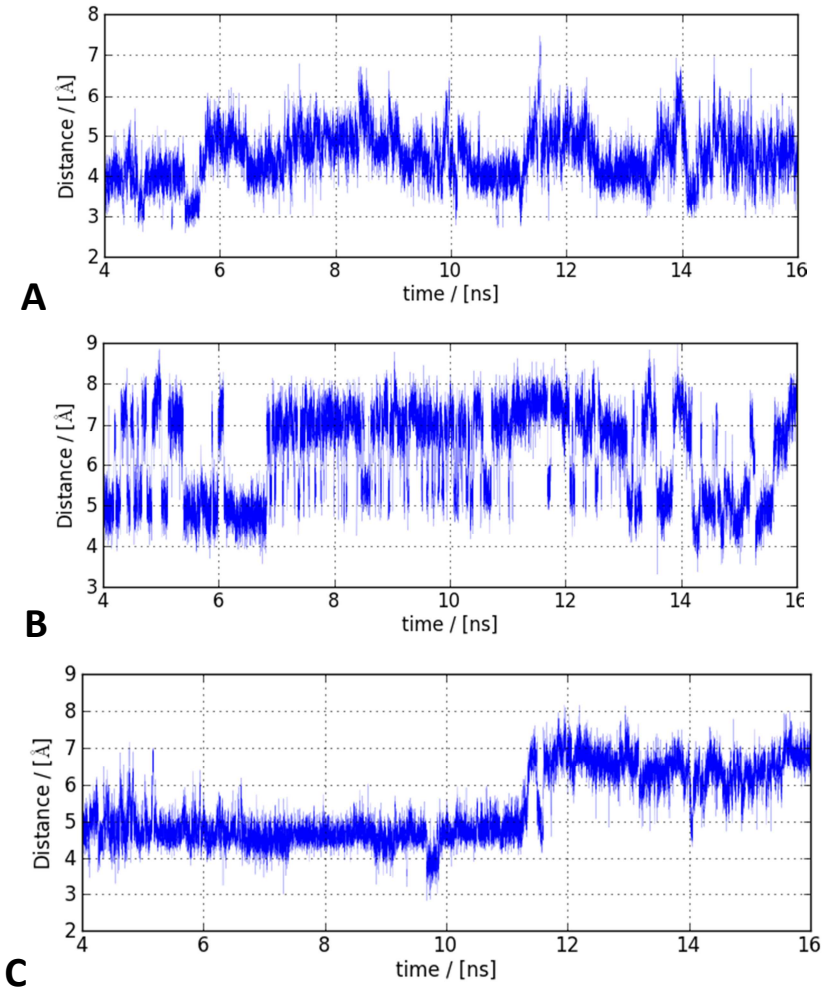

Figure 22: Graphical representation of the distance between Ser70 and Ser130 during the MD simulation in TEM-1 (A), TEM-180 (B) and TEM-201 (C).

The ASM analysis for TEM-180 has shown 3 HS: Lys73 ($\Delta\Delta G_{binding}$=3.98 ± 0.63 kcalmol^{-1}), Tyr105 ($\Delta\Delta G_{binding}$=2.00 ± 0.56 kcalmol^{-1}) and Glu166 ($\Delta\Delta G_{binding}$=6.86 ± 0.62 kcalmol-1) and in TEM-201 1 HS – Lys234 ($\Delta\Delta G_{binding}$=7.59 ± 0.64 kcalmol^{-1}). In TEM-180, Lys73 and Glu166 help stabilizing the bicyclic structure, mainly through hydrophobic interactions. Nevertheless, both can also bond by H-bonds with the oxygen groups from the ligand. Tyr105 has a major role by helping maintaining the acid inside the catalytic pocket (Figure 23).

Although, TEM-201 only presents 1HS (Lys234 with $\Delta\Delta G_{binding}$=7.59 ± 0.64 kcalmol-1) that forms a H-bond with clavulanic acid (Figure 23), it shows other relevant interactions.

No relevant interactions for the binding free energy were found in TEM-1. For this enzyme the small size of the ligand might be the reason for these findings as the enzyme cannot bind to the acid for a long period of time. This fact does not mean that it would be less prone to inhibition because if the enzyme cans acylate the acid and form the intermediary, it will be irreversibly inhibited. This surpasses the fact that it isn't as stable as in the ligands.

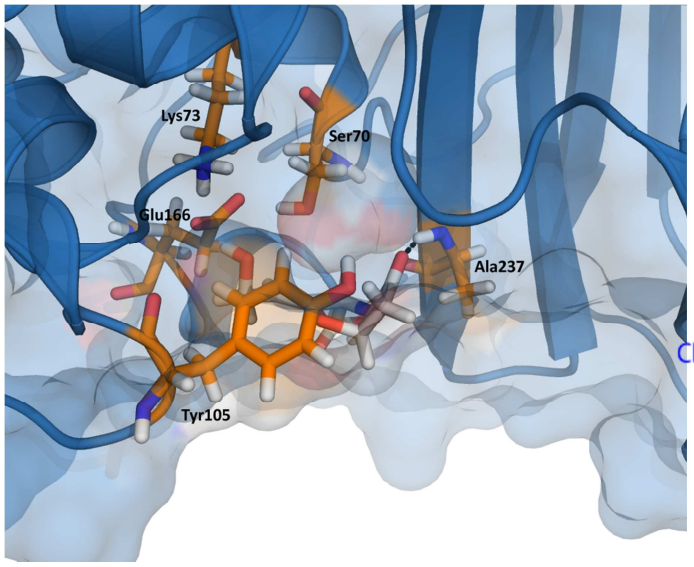

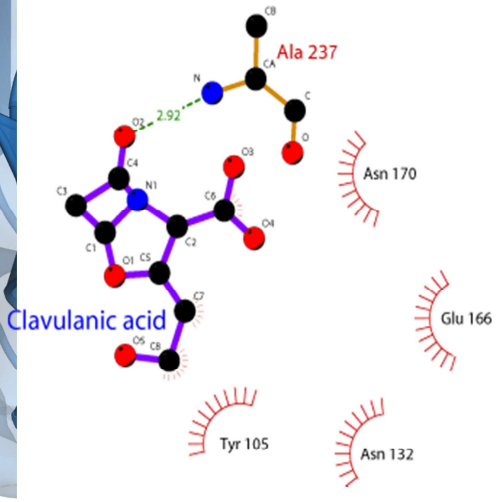

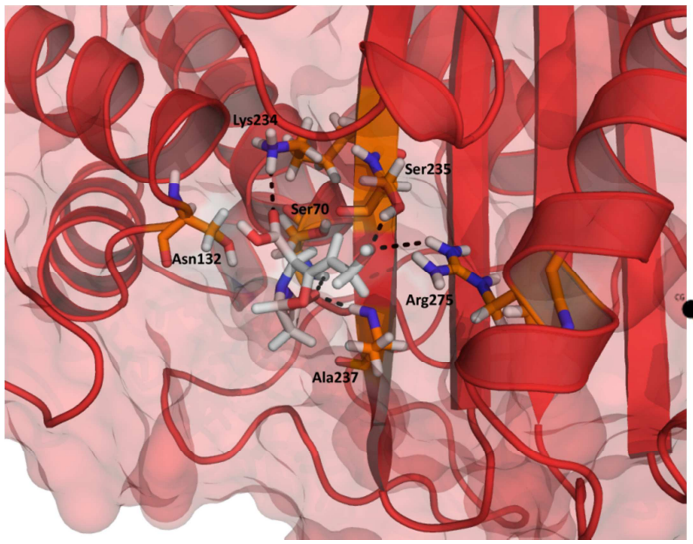

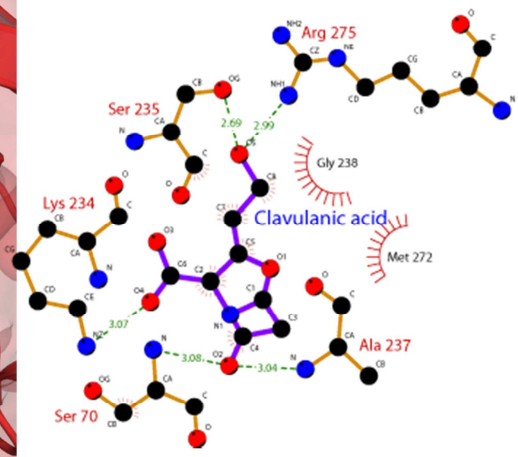

Figure 23: On the left panels are the complexes structures rendered in pymol[112] (blue for TEM-180, red for TEM-201 and green for TEM-1) and on the right panels are interaction maps made with ligplot[108]. The complexes correspond to the average structures from the MD simulations.

4.3.2. Analysis of complexes with Amoxicillin

The analysis of the interface with ASM (Table 11) shown that TEM-180 has more HS than the other two enzymes: Lys73 ($\Delta\Delta G_{binding}$=3.23 ± 0.62 kcalmol^{-1}), Tyr105 ($\Delta\Delta G_{binding}$=3.72 ± 0.61 kcalmol^{-1}), Asn132 ($\Delta\Delta G_{binding}$=2.11 ± 0.64 kcalmol^{-1}), Glu166 ($\Delta\Delta G_{binding}$=5.97 ± 0.0.7 kcalmol^{-1}) and Asn170 ($\Delta\Delta G_{binding}$=3.62 ± 0.65 kcalmol^{-1}).It is important to notice that the backbone of Ser70 and Ala237 form H-bridges with amoxicillin (Figure 24). The HS in this protein help to stabilize the ligand through hydrophobic interactions. Asn residues and Tyr105 are capable of forming H-bridges with the nitrogen and oxygen atoms from the side chain helping with its stabilization (Figure 24).

TEM-201 presented Glu166 ($\Delta\Delta G_{binding}$=8.49 ± 0.74 kcalmol^{-1}) and Glu239 ($\Delta\Delta G_{binding}$=7.86 ± 0.72 kcalmol^{-1}) as HS because (Table 11) these residues stabilize the ligand with H-bonds and hydrophobic interactions. Glu166 has an important role on the orientation and stabilization of the bicyclic structure and Glu239 helps protecting the aromatic side chain from the solvent and it stabilizes the aromatic ring. Ala237 have shown through the entire MD simulation a major role in stabilizing both the bicyclic structure. Its lateral side chain interacts with the antibiotic through H-bonds (backbone atoms) (Figure 24).

TEM-1 has Tyr105 ($\Delta\Delta G_{binding}$=2.95 ± 0.67 kcalmol^{-1}) and Glu166 ($\Delta\Delta G_{binding}$=7.18 ± 0.56 kcalmol^{-1}) as HS (Table 11). Tyr105 helps shielding the ligand from solvent and it stabilizes the lateral side chain of amoxicillin with its fenol structure. Glu166 helps stabilizing the bicyclic structure of the antibiotic with hydrophobic interactions. Although Asn132 does not have a $\Delta\Delta G_{binding}$ of 2Kcalmol^{-1} or higher (Table 11), it still forms strong interactions with the polar atoms near the β-lactam ring (Figure 24).

The only complex where it was possible to observe a conserved water molecule placed, most of the time near Glu166, was in complex TEM-201/amoxicillin. The fact that it is not observed in TEM-1 might justify why the catalytic activity against amoxicillin is inferior when compared to ampicillin (highly conserved water molecule near Glu166). Although in TEM-180/amoxicillin MD simulations, the presence of a water molecule near Glu166 is

inferior to 25% of the MD simulation time, it is still important to highlight that it has a highly conservative water molecule near Lys73. Lys73 has been previously described as a possible first base for the acylation process, and therefore can help to overcome the deficiency of a conserved water molecule near Glu166. It will lead to acylation of the antibiotic and biologic resistance to the antibiotic.

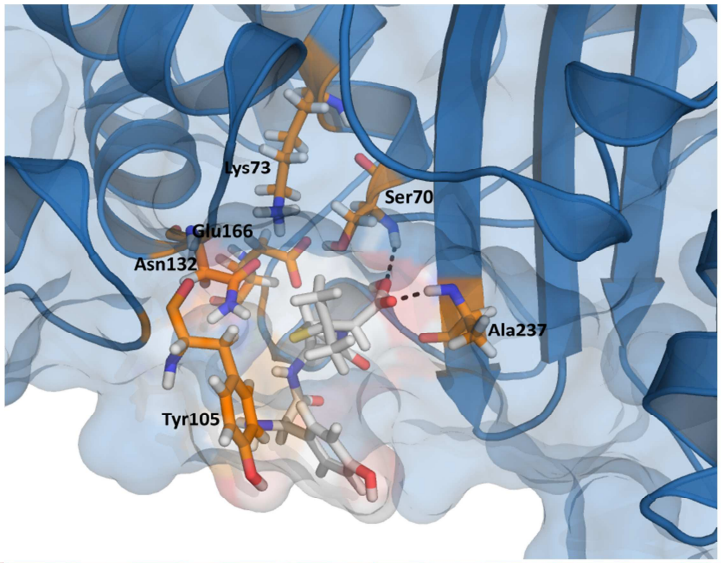

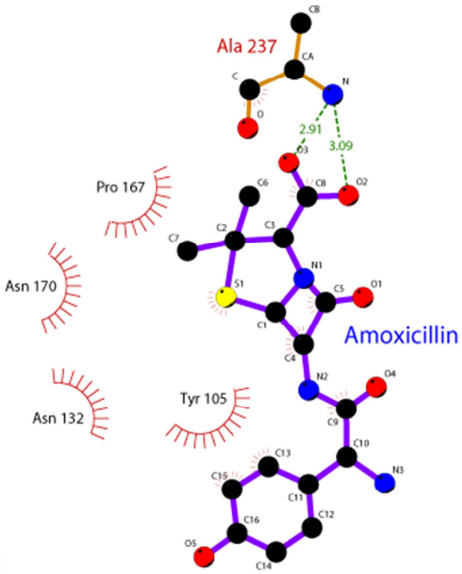

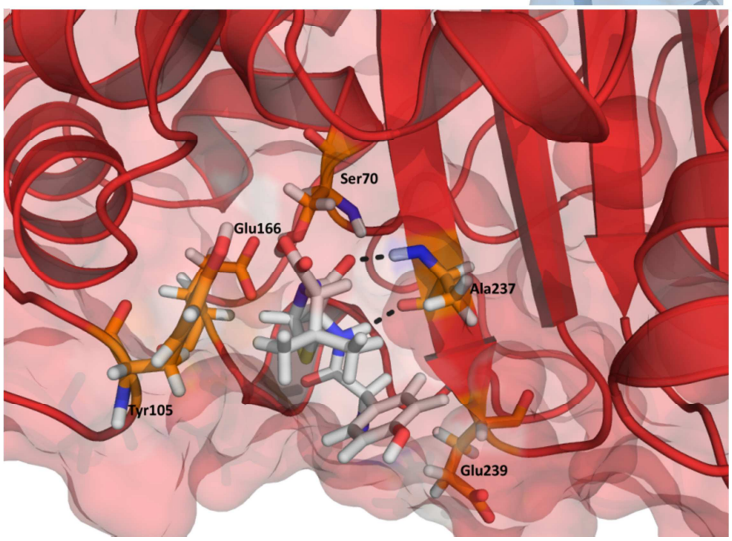

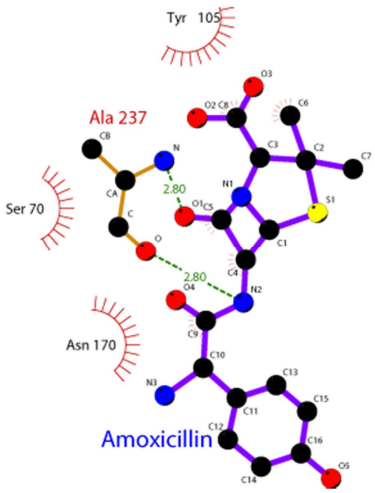

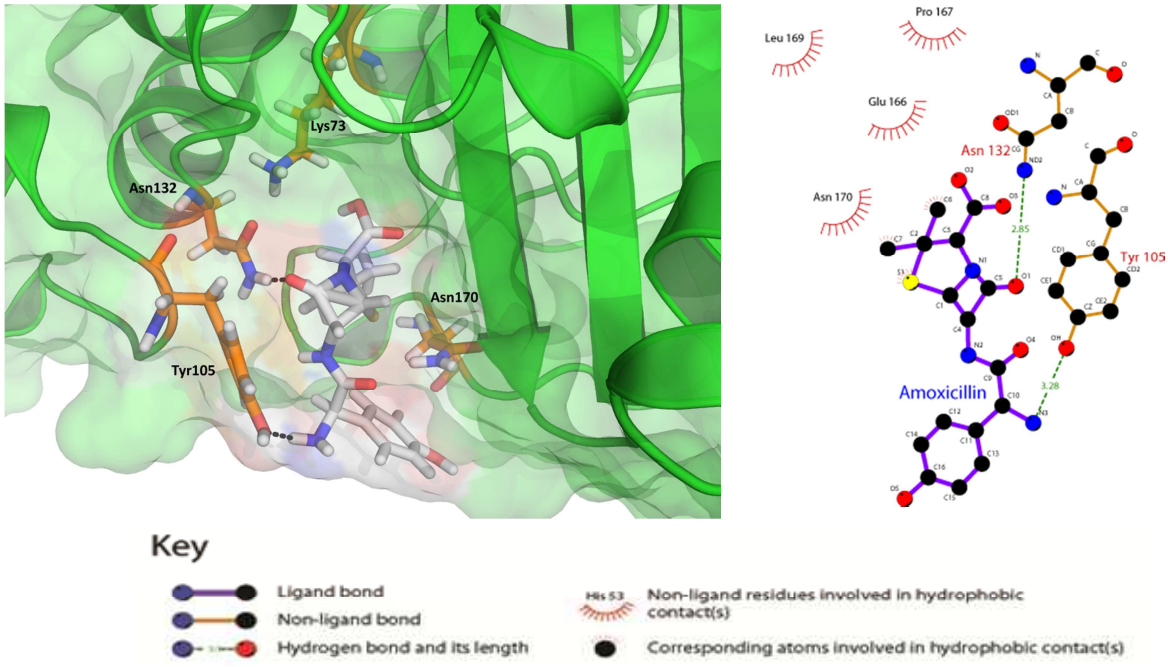

Figure 24: On the left panels are the complexes structures rendered in pymol[112] (blue for TEM-180, red for TEM-201 and green for TEM-1) and on the right panels are interaction maps made with ligplot[108]. The complexes correspond to the average structures from the MD

4.3.3. Analysis of complexes with Ampicillin

The complex TEM-180/ampicillin presented multiple HS (Table 11). Lys73 ($\Delta\Delta G_{binding}$=2.42 ± 0.72 kcalmol^{-1}), Tyr105 ($\Delta\Delta G_{binding}$=4.35 ± 0.77 kcalmol^{-1}) and Val216 ($\Delta\Delta G_{binding}$=2.76 ± 0.87 kcalmol^{-1}) are important for the binding of the antibiotic mainly because of the stabilization of the ligand *via* hydrophobic interactions while Asn132 (ΔΔGbinding=3.77 ± 0.73 kcalmol-1) and Glu166 ($\Delta\Delta G_{binding}$=1.24 ± 0.073 kcalmol^{-1} – not a HS) stabilize ampicillin's side chain with H-bonds. The interaction of this antibiotic with residues in the β3 chain is present through the entire simulation with particularly relevance of residues Gly236 and Ala237. Other interactions have been observed but with less significance.

The complex formed with TEM-201 also has multiple HS (Table 11). Lys73 ($\Delta\Delta G_{binding}$=2.19 ± 0.60 kcalmol^{-1}) and Tyr105 ($\Delta\Delta G_{binding}$=3.59 ± 0.61 kcalmol^{-1}) fulfill the same role as in the previously described complex. However, in this complex Glu166 ($\Delta\Delta G_{binding}$=2.41 ± 0.61 kcalmol^{-1}) and Asn170 ($\Delta\Delta G_{binding}$=5.41 ± 0.66 kcalmol^{-1}) also help to stabilizing the side chain of ampicillin with hydrophobic interactions as well but also with H-bonds (Figure 25). Asn 132 and Lys234 are also HS. Asn132 ($\Delta\Delta G_{binding}$=3.53 ± 0.60 kcalmol^{-1}) forms an H-bond with the oxygen in the side chain and Lys234 ($\Delta\Delta G_{binding}$=3.61 ± 0.67

kcalmol^{-1}) with the oxygen atom in the substituents of the bicyclic structure. Ala237 has also shown great importance by stabilizing the side chain with an H-bridge between its nitrogen atom and the oxygen from the carbonyl group in the β-lactam ring and between its oxygen and the nitrogen in the antibiotic side chain. Several other interactions have been identified, and although alone might not represent a great effect of the ligand binding, together might have reasonable effect (Figure 25).

TEM-1 presented only Lys73 ($\Delta\Delta G_{binding}$=2.30 ± 0.85 kcalmol^{-1}) and Tyr105 ($\Delta\Delta G_{binding}$=4.03 ± 0.88 kcalmol^{-1}) as HS because of their interactions with the core of the antibiotic (hydrophobic interactions) and the aromatic ring (π-π interactions) respectively.

Residues Asn170, Lys234 and Glu239 have shown inferior $\Delta\Delta G_{binding}$ (Table 11) than the previously discussed residues but they still show considerable importance for the interaction. Asn170 and Glu239 help stabilizing the ampicillin side chain, while Lys234 interacts with the methyl groups of the bicyclic structure (Figure 25). Like before, Ala237 have shown interaction with the antibiotic through the entire MD simulation.

The activity of the variants might still be inferior against ampicillin due to the fact that the conserved water molecule near Glu166 suffers displacement and is present near this residue less than 25% of the time in the MD simulation. The H-bond network is maintained almost through all the MD simulation being both the backbone and side chain of the residues involved more stable in the variants that in TEM-1.

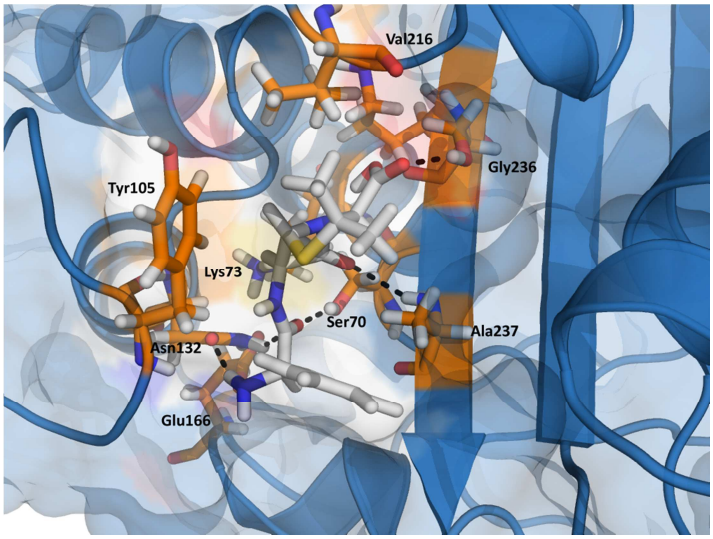
Val216
Gly236
Tyr105
Lys73
Ser70
Asn132
Ala237
Glu166

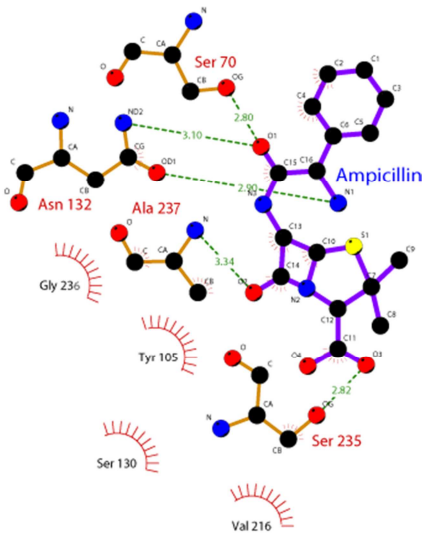
Ser 70
Ampicillin
Asn 132
Ala 237
Gly 236
Tyr 105
Ser 235
Ser 130
Val 216

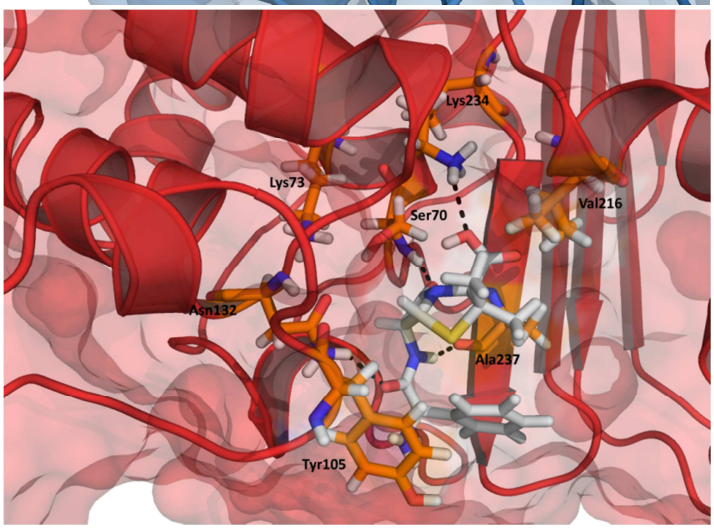
Lys234
Lys73
Ser70
Val216
Asn132
Ala237
Tyr105

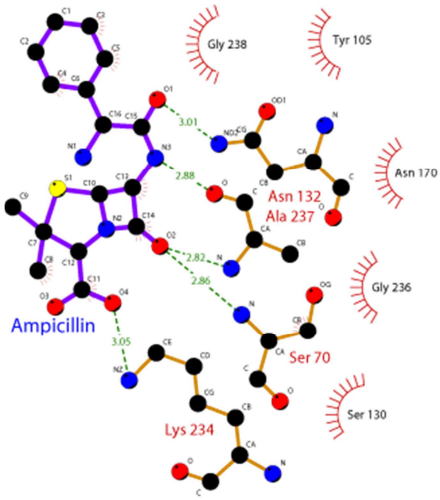
Gly 238
Tyr 105
Asn 170
Asn 132
Ala 237
Gly 236
Ampicillin
Ser 70
Ser 130
Lys 234

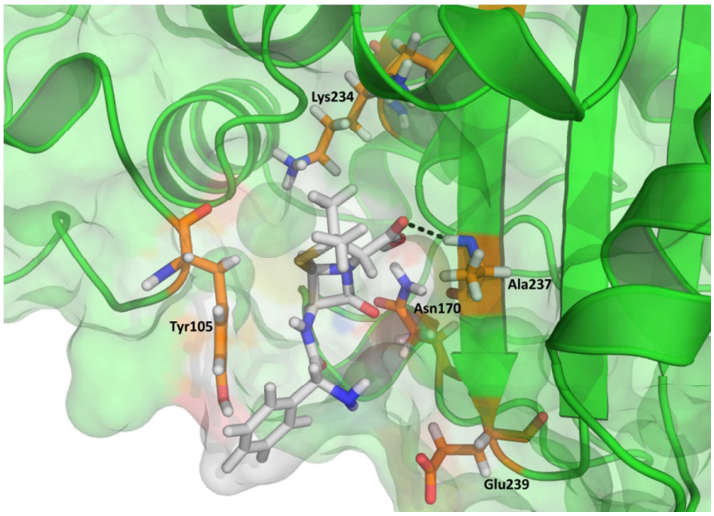
Lys234
Ala237
Asn170
Tyr105
Glu239

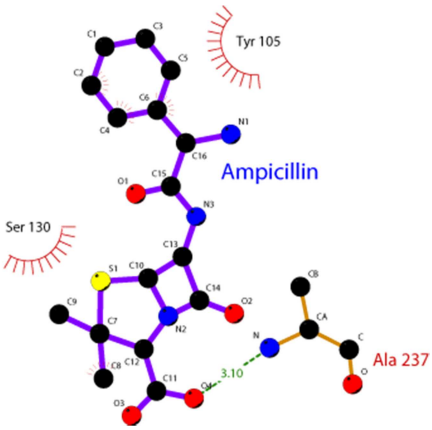
Tyr 105
Ampicillin
Ser 130
Ala 237


Key
Ligand bond
Non-ligand bond
Hydrogen bond and its length
His 53
Non-ligand residues involved in hydrophobic contact(s)
Corresponding atoms involved in hydrophobic contact(s)

Figure 25: On the left panels are the complexes structures rendered in pymol[112] (blue for TEM-180, red for TEM-201 and green for TEM-1) and on the right panels are interaction maps made with ligplot[108]. The complexes correspond to the average structures from the MD

4.3.4. Analysis of complexes with Cefpirome

The ASM analysis of the interface TEM-180/Cefpirome showed Lys73 ($\Delta\Delta G_{binding}$=4.59 ± 0.93 kcalmol^{-1}), Asn170 ($\Delta\Delta G_{binding}$=2.64 ± 0.95 kcalmol^{-1}), Val216 ($\Delta\Delta G_{binding}$=2.94 ± 1.03 kcalmol^{-1}) and Lys234 ($\Delta\Delta G_{binding}$=5.12 ± 1.00 kcalmol^{-1}) as HS (Table 11). With the exception of Asn170, all of them help positioning and stabilizing the ligand with hydrophobic interaction (Asn170 forms H-bonds with the polar atoms from the ligand side chain - Figure 27). In this complex Lys234 does not interact with the ligand *via* H-bonds because its side chain does not stay extended towards the catalytic pocket.

Ala237 is of great importance in the ligand binding, stabilizing both β-lactam ring and side chain with H-bonds.

The ASM analysis of the interface TEM-201/Cefpirome appointed Lys73 ($\Delta\Delta G_{binding}$=10.66 ± 0.73 kcalmol^{-1}), Tyr105 ($\Delta\Delta G_{binding}$=2.58 ± 0.61 kcalmol^{-1}), Asn170 ($\Delta\Delta G_{binding}$=2.56 ± 0.68 kcalmol^{-1}), Val216 ($\Delta\Delta G_{binding}$=2.00 ± 0.67 kcalmol^{-1}) and Lys234 ($\Delta\Delta G_{binding}$=10.34 ± 0.66 kcalmol^{-1}) as HS (Table 11).

Lys73 and Lys234 interact with the oxygen atoms from the bicyclics substituents (H-bonds) and Asn170 with the atoms at the end of the side chain (hydrophobic interactions and H-bonds). As in TEM-180, Val216 is a HS because in these complexes a high complementary can be achieved between the methyl groups from the Valine residue and the rings present in the substituent of the antibiotic (Figure 27).

Tyr105 clearly shows that it interacts with the side chain of Cefpirome forming H-bonds. However, most likely its important role comes from its ability to have π-π interactions with the ring in the antibiotic side chain.

Like in TEM-180, in the complex TEM-201/Cefpirome Ala237 stabilizes the β-lactam ring and the side chain with H-bonds.

The average distance in the TEM-180/Cefpirome complex between Ser70 and Lys73 has increased. However, during a big part of the MD simulation it is still at an acceptable

distance, so that the H-bond network is still functional (Figure 26). In TEM-201/Cefpirome no major differences have been observed in the H-bond triad (Table 10).

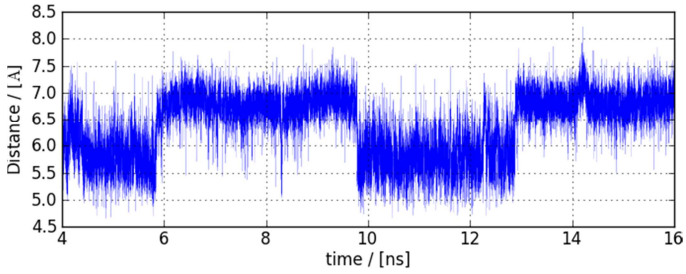

Figure 26: Graphical representation of the distance between Ser70-Oγand Lys73-Nζ during the simulation in TEM-180

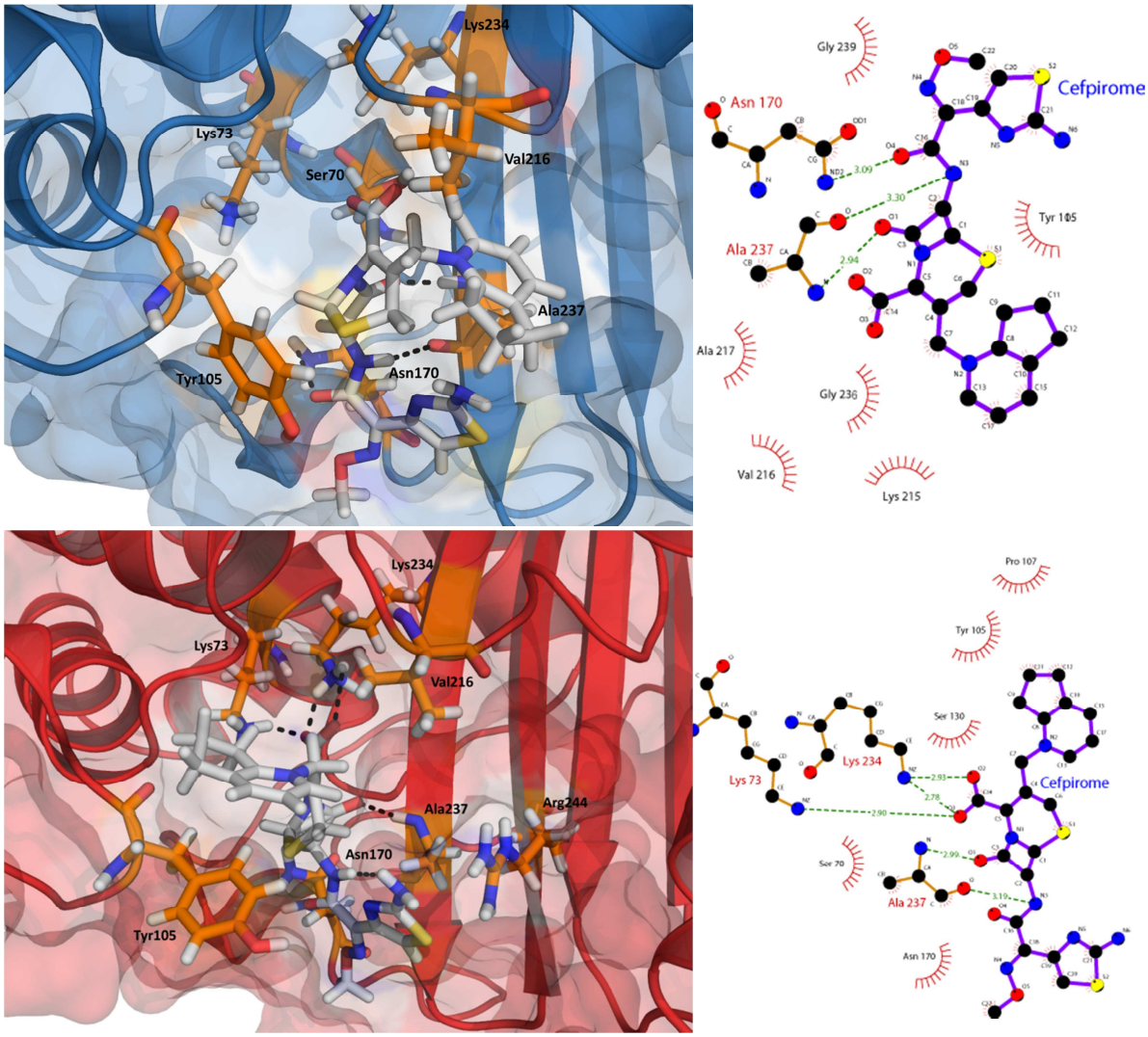

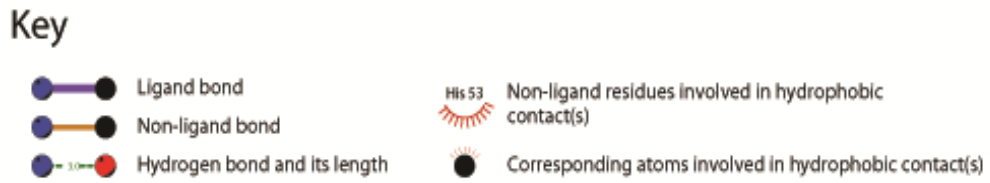

Figure 27: On the left panels are the complexes structures rendered in pymol[112] (blue for TEM-180 and red for TEM-201) and on the right panels are interaction maps made with ligplot[108]. The complexes correspond to the average structures from the MD

4.3.5. Analysis of complexes with Imipenem

In TEM-180/Imipenem complex Tyr105 and Glu166 have been detected as HS with $\Delta\Delta G_{binding}$=4.41 ± 0.67 kcalmol-1 and $\Delta\Delta G_{binding}$=5.84 ± 0.69 kcalmol-1, respectively (Table 11). Glu166 shows complementary between the carbon atoms in its side chain and the carbon atoms in the substituents near the β-lactam ring (Figure 28). It is possible that Glu166 interacts *via* H-bonds with the hydroxyl group of the same substituents. Tyr105 helps stabilizing the long side chain of Imipenem and it can have some complementary with the ring next to the β-lactam ring (Figure 28). Ala237 and Ser70 have shown to interact with the ligand during most of the simulation through H-bonds.

ASM of the interface TEM-201/Imipenem has shown that Lys73 ($\Delta\Delta G_{binding}$=2.38 ± 0.79 kcalmol-1), Tyr105 ($\Delta\Delta G_{binding}$=4.06 ± 0.70 kcalmol-1) and Glu166 ($\Delta\Delta G_{binding}$=6.89 ± 0.68 kcalmol-1) as HS (Table 11). Tyr105 has high complementary between its aromatic ring and the bicyclic structure of the antibiotic (Figure 28). Glu166 and Lys73 help with the stabilization of the bicyclic structure of the antibiotic. Ala237 kept constant interactions with the ligand through all the MD simulation.

In this complex, it is possible to observe that Arg244 interacts with the oxygen from one of the bicyclic structure substituents. It is notable that these ligands remain partially in contact with solvent causing destabilizing effects. It is the result of the Tyr105 not acting as a gate keeper fully locking the catalytic pocket, due to the size and freedom of movement of the long lateral side chain.

The H-bond network is very stable for these complexes (Table 8) and the distances between Ser70, Lys73 and Glu166 remains stable and within distances acceptable for the H-bond network to be functional (Table 10).

A conserved water molecule was identified in TEM-180/Imipenem near Glu166 during most of the MD simulation, while for TEM-201/Imipenem no water molecule near this residue was identified longer than 25%. It is important to refer that despite this fact, it is possible that a catalytic triad is formed with other residue or even a water molecule. We have also identified a conserved water molecule within 5Å of Ser130, Lys73 and Ser70. Any of these residues is capable of replacing the role of Glu166 as first base in the acylation process when near a water molecule, leading to acylation of the antibiotic.

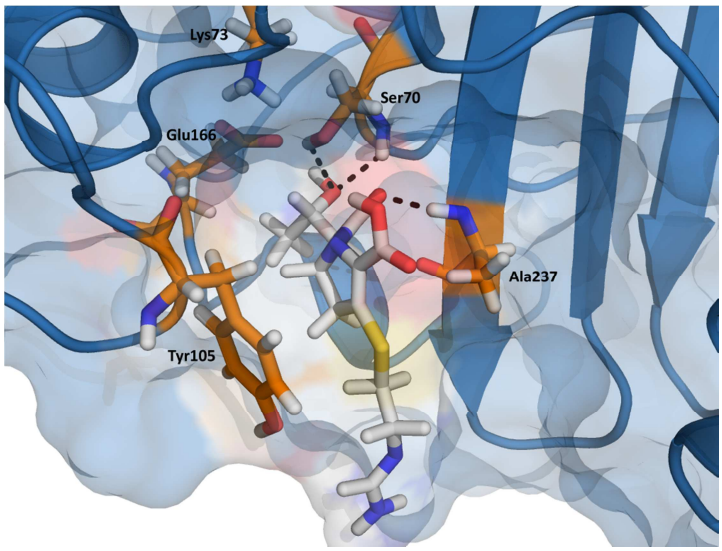

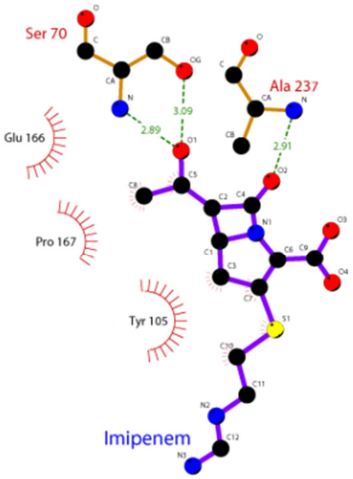

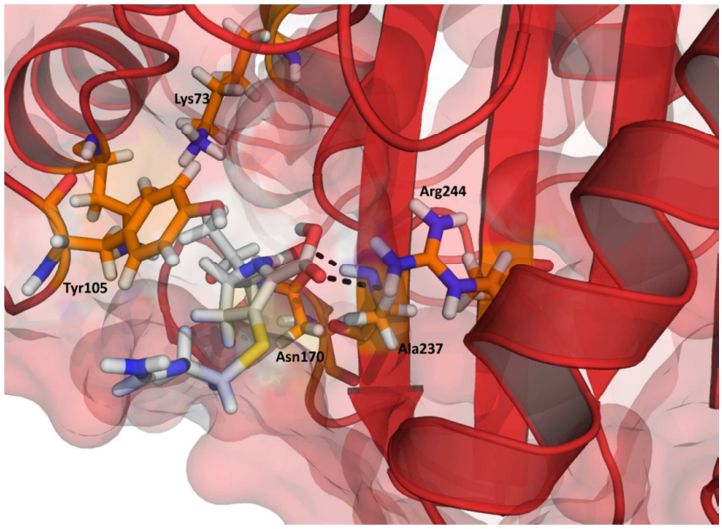

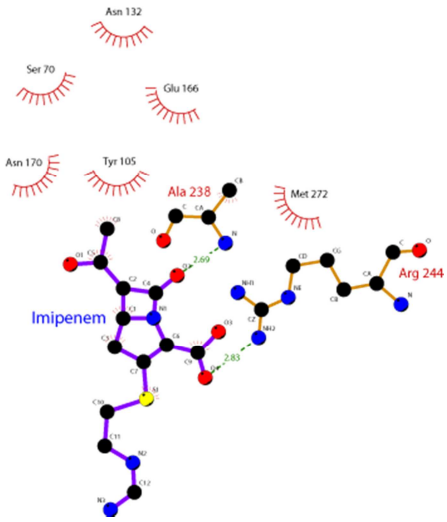

Figure 28: On the left panels are the complexes structures rendered in pymol[112] (blue for TEM-180 and red for TEM-201) and on the right panels are interaction maps made with ligplot[108]. The complexes correspond to the average structures from the MD simulation

4.3.6. Analysis of complexes with Meropenem

In the complex with TEM-180, Ser70, Lys73, Asn132 and Glu166 interact with the acidic group *via* H-bridges and Ser70 also interacts with the oxygen from the carboxylic group of the β-lactam ring. Tyr105 is involved in hydrophobic interactions with the bulky side chain and Val216 interacts with the methyl group of the substituents. Asn170 acts as the back wall of the catalytic pocket and contributes for the ligand binding free energy with Meropenem mainly with hydrophobic contacts.

Of all these residues Lys73 ($\Delta\Delta G_{binding}$=6.80 ± 0.86 kcalmol^{-1}), Tyr105 ($\Delta\Delta G_{binding}$=3.23 ± 0.78 kcalmol^{-1}), Glu166 ($\Delta\Delta G_{binding}$=4.81 ± 0.80 kcalmol^{-1}) and Asn170 ($\Delta\Delta G_{binding}$=3.95 ± 0.83 kcalmol^{-1}) have shown to have a greater effect on ligand binding energy than the rest of the residues in the interface (Table 11).

The ASM analysis of the interface of the complex TEM-201/Meropenem (Table 11) has shown less HS than for TEM-180: Tyr105 with $\Delta\Delta G_{binding}$=3.31 ± 0.52 kcalmol^{-1} and Asn170 with ($\Delta\Delta G_{binding}$=2.61 ± 0.54 kcalmol^{-1}).However, it has other important interactions that help stabilizing the bicyclic structure of the antibiotic (Ser70 and Lys234). Tyr105 has complementary with one of the rings of the core of the antibiotic but it has even more complementary (hydrophobic contacts with one of the substituents). The trade-off of this interaction might be less protection of the antibiotic from the solvent, which can have a destabilizing effect of the complex.

Asn170 stabilizes the ring present in the side chain and the oxygen from the carbonyl group of the tertiary amide.

In both complexes Glu239 interacts with the tertiary amine group of Meropenem side chain, which helps keeping the side chain of the antibiotic close to β3 allowing Ala237 to interact with the acidic group of the antibiotic with H-bonds. Glu239 might also help protecting the tertiary amine group from solvent.

In the complex TEM-201/Meropenem a highly conserved water molecule is presented near Glu166, which was not observer for the TEM-180/Meropenem complex.

As with other complexes, described previously, a new water molecule was identified near Lys73 and Ser130 for more than 40% of the MD simulation time. It might give the enzyme

the capability to hydrolyze this antibiotic, and therefore leads to biological antibiotic resistance.

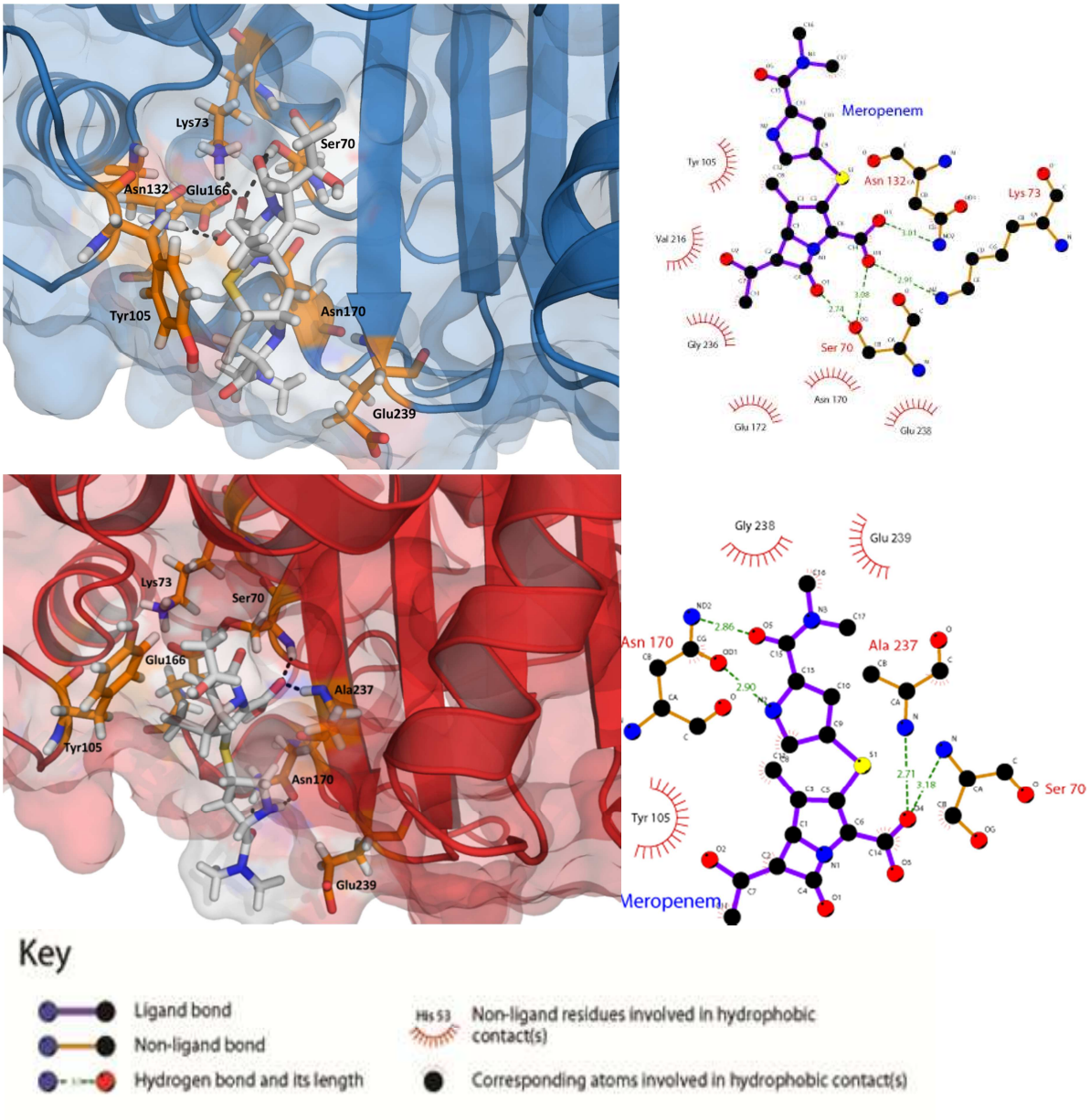

Figure 29: On the left panels are the complexes structures rendered in pymol[112] (blue for TEM-180 and red for TEM-201) and on the right panels are interaction maps made with ligplot[108]. The complexes correspond to the average structures from the MD simulation

4.3.7. Analysis of complexes with Methicillin

As described before, Methicillin inside the catalytic pocket of TEM-180 has an erratic behavior. So the structure represented above does not represent all the geometries observed for this ligand. The results from ASM (Table 11) indicate that there is only one HS (Tyr105 with $\Delta\Delta G_{binding}$=5.82 ± 0.56 kcalmol^{-1}) and that is due to the fact that this residue shows complementary either with the aromatic ring in the side chain (π-π interactions) and with the core of the antibiotic. There have also been identified other relevant residues (Lys73 and Asn170) due to their capability to form H-bonds with the polar atoms that in this ligand are present in great quantity.

In the complex TEM-201/Methicillin the same HS has been identified (Tyr105 with $\Delta\Delta G_{binding}$=2.38 ± 0.65 kcalmol^{-1}) but in this complex it only interacts with the bicyclic structure of the antibiotic and its methyl substituents.

The residues Asn170 and Glu239 have shown to be important to the stability of the complex, the first because it helps stabilizing the core of the antibiotic (hydrophobic contacts) and the latter for its complementary with the ortho-dimethoxyphenyl group, which also helps avoiding hindrance of the side chain.

Near Glu166 water molecules have been identified in both complexes but in none of the cases was identified one that stayed for more than 25% of the MD simulation time. Highly conserved water molecules were identified near Ser70 for both complexes and other near Lys73 for TEM-180/Methicillin.

It is important to refer that although there is not a conserved water molecule near Glu166 or in the case of the complex with TEM-201, near Lys73.

Other data that supports the strong possibility of these TEM variants being capable of acylate Methicillin is the fact that the distance between the Oγ of Ser70 (performs the nucleophilic attack after hydrogen abstraction by other base) and the carbon from the carbonyl group (C5) of the β-lactam ring is small through the MD simulation – maximum distance of 10Å with an average of 8 Å for TEM-201 and an average of 7Å for TEM-180.(Figure 30). Although these distances are high it is important to note that along the MD simulation much lower values can be found (less than 6 Å).

The number of water molecules at 4Å of Ser70 has also increased when compared to other complexes (4.76Å in TEM-180 and 3.56Å in TEM-201. In other complexes the number of water molecules at 4Å of this residue is usually lower than 1.5). The presence of new water molecules near this residue might also give the capability to acylate this antibiotic with the nucleophilic attack being performed by a water molecule.

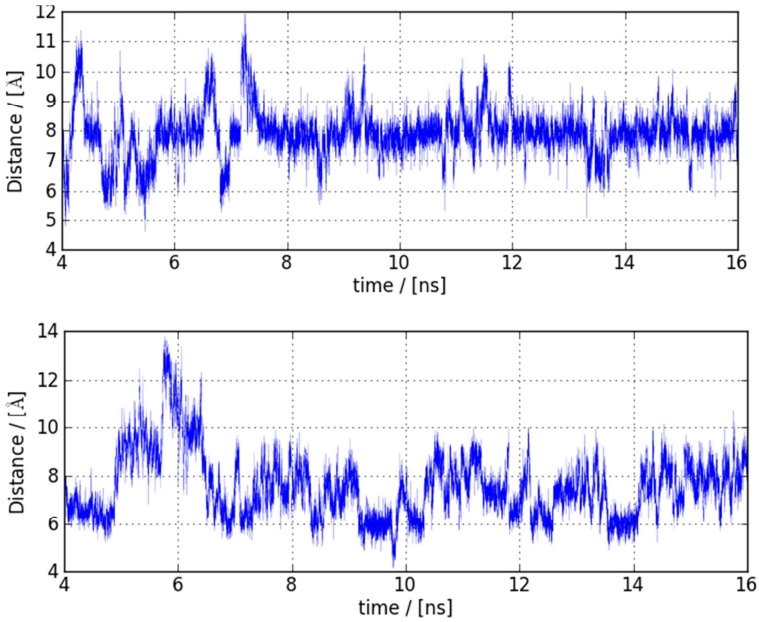

Figure 30: Graphical representation of the distance between Ser70-Oγ and Methicillin-C5 along the MD simulation, for the complexes TEM-201/Methicillin (A) and TEM-180/Methicillin (B).

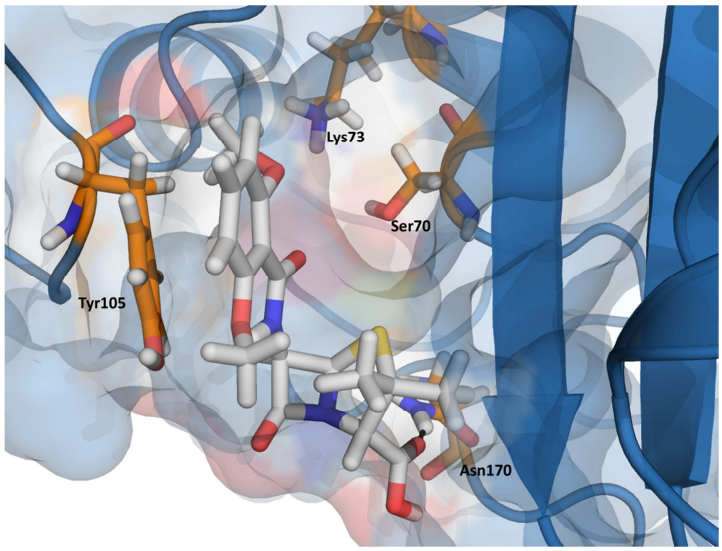

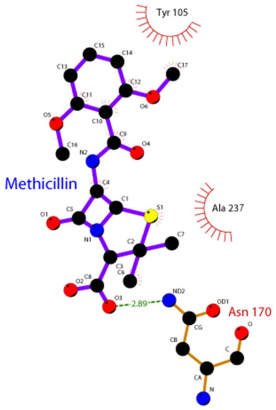

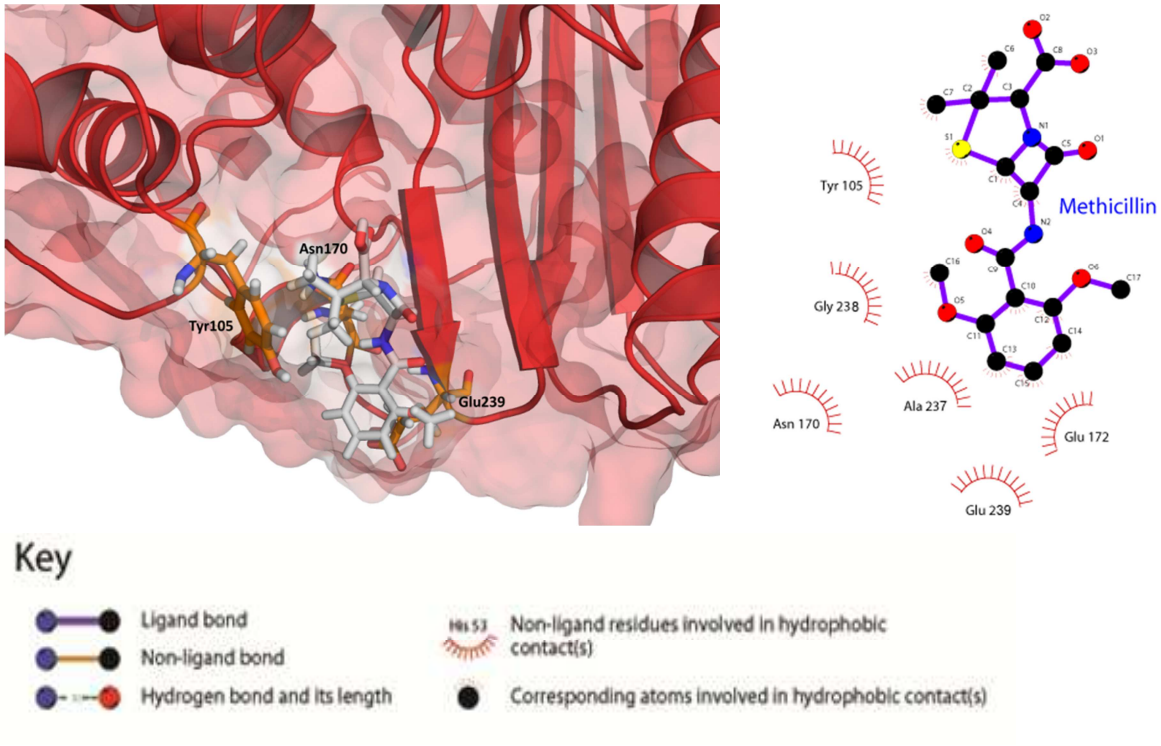

Figure 31: On the left panels are the complexes structures rendered in pymol[112] (blue for TEM-180 and red for TEM-201) and on the right panels are interaction maps made with ligplot[108]. The complexes correspond to the average structures from the MD

4.3.8. Hot spot analysis

As proposed with the O-ring structure, HS have shown to be shielded from water molecules. Even Tyr105 directly faces the solvent and has an important role in protecting the catalytic pocket from it, it still presents low number of water molecules for all the complexes when compared with other exposed residues. In all complexes this residue have shown similar behavior for RDFs even when it is not detected as HS. Therefor only one graphic of the calculated RDFs is shown as an example (Figure 32).

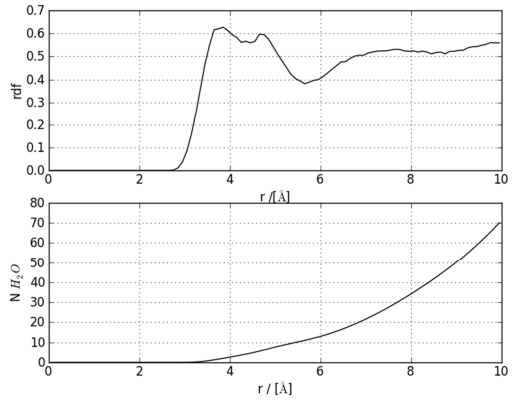

Figure 32: Graphical representation of the calculated RDFs of Tyr105, for the TEM-180/Ampicillin complex.

Glu239 that has been identified as HS in TEM-201/Amoxicillin complex ($\Delta\Delta G_{binding}$=7.86 ± 0.72 kcalmol^{-1}) and in other complexes has been identified as being important for the binding (Table 11). Glu239 is located in the extremity of β3 and has a relevant role for the stabilization of the ligand (discussed in sections 4.3.1 to 4.3.7). Due to its location is expected to have contact with water molecules and even protect the ligand from it.

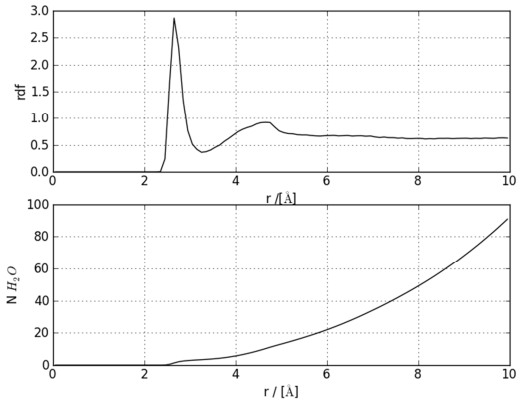

Figure 33: Graphical representation of the calculated RDFs of Glu239, for the TEM-201/Amoxicillin complex.

It is noticeable that residues that present a higher number of water molecules for all complexes have never been identified as HS, with the exception of the previously discussed Glu239 in TEM-201/Amoxicillin complex. This is, again in agreement with the proposed O-ring theory.

Because of the limitations of the ASM methodology (previously discussed in section 1.4.7) contributions of the backbone atoms cannot be estimated and Ala and Gly residues could not be analyzed with this protocol. As shown in the analysis of the complexes (sections 4.3.1-4.3.7) Ala237 has an important role for the stabilization of the ligand molecule for several complexes due to its capability to form H-bonds between its amino and carbonyl groups and the polar atoms of the ligand (both in the bicyclic structure and side chain). Therefore, this residue is likely to have a great contribution for the free binding energy of the various complexes

5. Experimental results

The halos were measured and registered, after 24h at 37°C.

We chose to follow the procedure described previously (Experimental Methods) to ensure that the bacteria, which we use to perform the susceptibility tests, only produce the enzymes required for this study.

As shown in Table 12 the cloned bacteria are resistant to combinations of combinations of β-lactam antibiotics/β-lactamase inhibitors as bacteria presented a normal grow, without the formation of a halo. These combinations are TZP and APSM. Normal bacteria growth was also observed when using disks with penicillin G, FD, SXT, VA, SAM, CEC, LZD and DA. These results show that the cloned *E. coli* is resistant to these antibiotics due to the catalytic action of the TEM variants.

Several halos were measured with radii under 10mm. This might be due to the fact that the enzymes have the ability to acylate the antibiotics. Nevertheless, this acylation is not as efficient as in the cases where no halo was formed.

Table 12: Radii, in mm, of the halo observed in the antibiotic susceptibility test

	CAZ	APSM	CTX	FOX	CRO	CXM	TZP	AZM
TEM-201	12	NA	15	12	13	6	NA	10
TEM-180	11	NA	15	11	15	6	NA	9
	OX	P	CIP	NOR	LEV	MXF	F	SAM
TEM-201	NA	NA	10	10	14	10	14	NA
TEM-180	NA	NA	11	13	14	11	15	NA
	CN	FD	SXT	IMI	VA	E	TOB	DA
TEM-201	12	NA	14	15	NA	5	9	NA
TEM-180	11	NA	14	15	NA	7	10	NA
	CLR	CEC	TEC	MUP	RD	LZD		
TEM-201	5	NA	NA	6	NA	NA		
TEM-180	7	NA	NA	9	4	NA		

6. Comparison of results obtained from the methodologies followed

The complexes analyzed with the computational methodologies part were ampicillin, amoxicillin, methicillin, clavulanic acid, cefpirome, Imipenem and Meropenem. In the susceptibility experiments we used CAZ, SAM, CTX, FOX, CRO, CXM, TZP, CN, FD, SXT,IMI, VA, E, TOB, OX, P ,CIP, NOR, LEV, MXF, F, CLR, CFC, TEC, MUP, RD and L. Although many several antibiotics analyzed with computational methodologies were not tested, some are closely related (methicillin and oxacillin are very similar penicillins but oxacillin has been replacing methicillin in clinical use). The inhibitors always inhibit β-lactamases as discussed in 1.2.4 Inhibitors resistant beta lactamases - IRT and therefore, resistance to these antibiotics can be compared in this study.

The predicted activity of TEM-180 and TEM-201 with computational methods is supported by the experimental results obtained (Table 12). The ability to resist to inhibition is supported by the structural data that shows an increased distance between Ser70 and Ser130 avoiding the formation of the intermediate. Therefore, it leads to the irreversible inactivation of Ser130 and ultimately the enzyme.

Experimentally, our computational hypotheses were verified. These enzymes have the capability to acylate several penicillins, even those, classified as penicillinase-resistant penicillins (used to treat infections caused by Gram-positive bacteria such as *S. aureus*).

The cloned *E. coli* was not resistant to Imipenem and as discussed in 4.3.5 Analysis of complexes with Imipenem. It can result from the exposure of the antibiotic to the solvent molecules in TEM-180/Imipenem complex. In TEM-201/Imipenem complex, no conserved water molecule was identified near Glu166.

These results show that methodologies used in Computational Biochemistry are very reliable and can be used to justify the activity of enzymes. Although it would be possible to obtain the results experimentally, it will be time and money expensive.

Chapter IV – Conclusion & Future Prospects

7. Conclusion

The objectives proposed for this study were fulfilled. The structures of the two enzymes studied were obtained and major studied differences between them and TEM-1 were appointed. The two mutants present differences in several secondary structures. The most noticeable and also related to the phenotype presented by them are the differences observed between β3 and β4-H11 and also the displacement of the α-helices on the opposite side of the catalytic pocket, relatively to H11. These modifications are similar in TEM-180 and TEM-201, although they are more marked in TEM-201. These facts can be appointed as the reasons why these enzymes can acylate antibiotics with bulky side chain and even protect the side chain of antibiotics like methicillin from solvent allowing its degradation. The displacement of the helical structures close to Ser130 and Ser70 are likely the cause to their capability to resist to inhibition due to increased distance between these residues.

In the literature, it has been described that this type of enzymes acquires either the capability to resist to inhibition or the capability to hydrolyzed very large antibiotics. It was demonstrated in this study that both variants under study present characteristics that allow them to be simultaneously resistant to inhibition and capable of hydrolyzing large antibiotics. This might be the effect of high plasticity of the enzymes to the antibiotics, allowing them to form a strong complex with a variety of antibiotics. These complexes show significant differences in structural (orientation of side chains, presence of water molecules and modifications in secondary structures) and energetic (HS can vary depending on the antibiotic) terms.

Computational ASM have shown that some residues are responsible for an important contribution for the binding free energy in a great number of the analyzed complexes. Tyr105 was identified as HS in almost all the complexes and presented a low number of water molecules, even though is facing the exterior of the catalytic pocket. Although, Glu166 and Lys73 are typically described as very important for the acylation of antibiotics due to their role in the hydrogen transfer network, they have been identified as HS in several complexes. This shows that their role for enzymatic catalysis is not only for proton transfer but they can also play a key role in stabilization of the ligand. Ala237 could not be analyzed with computational ASM but it was an interacting residue in most complexes,

with the ligands. These interactions seem to help stabilizing the ligand (bicyclic structure and side chain).

The distance between Ser70 and Ser130 has been appointed as the reason why these enzymes resist inhibition. As described in 1.2.4 Inhibitors resistant beta lactamases - IRT, this fact usually leads to decreased acylation of other antibiotics. However, in both TEMs studied that does not appear to be the case since the cloned *E. coli* have presented resistance to several antibiotics. This has to be confirmed in further experiments.

8. Future Prospects

Given the apparent complexity of TEM-180 and TEM201, several properties need to be investigated with computational and experimental methodologies.

The next step in Computational biochemistry will be to characterize the secondary structures observed in TEM-1. This will be investigated plotting DSSP Helix/Sheet assignments and estimating the structural variance of several secondary structures.

Within the experimental methodologies, enzymatic kinetics will be calculated with several antibiotics, as well as, the ability of these plasmids to allow other bacteria (i.e. *S. aureus*) to resist to antibiotics such as methicillin and oxacillin. It is still necessary to perform susceptibility tests with all the antibiotics that were tested with computational methodologies.

Obtaining the X-ray structures of both TEM-180 and TEM-201 would also be very important.

Chapter V – Supporting information

9. Supporting Information (S.I.)

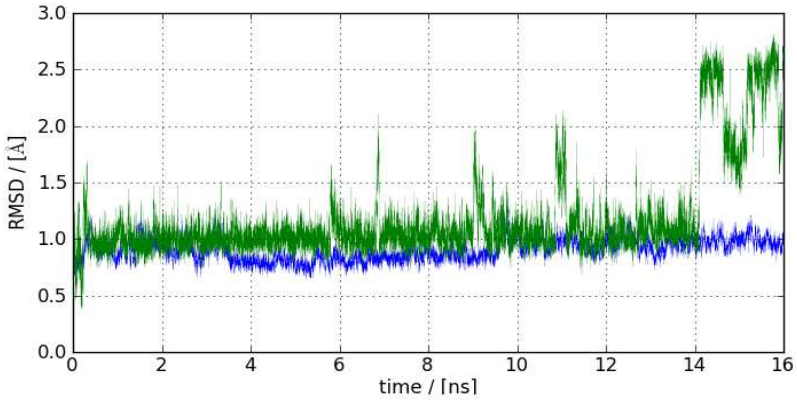

Figure 34: Graphic representation of the RMSD of the TEM-180/Amoxicillin complex. In blue is the RMSD for the protein backbone and in green the RMSD of Amoxicillin

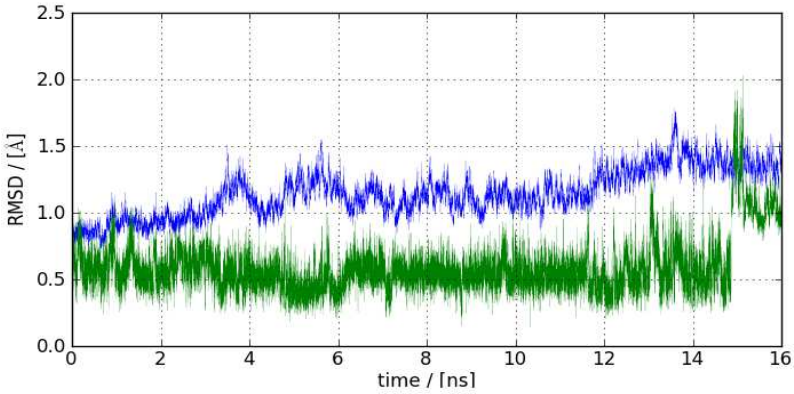

Figure 35: Graphic representation of the RMSD of the TEM-201/Amoxicillin complex. In blue is the RMSD for the protein backbone and in green the RMSD of Amoxicillin

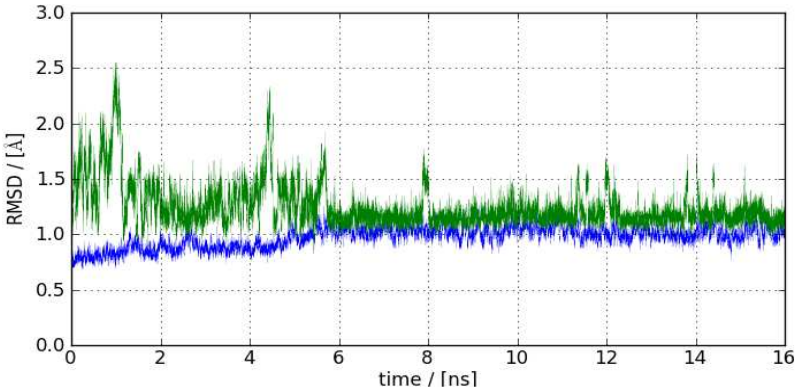

Figure 36: Graphic representation of the RMSD of the TEM-1/Amoxicillin complex. In blue is the RMSD for the protein backbone and in green the RMSD of Amoxicillin

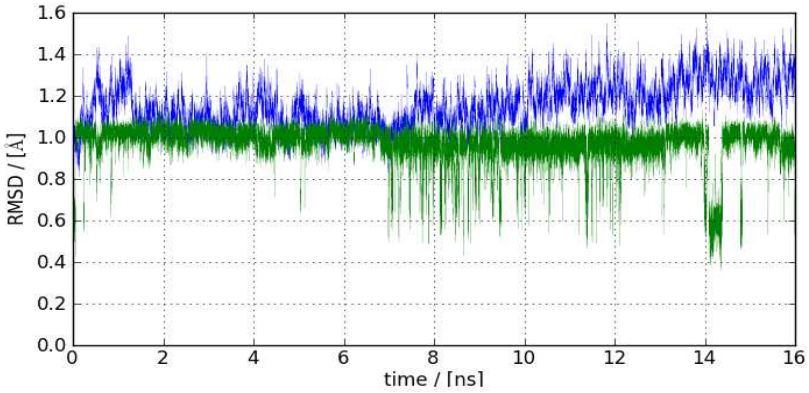

Figure 37: Graphic representation of the RMSD of the TEM-180/Clavulanic acid. In blue is the RMSD for the protein backbone and in green the RMSD of Clavulanic acid

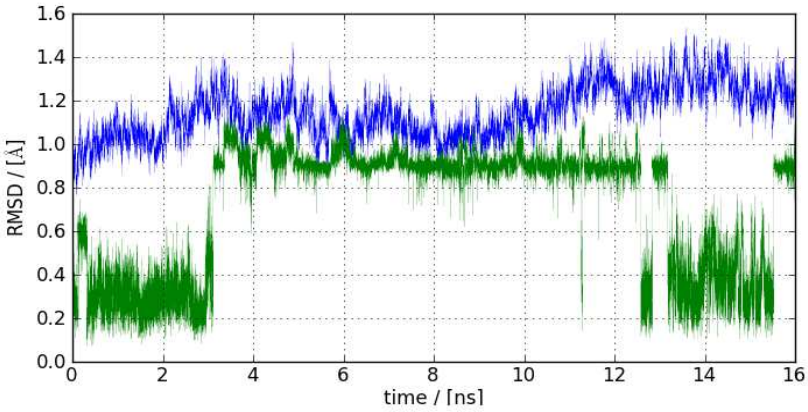

Figure 38: Graphic representation of the RMSD of the TEM-201/Clavulanic acid. In blue is the RMSD for the protein backbone and in green the RMSD of Clavulanic acid

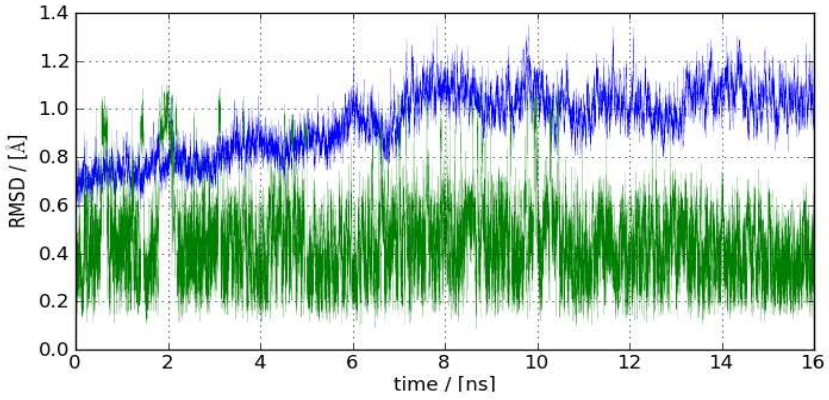

Figure 39: Graphic representation of the RMSD of the TEM-1/Clavulanic acid. In blue is the RMSD for the protein backbone and in green the RMSD of Clavulanic acid

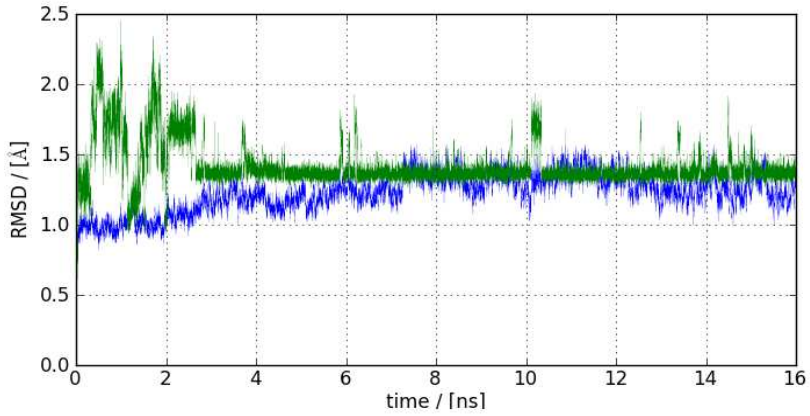

Figure 40: Graphic representation of the RMSD of the TEM-180/Cefpirome. In blue is the RMSD for the protein backbone and in green the RMSD of Cefpirome

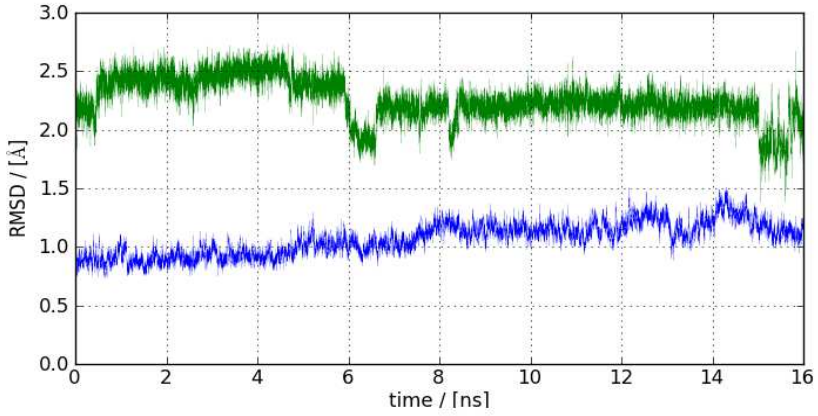

Figure 41: Graphic representation of the RMSD of the TEM-201/Cefpirome. In blue is the RMSD for the protein backbone and in green the RMSD of Cefpirome

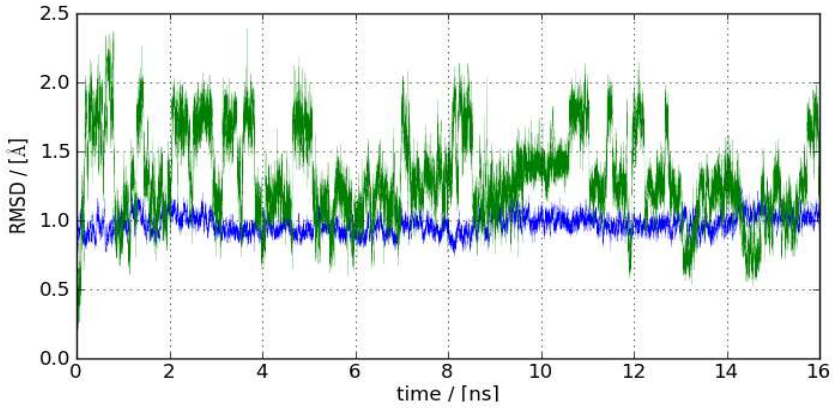

Figure 42: Graphic representation of the RMSD of the TEM-180/Imipenem. In blue is the RMSD for the protein backbone and in green the RMSD of Imipenem

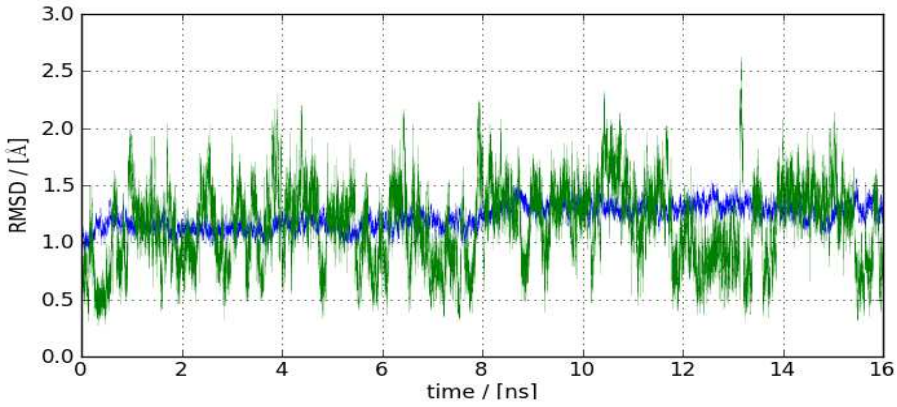

Figure 43: Graphic representation of the RMSD of the TEM-201/Imipenem. In blue is the RMSD for the protein backbone and in green the RMSD of Imipenem

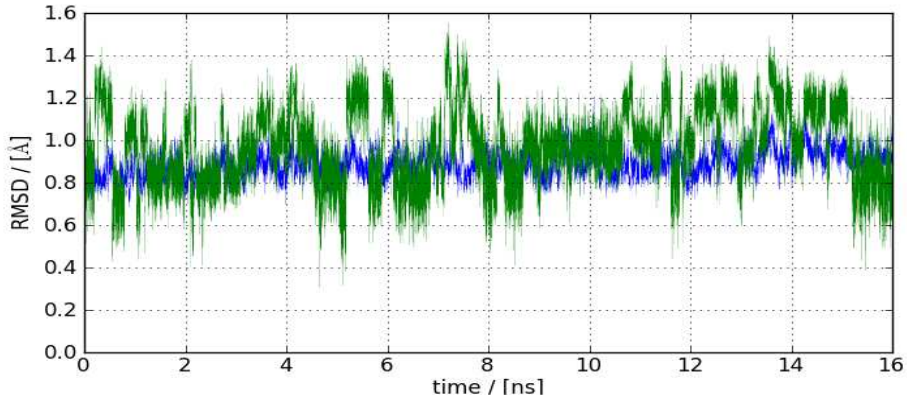

Figure 44: Graphic representation of the RMSD of the TEM-180/Meropenem. In blue is the RMSD for the protein backbone and in green the RMSD of Meropenem

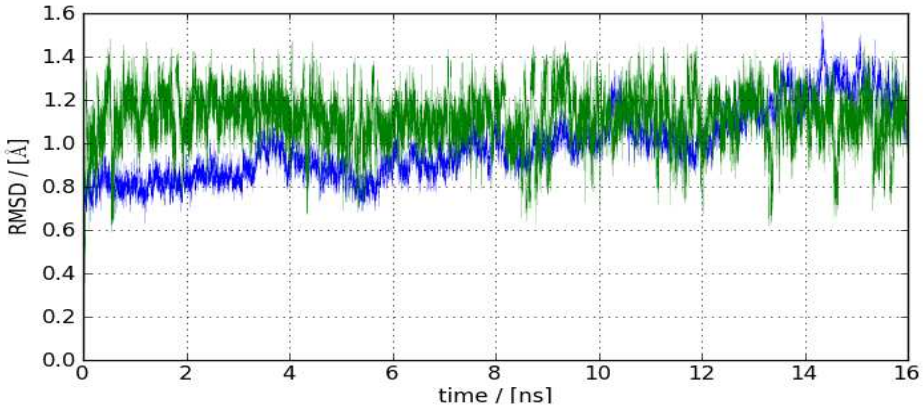

Figure 45: Graphic representation of the RMSD of the TEM-201/Meropenem. In blue is the RMSD for the protein backbone and in green the RMSD of Meropenem

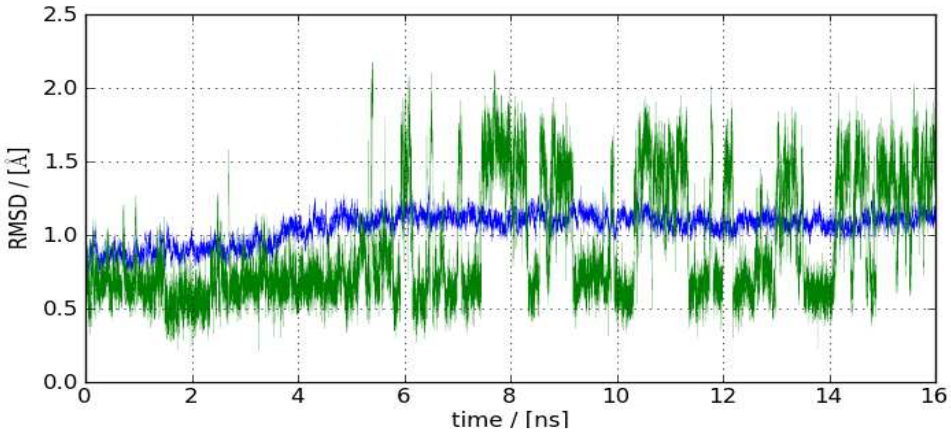

Figure 46: Graphic representation of the RMSD of the TEM-180/Methicillin. In blue is the RMSD for the protein backbone and in green the RMSD of Methicillin

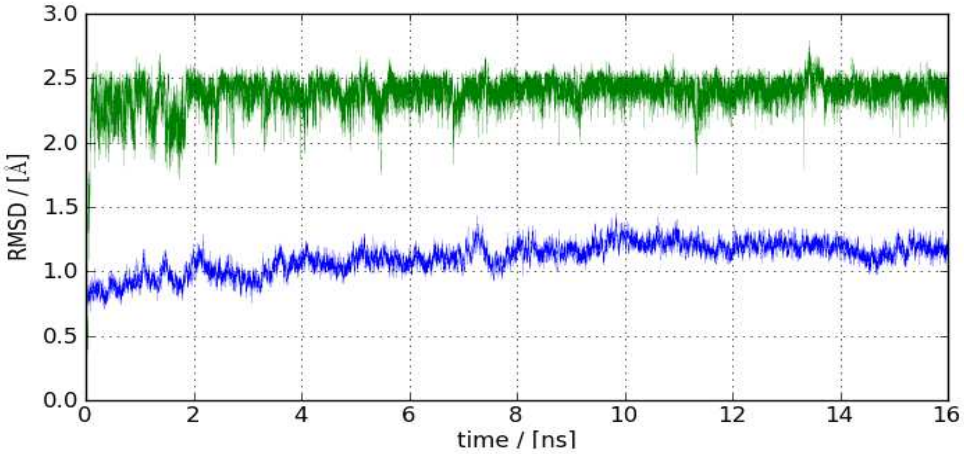

Figure 47: Graphic representation of the RMSD of the TEM-201/Methicillin. In blue is the RMSD for the protein backbone and in green the RMSD of Methicillin

Chapter VI – Bibliography

10.Bibliography

1.Bradford, P. A., Extended-spectrum beta-lactamases in the 21st century: characterization, epidemiology, and detection of this important resistance threat. *Clin Microbiol Rev* 2001, 14, 933-51, table of contents.

2.Salverda, M. L.; De Visser, J. A.; Barlow, M., Natural evolution of TEM-1 β-lactamase: experimental reconstruction and clinical relevance. *FEMS Microbiol Rev* 2010, 34, 1015-36.

3.Bush, K., The evolution of beta-lactamases. *Ciba Found Symp* 1997, 207, 152-63; discussion 163-6.

4.Bush, K., beta-Lactamases of increasing clinical importance. *Curr Pharm Des* 1999, 5, 839-45.

5.Fisher, J. F.; Meroueh, S. O.; Mobashery, S., Bacterial Resistance to β-Lactam Antibiotics: Compelling Opportunism, Compelling Opportunity†. *Chemical Reviews* 2005, 105, 395-424.

6.Llarrull, L. I.; Testero, S. A.; Fisher, J. F.; Mobashery, S., The future of the β-lactams. *Current Opinion in Microbiology* 2010, 13, 551-557.

7.Wilke, M. S.; Lovering, A. L.; Strynadka, N. C. J., β-Lactam antibiotic resistance: a current structural perspective. *Current Opinion in Microbiology* 2005, 8, 525-533.

8.Abraham Ep Fau - Chain, E.; Chain, E., An enzyme from bacteria able to destroy penicillin. 1940.

9.Bush, K.; Fisher, J. F., Epidemiological Expansion, Structural Studies, and Clinical Challenges of New beta-Lactamases from Gram-Negative Bacteria. In *Annual Review of Microbiology, Vol 65*, Gottesman, S.; Harwood, C. S., Eds. Annual Reviews: Palo Alto, 2011; Vol. 65, pp 455-478.

10.Bös, F.; Pleiss, J., Conserved Water Molecules Stabilize the Ω-Loop in Class A β-Lactamases. *Antimicrobial Agents and Chemotherapy* 2008, 52, 1072-1079.

11.Stapleton, P. D.; Shannon, K. P.; French, G. L., Construction and characterization of mutants of the TEM-1 beta-lactamase containing amino acid substitutions associated with both extended-spectrum resistance and resistance to beta-lactamase inhibitors. *Antimicrob Agents Chemother* 1999, 43, 1881-7.

12.Wang, X.; Minasov, G.; Shoichet, B. K., Evolution of an antibiotic resistance enzyme constrained by stability and activity trade-offs. *J Mol Biol* 2002, 320, 85-95.

13.Stec, B.; Holtz, K. M.; Wojciechowski, C. L.; Kantrowitz, E. R., Structure of the wild-type TEM-1 beta-lactamase at 1.55 A and the mutant enzyme Ser70Ala at 2.1 A suggest the mode of noncovalent catalysis for the mutant enzyme. *Acta Crystallogr D Biol Crystallogr* 2005, 61, 1072-9.

14.Bush, K.; Jacoby, G., Nomenclature of TEM beta-lactamases. *J Antimicrob Chemother* 1997, 39, 1-3.

15.Doucet, N.; Savard, P. Y.; Pelletier, J. N.; Gagné, S. M., NMR investigation of Tyr105 mutants in TEM-1 beta-lactamase: dynamics are correlated with function. *J Biol Chem* 2007, 282, 21448-59.

16.Bernstein, F. C.; Koetzle, T. F.; Williams, G. J.; Meyer, E. F.; Brice, M. D.; Rodgers, J. R.; Kennard, O.; Shimanouchi, T.; Tasumi, M., The Protein Data Bank. A computer-based archival file for macromolecular structures. *Eur J Biochem* 1977, 80, 319-24.

17.Fisette, O.; Morin, S.; Savard, P. Y.; Lagüe, P.; Gagné, S. M., TEM-1 backbone dynamics-insights from combined molecular dynamics and nuclear magnetic resonance. *Biophys J* 2010, 98, 637-45.

18.Minasov, G.; Wang, X.; Shoichet, B. K., An ultrahigh resolution structure of TEM-1 beta-lactamase suggests a role for Glu166 as the general base in acylation. *J Am Chem Soc* 2002, 124, 5333-40.

19.Page, M. G., Extended-spectrum beta-lactamases: structure and kinetic mechanism. *Clin Microbiol Infect* 2008, 14 Suppl 1, 63-74.

20.Meroueh, S. O.; Roblin, P.; Golemi, D.; Maveyraud, L.; Vakulenko, S. B.; Zhang, Y.; Samama, J. P.; Mobashery, S., Molecular dynamics at the root of expansion of function in the M69L inhibitor-resistant TEM beta-lactamase from Escherichia coli. *J Am Chem Soc* 2002, 124, 9422-30.

21.Thomas, V. L.; Golemi-Kotra, D.; Kim, C.; Vakulenko, S. B.; Mobashery, S.; Shoichet, B. K., Structural consequences of the inhibitor-resistant Ser130Gly substitution in TEM beta-lactamase. *Biochemistry* 2005, 44, 9330-8.

22.Massova, I.; Kollman, P. A., pKa, MM, and QM studies of mechanisms of β-lactamases and penicillin-binding proteins: Acylation step. *Journal of Computational Chemistry* 2002, 23, 1559-1576.

23.Hermann, J. C.; Pradon, J.; Harvey, J. N.; Mulholland, A. J., High level QM/MM modeling of the formation of the tetrahedral intermediate in the acylation of wild type and K73A mutant TEM-1 class A beta-lactamase. *J Phys Chem A* 2009, 113, 11984-94.

24.Brown, N. G.; Pennington, J. M.; Huang, W.; Ayvaz, T.; Palzkill, T., Multiple global suppressors of protein stability defects facilitate the evolution of extended-spectrum TEM β-lactamases. *J Mol Biol* 2010, 404, 832-46.

25.Jacoby, G. ß-Lactamase Classification and Amino Acid Sequences for TEM, SHV and OXA Extended-Spectrum and Inhibitor Resistant Enzymes. http://www.lahey.org/Studies/.

26.Wang, X.; Minasov, G.; Shoichet, B. K., The structural bases of antibiotic resistance in the clinically derived mutant beta-lactamases TEM-30, TEM-32, and TEM-34. *J Biol Chem* 2002, 277, 32149-56.

27.Brown, N. G.; Shanker, S.; Prasad, B. V.; Palzkill, T., Structural and biochemical evidence that a TEM-1 beta-lactamase N170G active site mutant acts via substrate-assisted catalysis. *J Biol Chem* 2009, 284, 33703-12.

28.Marciano, D. C.; Pennington, J. M.; Wang, X.; Wang, J.; Chen, Y.; Thomas, V. L.; Shoichet, B. K.; Palzkill, T., Genetic and structural characterization of an L201P global suppressor substitution in TEM-1 beta-lactamase. *J Mol Biol* 2008, 384, 151-64.

29.Knox, J. R., Extended-spectrum and inhibitor-resistant TEM-type beta-lactamases: mutations, specificity, and three-dimensional structure. *Antimicrob Agents Chemother* 1995, 39, 2593-601.

30.Saves, I.; Burlet-Schiltz, O.; Swarén, P.; Lefèvre, F.; Masson, J. M.; Promé, J. C.; Samama, J. P., The asparagine to aspartic acid substitution at position 276 of TEM-35 and TEM-36 is involved in the beta-lactamase resistance to clavulanic acid. *J Biol Chem* 1995, 270, 18240-5.
31.Chaïbi, E. B.; Sirot, D.; Paul, G.; Labia, R., Inhibitor-resistant TEM beta-lactamases: phenotypic, genetic and biochemical characteristics. *J Antimicrob Chemother* 1999, 43, 447-58.
32.Swarén, P.; Golemi, D.; Cabantous, S.; Bulychev, A.; Maveyraud, L.; Mobashery, S.; Samama, J. P., X-ray structure of the Asn276Asp variant of the Escherichia coli TEM-1 beta-lactamase: direct observation of electrostatic modulation in resistance to inactivation by clavulanic acid. *Biochemistry* 1999, 38, 9570-6.
33.Vakulenko, S.; Golemi, D., Mutant TEM beta-lactamase producing resistance to ceftazidime, ampicillins, and beta-lactamase inhibitors. *Antimicrob Agents Chemother* 2002, 46, 646-53.
34.Robin, F.; Delmas, J.; Schweitzer, C.; Tournilhac, O.; Lesens, O.; Chanal, C.; Bonnet, R., Evolution of TEM-type enzymes: biochemical and genetic characterization of two new complex mutant TEM enzymes, TEM-151 and TEM-152, from a single patient. *Antimicrob Agents Chemother* 2007, 51, 1304-9.
35.Chaibi, E. B.; Péduzzi, J.; Farzaneh, S.; Barthélémy, M.; Sirot, D.; Labia, R., Clinical inhibitor-resistant mutants of the beta-lactamase TEM-1 at amino-acid position 69. Kinetic analysis and molecular modelling. *Biochim Biophys Acta* 1998, 1382, 38-46.
36.Jelsch, C.; Mourey, L.; Masson, J. M.; Samama, J. P., Crystal structure of Escherichia coli TEM1 beta-lactamase at 1.8 A resolution. *Proteins* 1993, 16, 364-83.
37.Giakkoupi, P.; Hujer, A. M.; Miriagou, V.; Tzelepi, E.; Bonomo, R. A.; Tzouvelekis, L. S., Substitution of Thr for Ala-237 in TEM-17, TEM-12 and TEM-26: alterations in beta-lactam resistance conferred on Escherichia coli. *FEMS Microbiol Lett* 2001, 201, 37-40.
38.Cantu, C.; Palzkill, T., The role of residue 238 of TEM-1 beta-lactamase in the hydrolysis of extended-spectrum antibiotics. *J Biol Chem* 1998, 273, 26603-9.
39.Blázquez, J.; Negri, M. C.; Morosini, M. I.; Gómez-Gómez, J. M.; Baquero, F., A237T as a modulating mutation in naturally occurring extended-spectrum TEM-type beta-lactamases. *Antimicrob Agents Chemother* 1998, 42, 1042-4.
40.Labia, R.; Morand, A.; Tiwari, K.; Sirot, J.; Sirot, D.; Petit, A., Interactions of new plasmid-mediated beta-lactamases with third-generation cephalosporins. *Rev Infect Dis* 1988, 10, 885-91.
41.Venkatachalam, K. V.; Huang, W.; LaRocco, M.; Palzkill, T., Characterization of TEM-1 beta-lactamase mutants from positions 238 to 241 with increased catalytic efficiency for ceftazidime. *J Biol Chem* 1994, 269, 23444-50.
42.Imtiaz, U.; Manavathu, E. K.; Mobashery, S.; Lerner, S. A., Reversal of clavulanate resistance conferred by a Ser-244 mutant of TEM-1 beta-lactamase as a result of a second mutation (Arg to Ser at position 164) that enhances activity against ceftazidime. *Antimicrob Agents Chemother* 1994, 38, 1134-9.
43.Kong, K.-F.; Schneper, L.; Mathee, K., Beta-lactam antibiotics: from antibiosis to resistance and bacteriology. *APMIS* 2010, 118, 1-36.
44.Chen, Y.; Zhang, W.; Shi, Q.; Hesek, D.; Lee, M.; Mobashery, S.; Shoichet, B. K., Crystal Structures of Penicillin-Binding Protein 6 from Escherichia coli. *Journal of the American Chemical Society* 2009, 131, 14345-14354.
45.Knox, J. R.; Moews, P. C.; Frere, J.-M., Molecular evolution of bacterial ²-lactam resistance. *Chemistry & biology* 1996, 3, 937-947.
46.Long, A. J.; Clifton, I. J.; Roach, P. L.; Baldwin, J. E.; Rutledge, P. J.; Schofield, C. J., Structural studies on the reaction of isopenicillin N synthase with the truncated substrate analogues delta-(L-alpha-aminoadipoyl)-L-cysteinyl-glycine and delta-(L-alpha-aminoadipoyl)-L-cysteinyl-D-alanine. *Biochemistry* 2005, 44, 6619-28.
47.Fonseca, F.; Chudyk, E. I.; van der Kamp, M. W.; Correia, A.; Mulholland, A. J.; Spencer, J., The Basis for Carbapenem Hydrolysis by Class A β-Lactamases: A Combined Investigation using Crystallography and Simulations. *Journal of the American Chemical Society* 2012, 134, 18275-18285.
48.Mainardi, J.-L.; Hugonnet, J.-E.; Rusconi, F.; Fourgeaud, M.; Dubost, L.; Moumi, A. N.; Delfosse, V.; Mayer, C.; Gutmann, L.; Rice, L. B.; Arthur, M., Unexpected Inhibition of Peptidoglycan LD-Transpeptidase from Enterococcus faecium by the β-Lactam Imipenem. *Journal of Biological Chemistry* 2007, 282, 30414-30422.
49.Sacco, E.; Hugonnet, J.-E.; Josseaume, N.; Cremniter, J.; Dubost, L.; Marie, A.; Patin, D.; Blanot, D.; Rice, L. B.; Mainardi, J.-L.; Arthur, M., Activation of the l,d-transpeptidation peptidoglycan cross-linking pathway by a metallo-d,d-carboxypeptidase in Enterococcus faecium. *Molecular Microbiology* 2010, 75, 874-885.
50.Hellinger, W. C.; Brewer, N. S., Carbapenems and monobactams: imipenem, meropenem, and aztreonam. *Mayo Clin Proc* 1999, 74, 420-34.
51.Brewer, N. S.; Hellinger, W. C., The monobactams. *Mayo Clin Proc* 1991, 66, 1152-7.
52.Drawz, S. M.; Bonomo, R. A., Three decades of beta-lactamase inhibitors. *Clin Microbiol Rev* 2010, 23, 160-201.
53.Akova, M., Sulbactam-containing beta-lactamase inhibitor combinations. *Clin Microbiol Infect* 2008, 14 Suppl 1, 185-8.
54.Livermore, D. M.; Hope, R.; Mushtaq, S.; Warner, M., Orthodox and unorthodox clavulanate combinations against extended-spectrum beta-lactamase producers. *Clin Microbiol Infect* 2008, 14 Suppl 1, 189-93.
55.Oelschlaeger, P.; Ai, N.; Duprez, K. T.; Welsh, W. J.; Toney, J. H., Evolving carbapenemases: can medicinal chemists advance one step ahead of the coming storm? *J Med Chem* 2010, 53, 3013-27.
56.Allinger, N. L., Understanding molecular structure from molecular mechanics. *J Comput Aided Mol Des* 2011, 25, 295-316.
57.Leach, A. R., *Molecular Modelling - Principles and applications*. second edition ed.; 2001.

58.Ramachandran, K. I.; Deepa, G.; Namboori, K., *Computational Chemistry and Molecular Modeling - Principles and Applications*. Springer-Verlag Berlin Heidelberg: 2008.
59.Case, D. A.; Cheatham, T. E.; Darden, T.; Gohlke, H.; Luo, R.; Merz, K. M.; Onufriev, A.; Simmerling, C.; Wang, B.; Woods, R. J., The Amber biomolecular simulation programs. *J Comput Chem* 2005, 26, 1668-88.
60.Brooks, B. R.; Brooks, C. L.; Mackerell, A. D.; Nilsson, L.; Petrella, R. J.; Roux, B.; Won, Y.; Archontis, G.; Bartels, C.; Boresch, S.; Caflisch, A.; Caves, L.; Cui, Q.; Dinner, A. R.; Feig, M.; Fischer, S.; Gao, J.; Hodoscek, M.; Im, W.; Kuczera, K.; Lazaridis, T.; Ma, J.; Ovchinnikov, V.; Paci, E.; Pastor, R. W.; Post, C. B.; Pu, J. Z.; Schaefer, M.; Tidor, B.; Venable, R. M.; Woodcock, H. L.; Wu, X.; Yang, W.; York, D. M.; Karplus, M., CHARMM: the biomolecular simulation program. *J Comput Chem* 2009, 30, 1545-614.
61.Hetzel, R.; Wüthrich, K.; Deisenhofer, J.; Huber, R., Dynamics of the aromatic amino acid residues in the globular conformation of the basic pancreatic trypsin inhibitor (BPTI). II. Semi-empirical energy calculations. *Biophys Struct Mech* 1976, 2, 159-80.
62.Alder, B. J.; Wainwright, T. E., Studies in Molecular Dynamics. I. General Method. *Journal of Chemical Physics* 1959, 31.
63. Rahman, A., Correlations in the Motion of Atoms in Liquid Argon. *Physical Review* 1964, 136, A405-A411.
64.Karplus, M.; McCammon, J. A., Molecular dynamics simulations of biomolecules. *Nat Struct Mol Biol* 2002, 9, 646-652.
65.Chandler, D., *Introduction to Modern Statistical Mechanics*. Oxford University Press, 1987; p 288.
66.Ryckaert, J.-P.; Ciccotti, G.; Berendsen, H. J. C., Numerical integration of the cartesian equations of motion of a system with constraints: molecular dynamics of n-alkanes. *Journal of Computational Physics* 1977, 23, 327-341.
67.William, G. H., *Computational Statistical Mechanics*. Elsevier Science Publishers Ltd.: 1991; p 314.
68.Nose, S., A unified formulation of the constant temperature molecular dynamics methods. *The Journal of Chemical Physics* 1984, 81, 511-519.
69.Berendsen, H. J. C.; Postma, J. P. M.; van Gunsteren, W. F.; DiNola, A.; Haak, J. R., Molecular dynamics with coupling to an external bath. *The Journal of Chemical Physics* 1984, 81, 3684-3690.
70.Loncharich, R. J.; Brooks, B. R.; Pastor, R. W., Langevin dynamics of peptides: The frictional dependence of isomerization rates of N-acetylalanyl-N'-methylamide. *Biopolymers* 1992, 32, 523-535.
71.Izaguirre, J. A.; Catarello, D. P.; Wozniak, J. M.; Skeel, R. D., Langevin stabilization of molecular dynamics. *The Journal of Chemical Physics* 2001, 114, 2090-2098.
72.Darden, T.; York, D.; Pedersen, L., Particle mesh Ewald: An N [center-dot] log(N) method for Ewald sums in large systems. *The Journal of Chemical Physics* 1993, 98, 10089-10092.
73.Ewald, P. P., Die Berechnung optischer und elektrostatischer Gitterpotentiale. *Annalen der Physik* 1921, 369, 253-287.
74.Essmann, U.; Perera, L.; Berkowitz, M. L.; Darden, T.; Lee, H.; Pedersen, L. G., A smooth particle mesh Ewald method. *The Journal of Chemical Physics* 1995, 103, 8577-8593.
75.Sagui, C.; Darden, T. A., Molecular dynamics simulations of biomolecules: long-range electrostatic effects. *Annu Rev Biophys Biomol Struct* 1999, 28, 155-79.
76. Teague, S. J., Implications of protein flexibility for drug discovery. *Nat Rev Drug Discov* 2003, 2, 527-41.
77.Carlson, H. A., Protein flexibility and drug design: how to hit a moving target. *Curr Opin Chem Biol* 2002, 6, 447-52.
78.Carlson, H. A., Protein flexibility is an important component of structure-based drug discovery. *Curr Pharm Des* 2002, 8, 1571-8.
79.Sousa, S. F.; Fernandes, P. A.; Ramos, M. J., Protein-ligand docking: current status and future challenges. *Proteins* 2006, 65, 15-26.
80.Schnecke, V.; Swanson, C. A.; Getzoff, E. D.; Tainer, J. A.; Kuhn, L. A., Screening a peptidyl database for potential ligands to proteins with side-chain flexibility. *Proteins* 1998, 33, 74-87.
81.Hart, T. N.; Read, R. J., A multiple-start Monte Carlo docking method. *Proteins* 1992, 13, 206-22.
82.Oshiro, C. M.; Kuntz, I. D.; Dixon, J. S., Flexible ligand docking using a genetic algorithm. *J Comput Aided Mol Des* 1995, 9, 113-30.
83.Kitchen, D. B.; Decornez, H.; Furr, J. R.; Bajorath, J., Docking and scoring in virtual screening for drug discovery: methods and applications. *Nat Rev Drug Discov* 2004, 3, 935-49.
84.Bissantz, C.; Folkers, G.; Rognan, D., Protein-based virtual screening of chemical databases. 1. Evaluation of different docking/scoring combinations. *J Med Chem* 2000, 43, 4759-67.
85.Kawatkar, S.; Moustakas, D.; Miller, M.; Joseph-McCarthy, D., Virtual fragment screening: exploration of MM-PBSA re-scoring. *J Comput Aided Mol Des* 2012, 26, 921-34.
86.Morris, G. M.; Huey, R.; Lindstrom, W.; Sanner, M. F.; Belew, R. K.; Goodsell, D. S.; Olson, A. J., AutoDock4 and AutoDockTools4: Automated docking with selective receptor flexibility. *J Comput Chem* 2009, 30, 2785-91.
87.Huey, R.; Morris, G. M.; Olson, A. J.; Goodsell, D. S., A semiempirical free energy force field with charge-based desolvation. *J Comput Chem* 2007, 28, 1145-52.
88.Kollman, P., Free energy calculations: Applications to chemical and biochemical phenomena. *Chemical Reviews* 1993, 93, 2395-2417.
89.Hou, T.; Wang, J.; Li, Y.; Wang, W., Assessing the performance of the MM/PBSA and MM/GBSA methods. 1. The accuracy of binding free energy calculations based on molecular dynamics simulations. *J Chem Inf Model* 2011, 51, 69-82.

90.Fogolari, F.; Brigo, A.; Molinari, H., Protocol for MM/PBSA Molecular Dynamics Simulations of Proteins. *Biophysical Journal* 2003, 85, 159-166.
91.Massova, I.; Kollman, P., Combined molecular mechanical and continuum solvent approach (MM-PBSA/GBSA) to predict ligand binding. *Perspectives in Drug Discovery and Design* 2000, 18, 113-135.
92.Moreira, I. S.; Fernandes, P. A.; Ramos, M. J., Computational alanine scanning mutagenesis--an improved methodological approach. *J Comput Chem* 2007, 28, 644-54.
93.Clackson, T.; Wells, J. A., A hot spot of binding energy in a hormone-receptor interface. *Science (New York, N.Y.)* 1995, 267, 383-386.
94.Moreira, I. S.; Fernandes, P. A.; Ramos, M. J., Hot spots--a review of the protein-protein interface determinant amino-acid residues. *Proteins* 2007, 68, 803-12.
95.Bogan, A. A.; Thorn, K. S., Anatomy of hot spots in protein interfaces. *J Mol Biol* 1998, 280, 1-9.
96.Moreira, I. S.; Fernandes, P. A.; Ramos, M. J., Hot spot occlusion from bulk water: a comprehensive study of the complex between the lysozyme HEL and the antibody FVD1.3. *J Phys Chem B* 2007, 111, 2697-706.
97.Clackson, T.; Wells, J. A., A hot spot of binding energy in a hormone-receptor interface. *Science* 1995, 267, 383-6.
98.Thorn Ks Fau - Bogan, A. A.; Bogan, A. A., ASEdb: a database of alanine mutations and their effects on the free energy of binding in protein interactions.
99.Conte, L. L.; Chothia, C.; Janin, J., The atomic structure of protein-protein recognition sites. *Journal of Molecular Biology* 1999, 285, 2177-2198.
100.Lichtarge O Fau - Bourne, H. R.; Bourne Hr Fau - Cohen, F. E.; Cohen, F. E., An evolutionary trace method defines binding surfaces common to protein families.
101.Moreira, I. S.; Martins, J. M.; Ramos, R. M.; Fernandes, P. A.; Ramos, M. J., Understanding the importance of the aromatic amino-acid residues as hot-spots. *Biochim Biophys Acta* 2012.
102.Thompson, J. D.; Higgins, D. G.; Gibson, T. J., CLUSTAL W: improving the sensitivity of progressive multiple sequence alignment through sequence weighting, position-specific gap penalties and weight matrix choice. *Nucleic Acids Research* 1994, 22, 4673-4680.
103.Schrödinger, L. *Maestro, version 9.2*, 2011.
104.Cornell, W. D.; Cieplak, P.; Bayly, C. I.; Gould, I. R.; Merz, K. M.; Ferguson, D. M.; Spellmeyer, D. C.; Fox, T.; Caldwell, J. W.; Kollman, P. A., A Second Generation Force Field for the Simulation of Proteins, Nucleic Acids, and Organic Molecules. *Journal of the American Chemical Society* 1995, 117, 5179-5197.
105.Duan, Y.; Wu, C.; Chowdhury, S.; Lee, M. C.; Xiong, G.; Zhang, W.; Yang, R.; Cieplak, P.; Luo, R.; Lee, T.; Caldwell, J.; Wang, J.; Kollman, P., A point-charge force field for molecular mechanics simulations of proteins based on condensed-phase quantum mechanical calculations. *Journal of Computational Chemistry* 2003, 24, 1999-2012.
106.Jorgensen, W. L.; Chandrasekhar, J.; Madura, J. D.; Impey, R. W.; Klein, M. L., Comparison of simple potential functions for simulating liquid water. *The Journal of Chemical Physics* 1983, 79, 926-935.
107.Bolton, E. E.; Wang, Y.; Thiessen, P. A.; Bryant, S. H., Chapter 12 PubChem: Integrated Platform of Small Molecules and Biological Activities. In *Annual Reports in Computational Chemistry*, Ralph, A. W. a. D. C. S., Ed. Elsevier: 2008; Vol. Volume 4, pp 217-241.
108.Wallace Ac Fau - Laskowski, R. A.; Laskowski Ra Fau - Thornton, J. M.; Thornton, J. M., LIGPLOT: a program to generate schematic diagrams of protein-ligand interactions.
109.Bayly, C. I.; Cieplak, P.; Cornell, W.; Kollman, P. A., A well-behaved electrostatic potential based method using charge restraints for deriving atomic charges: the RESP model. *The Journal of Physical Chemistry* 1993, 97, 10269-10280.
110.Wang, J.; Wolf, R. M.; Caldwell, J. W.; Kollman, P. A.; Case, D. A., Development and testing of a general amber force field. *Journal of Computational Chemistry* 2004, 25, 1157-1174.
111.Humphrey, W.; Dalke, A.; Schulten, K., VMD: Visual molecular dynamics. *Journal of Molecular Graphics* 1996, 14, 33-38.
112. DeLano, W. L., The PyMOL Molecular Graphics System. DeLano Scientific, San Carlos, CA, USA.: 2002.
113.Huo, S.; Massova, I.; Kollman, P. A., Computational alanine scanning of the 1 : 1 human growth hormone-receptor complex. *Journal of Computational Chemistry* 2002, 23, 15-27.
114.D.A. Case, T. A. D., T.E. Cheatham, III, C.L. Simmerling, J. Wang, R.E. Duke, R. Luo,; M. Crowley, R. C. W., W. Zhang, K.M. Merz, B.Wang, S. Hayik, A. Roitberg, G. Seabra, I.; Kolossváry, K. F. W., F. Paesani, J. Vanicek, X.Wu, S.R. Brozell, T. Steinbrecher, H. Gohlke,; L. Yang, C. T., J. Mongan, V. Hornak, G. Cui, D.H. Mathews, M.G. Seetin, C. Sagui, V. Babin,; Kollman, a. P. A., AMBER 10, University of Calirfonia, San Francisco. 2008.
115.Moreira, I. S.; Fernandes, P. A.; Ramos, M. J., Detailed microscopic study of the full ZipA : FtsZ interface. *Proteins-Structure Function and Bioinformatics* 2006, 63, 811-821.
116.Moreira, I. S.; Fernandes, P. A.; Ramos, M. J., Unraveling the importance of protein-protein interaction: Application of a computational alanine-scanning mutagenesis to the study of the IgG1 streptococcal protein G (C2 fragment) complex. *Journal of Physical Chemistry B* 2006, 110, 10962-10969.
117.Moreira, I. S.; Fernandes, P. A.; Ramos, M. J., Unravelling Hot Spots: a comprehensive computational mutagenesis study. *Theoretical Chemistry Accounts* 2007, 117, 99-113.
118.Moreira, I. S.; Fernandes, P. A.; Ramos, M. J., Hot spot computational identification: Application to the complex formed between the hen egg white lysozyme (HEL) and the antibody HyHEL-10. *International Journal of Quantum Chemistry* 2007, 107, 299-310.

119.Moreira, I. S.; Fernandes, P. A.; Ramos, M. J., Computational alanine scanning mutagenesis - An improved methodological approach. *Journal of Computational Chemistry* 2007, 28, 644-654.
120.Moreira, I. S.; Fernandes, P. A.; Ramos, M. J., Backbone importance for protein-protein binding. *Journal of Chemical Theory and Computation* 2007, 3, 885-893.
121.Moreira, I. S.; Fernandes, P. A.; Ramos, M. J., Hot spot occlusion from bulk water: A comprehensive study of the complex between the lysozyme HEL and the antibody FVD1.3. *Journal of Physical Chemistry B* 2007, 111, 2697-2706.
122.Moreira, I. S.; Fernandes, P. A.; Ramos, M. J., Protein-protein recognition: a computational mutagenesis study of the MDM2-P53 complex. *Theoretical Chemistry Accounts* 2008, 120, 533-542.
123.Chong, L. T.; Duan, Y.; Wang, L.; Massova, I.; Kollman, P. A., Molecular dynamics and free-energy calculations applied to affinity maturation in antibody 48G7. *Proceedings of the National Academy of Sciences of the United States of America* 1999, 96, 14330-14335.
124.Kollman, P. A.; Massova, I.; Reyes, C.; Kuhn, B.; Huo, S. H.; Chong, L.; Lee, M.; Lee, T.; Duan, Y.; Wang, W.; Donini, O.; Cieplak, P.; Srinivasan, J.; Case, D. A.; Cheatham, T. E., Calculating structures and free energies of complex molecules: Combining molecular mechanics and continuum models. *Accounts of Chemical Research* 2000, 33, 889-897.
125.Bradshaw, R. T.; Patel, B. H.; Tate, E. W.; Leatherbarrow, R. J.; Gould, I. R., Comparing experimental and computational alanine scanning techniques for probing a prototypical protein-protein interaction. *Protein Engineering Design & Selection* 2011, 24, 197-207.
126.Martins, J.; Ramos, R.; Moreira, I., Structural determinats of a typical leucine-rich repeat protein. *Communications in computational physics* 2013, 13, 238-255.
127.Moreira, I. S.; Martins, J. M.; Ramos, M. J.; Fernandes, P. A.; Ramos, M. J., Understanding the importance of the aromatic amino-acid residues as hot-spots. *Biochem. Biophys. Acta* 2013, 1834, 401-414.
128.Ribeiro, J. V.; Cerqueira, N. M. F. S. A.; Moreira, I. S.; Fernandes, P. A.; Ramos, M. J., CompASM: an Amber-VMD Alanine Scanning Mutagenesis plug-in. *Theoretical Chemistry Accounts- In press.* 2012.
129.Rocchia, W.; Alexov, E.; Honig, B., Extending the applicability of the nonlinear Poisson-Boltzmann equation: Multiple dielectric constants and multivalent ions. *Journal of Physical Chemistry B* 2001, 105, 6507-6514.
130.Rocchia, W.; Sridharan, S.; Nicholls, A.; Alexov, E.; Chiabrera, A.; Honig, B., Rapid grid-based construction of the molecular surface and the use of induced surface charge to calculate reaction field energies: Applications to the molecular systems and geometric objects. *Journal of Computational Chemistry* 2002, 23, 128-137.
131.Moreira, I. S.; Fernandes, P. A.; Ramos, M. J., Accuracy of the numerical solution of the Poisson-Boltzmann equation. *Journal of Molecular Structure-Theochem* 2005, 729, 11-18.
132.Sitkoff, D.; Sharp, K. A.; Honig, B., Accurate calculation of hydration free-energies using macroscopic solvent models *Journal of Physical Chemistry* 1994, 98, 1978-1988.
133.Connolly, M. L., Analytical molecular surface calculation *Journal of Applied Crystallography* 1983, 16, 548-558.